Title
Flexible Control of the Target Template during Visual Search

Permalink
https://escholarship.org/uc/item/82s7b4b0

Author
Yu, Xinger

Publication Date
2021

Flexible Control of the Target Template during Visual Search

By

XINGER YU
DISSERTATION

Submitted in partial satisfaction of the requirements for the degree of

DOCTOR OF PHILOSOPHY

in

Psychology

in the

OFFICE OF GRADUATE STUDIES

of the

UNIVERSITY OF CALIFORNIA

DAVIS

Approved:

Joy J. Geng, Chair

George R. Mangun

Timothy D. Hanks

Committee in Charge

2022

Acknowledgements

First and foremost, I would like to express my gratitude and appreciation for my advisor Joy Geng whose guidance, support, and encouragement has been invaluable throughout this dissertation. Her high standards and thoughtful feedback constantly motivated my work and helped me to become an independent scientist. Joy, I will forever be grateful for the role you continue to play in my life. I look forward to years of learning from you.

I would like to thank my dissertation committee, Ron Mangun and Tim Hanks. Thank you all very much for your time and support.

I have also received enormous professional and personal support from many past and present Geng lab members. Special thanks go to Bo Yeong Won for being an incredible teacher and friend when I first arrived at Davis. Jeongmi Lee has so generously shared her neuroimaging knowledge with me. Phillip Witkowski has helped me with my neuroimaging data collection presented in Chapter 3. Zhiheng Zhou has been the most wonderful office mate, friend, collaborator as well as my unofficial second advisor. Thanks to Joe Nah, Raisa Rahim, Shea Duarte and Beth Hall for their valuable feedback during the lab meetings. All of your support and friendship have improved the science and welfare of the entire lab.

Last but not least, I would like to express my gratitude to my wonderful family. Mom and Dad, everything I have and everything I am, I owe it all to you. Thank you for always staying right by my side and never questioning my choices. Sharky, my lovely kitten, thank you for providing the much needed support to finish this dissertation. Your tiny paws will always have a special place in my heart.

Abstract

When searching for a target object (e.g., a friend at a party), we engage in a continuous “look-identify” cycle in which we use known features (e.g., hair color) to guide attention and eye gaze towards potential targets and then to decide if it is indeed the target. Theories of attention refer to the information about the target in memory as the “target” or “attentional” template and typically characterize it as a single, fixed, source of information. In this doctoral thesis, I provide evidence that templates do not necessarily represent the veridical properties of the target item, but rather are adapted to the current context (e.g., distractors, task demands, etc.) to improve visual search efficiency. In Chapter 2, I investigated the behavioral mechanisms by which modulations in the target template might increase the representational distinctiveness of targets from expected distractors. I argue that template *shifting and asymmetrical sharpening* are two mechanisms that increase the template-to-distractor distinctiveness, which makes target selection and decisions more efficient. In Chapter 3, I assessed the brain mechanisms that support these changes in target representations to optimize target-match decisions. I found that sensory-veridical target information is transformed in *lateral prefrontal cortex* into an adaptive code of target-relevant information that optimize decision processes during visual search. In Chapter 4 and 5, I investigated how template information operates to guide attention and make identity decisions during visual search. I argue that attentional guidance operates on a *coarser* code to weight sensory information and target match decisions use a more *precise* representation to determine identity. Across these studies, the results reveal the flexible nature of target templates that are used to guide visual search.

Table of Contents

Chapter 1: Introduction

Every day we perform numerous visual search tasks: looking for a key in a living room, a textbook in a bookstore or a friend in crowd. In each of these scenarios, the objects are hard to find because they are “hidden” amongst countless other objects, and there is a limit on how much information can be processed in any given moment. However, we are still somehow able to limit our search to plausible objects. Traditional theories of attention hypothesize that we accomplish the task by holding a veridical copy of the target, akin to a photograph of the target object, in working memory and then moving attention and the eyes to candidate objects that might match target features. For example, imagine you are searching for car keys on a cluttered table. Being familiar with the keys, an image comes to your mind of shiny metal. This knowledge can help you limit your search to objects with shiny metal, instead of searching in a random order or inspecting each object on the table. This internal representation of target features held in working or long-term memory during visual search is often known as “attentional” or “target” template (Duncan & Humphreys, 1989; Eriksen, 1953; Green & Anderson, 1956; Olivers et al., 2011). The contents of the template are critical for defining “task-relevance” at multiple stages of attentive processing (Geng & Witkowski, 2019; Hout & Goldinger, 2015; Malcolm & Henderson, 2009; Wolfe, 2021). However, despite its important role in the study of attention, there are still many open questions regarding what information is stored in the template and how its contents affect visual search performance. The purpose of the work presented here is to demonstrate the flexibility of the template contents and investigate how the template-to-distractor distinctiveness impacts visual search efficiency.

Attentional guidance and decision

As introduced earlier, the attentional template contributes to visual search by directing selective attention and eye-movements toward objects with template-matching attributes. This is presumed to occur because information in the target template is used to modulate sensory gain (Desimone & Duncan, 1995; Reynolds & Heeger, 2009; Treisman & Gelade, 1980). For example, when searching for a red colored object, mechanisms of gain enhancement will selectively increase the responsivity of sensory neurons that preferentially encode “red”, resulting in increased attentional priority to all red stimuli in the visual field (Liu et al., 2007; Serences et al., 2009; Treue & Trujillo, 1999).

Once attention selects a candidate object, however, a decision must be made regarding the exact identity of the stimulus as a match or non-match to the target (Bravo & Farid, 2012, 2016; Castelhano et al., 2008; Rajsic & Woodman, 2020; Wolfe, 2012). To do this, the memory template can be compared against visual inputs through a drift diffusion process for target verification or rejection (Ratcliff et al., 2016; Ratcliff & McKoon, 2008; Wolfe, 2021). This decision component is a time-consuming portion of visual search and the critical final stage for making a correct or incorrect response. Despite the importance of this decision process on visual search, knowledge of how target representations are modulated to facilitate target-match decisions is still poorly understood.

The two distinct subprocesses of visual search are often hypothesized to rely on the same informational content of the target. However, this notion is challenged by recent evidence showing the precision of template information may differ based on the stage of processing. For example, Kerzel (2019) found that colors that were less similar to the target could still capture attention, despite a very precise memory representation of the target (see also Anderson, 2014). These results suggest that attentional guidance is a less precise subprocess during visual search. In contrast, the decision process requires a more specific template (Castelhano et al., 2008). For instance, Rajsic and Woodman (2020) found that the benefit of weighting the target template over accessory memory representations in a dual-memory search task mainly lies in enhancing target recognition rather than more efficient localization of the target. Consistent with those findings, Wolfe (2021) recently argued that the search template can (and should) be divided into two: a "guiding" template in working memory that is used to direct attention to potential targets; and a "target" template in long-term memory that is used to determine if a candidate object is the target. Based the stage of processing, the appropriate template is recruited to define task relevance. Although there is good evidence for coarse guidance and precise decisions separately, few studies have directly tested whether the informational content of the target is used differently on these two subprocesses of visual search.

"Off-veridical" target template

If the attentional template serves to filter stimuli entering the visual system and "gate keep" the outcome accuracy of object localization, it follows that the precision of templates should improve visual search by enhancing attentional guidance to the correct target object (Nako et al., 2014; Schmidt & Zelinsky, 2009) and by facilitating recognition and decision processes (Castelhano et al., 2008; Rajsic & Woodman, 2020). For example, Hout and Goldringer (2015) provided observers with one of the following three types of cues for a subsequent target in a visual search display: an exact match, the same object from a different viewpoint, or a different exemplar object from the same category. The authors found that less precise cues increased both the time to locate the correct target and the time to decide if it was the target. The advantages of specific search templates were also observed in visually complex real-world environment (Malcolm & Henderson, 2009, 2010). Picture cues, rather than verbal cues, allowed observers to more efficiently allocate attention to target items, and to more quickly verify the target once fixated.

Although these studies argue for the advantage of template specificity, a distorted version of the veridical target may actually be more optimal if it increases the psychological distance between targets and distractors (Becker, 2010; Geng et al., 2017; Geng & Witkowski, 2019; Hodsoll & Humphreys, 2001; Kerzel, 2020; Navalpakkam & Itti, 2007; Scolari & Serences, 2009). For example, a key finding of Navalpakkam and Itti (2007) suggests that the target template shifted in feature space when presented with highly similar and linearly separable distractors (e.g., an orange target amongst red distractors). Throughout the visual search trials, a probe task would appear which presented the target amongst distractors and an “exaggerated” target (e.g. the slightly yellower version of the orange target). Participants were more likely to choose the exaggerated one as the target than the actual target, suggesting that their target representation was shifted to optimize the template-to-distractor distinctiveness (Hodsoll & Humphreys, 2001; Scolari et al., 2012). The shifts in target representations occur not only when searching for simple target features, but also when searching for “high level” objects such as a face depicting an emotion (Won et al., 2020). This suggests that shifting is not simply due to an adaptation or contrast effect in the visual system, but a strategic adjustment of the target template.

Although it is clear that the shifted template is more effective to discriminate the target from linearly separable distractors, different underlying mechanisms have been proposed. Becker and colleagues (Becker, 2010; Becker et al., 2014; Martin & Becker, 2018) argue that this attentional bias was due to observers using a “relational” rule to guide attention and first saccades towards the “yellowest” object in the visual environment. The relational account hypothesizes that target features are represented relative to distractors rather than by specific features. Non-targets sharing the target’s feature relation to distractors will capture attention even if the specific features are different. The optimal model using the probe task and the relational account using first saccade destinations provided conflicting results and explanations of template shifting. Therefore, it is important to address this debate.

In addition to shifting target representations away from specific features, there is also evidence that the template is sharpened when distractor competition is strong (Geng et al., 2017). Sharpening has been observed in sensory neurons in response to attentional selection and has long been hypothesized to decrease the selectivity of task-irrelevant stimulus features (Martinez-Trujillo & Treue, 2004; Scolari & Serences, 2009; Serences et al., 2009). For instance, Geng et al. (2017) demonstrated that the sharpness of the target template asymmetrically increased on the distractor side when highly competitive distractors were more frequent. This was presumably due to a greater need to counteract competitive pressure from highly similar distractors. Although these changes in the target template are presumed to increase the template-to-distractor psychological distinctiveness and lead to better attentional selection, it remains unclear what characteristics of the distractor context produce shifting vs. sharpening of the target template.

Overview of current work

The focus of the following work will be on the further understanding of how the target representation is shaped by the distractor context and moreover, how the target information is used to perform visual search. First, recent evidence suggests that expectations regarding the distractor context might shift and asymmetrically sharpen the attentional template to increase the psychological distinctiveness between the target and distractors, but it remains unknown if different distractor characteristics produce shifting vs. sharpening. In Chapter 2, we extend those demonstrations to investigate the exact properties of the visual context that alter tuning properties of the target template. Specifically, we investigate two distractor features: linear separability and the strength of distractor competition. We expect that when distractor colors are predictable and linearly separable from the target, the central tendency of the target representation will shift away from distractor values, but this will occur irrespective of exactly how similar the distractors are to the target. In contrast, we hypothesize that asymmetrical sharpening will occur in response to increasing competition from target-similar distractors.

In Chapter 3, we conducted a pattern-based fMRI study to assess how template information is encoded to optimize target-match decisions during visual search. To ensure that match decisions reflect visual search demands, we used the visual search paradigm in Chapter 2 in which all distractors were linearly separable but highly similar to the target and were known to induce a bias in the target template. We measured the target representation used for match decisions in a separate match-to-sample probe task. We expect that the “off-veridical” template representation would be stored and used to optimize target-match decisions in lateral prefrontal cortex within the frontoparietal network.

In Chapter 4, we investigate how the off-veridical target representation, shaped by the distractor context, in turn affect visual search processing through sensory gain and decisional processes. Using a visual search task for a target amongst linearly separable distractors, we test the hypothesis that early attentional guidance will be based on relational information whereas subsequent match decisions will be made against an “optimal” off-target feature. If true, this would suggest that attentional guidance operates on a coarser code to weight sensory information and target match decisions use a more precise representation to determine identity. Real-world search targets, however, are infrequently linearly separable from distractors. In Chapter 5, we test if the differences between the precision of template information used for guidance compared to target decisions also applies under more typical search conditions.

Taken together, the findings presented here extend our knowledge of target template. By understanding how the template information is flexibly controlled and used we can better explain attention and visual search in general.

Chapter 2: The Attentional Template is Shifted and Asymmetrically Sharpened by Distractor Context

The following chapter consists of a manuscript that has been submitted for publication at *Journal of Experimental Psychology: Human Perception and Performance*

Abstract

Theories of attention hypothesize the existence of an “attentional template” that contains target features in working or long-term memory. It is often assumed that the template contents are veridical, but recent studies have found that this is not true when the distractor set is linearly separable from the target (e.g., all distractors are “yellower” than an orange colored target). In such cases, the target representation in memory shifts away from distractor features (Navalpakkam & Itti, 2007) and develop a sharper boundary with distractors (Geng, DiQuattro & Helm, 2017). These changes in the target template are presumed to increase the target-to-distractor psychological distinctiveness and lead to better attentional selection, but it remains unclear what characteristics of the distractor context produce shifting vs. sharpening. Here, we test the hypothesis that the template representation shifts whenever the distractor set (i.e., all of the distractors) is linearly separable from the target, but that asymmetrical sharpening only occurs when linearly separable distractors are highly target-similar. Our results were consistent, suggesting that *template shifting and asymmetrical sharpening* are two mechanisms that increase the representational distinctiveness of targets from expected distractors and improve visual search performance.

Introduction

It is impossible for humans to simultaneously process all available information in complex visual scenes. Thus, when searching for a target object (e.g., a friend at a party), we must use known features (e.g., hair color) to guide our attention and gaze. Theories of attention posit that this occurs by using information held within a memory representation (i.e., the *attentional or target template*) to bias sensory processing towards target features and serve as a decisional boundary for target selection (Bundesen, 1990; Desimone & Duncan, 1995; Duncan & Humphreys, 1989; Reynolds & Heeger, 2009; Treue & Martínez-Trujillo, 1999; Liu, Larsson, & Carrasco, 2007; Wolfe, 2007). Importantly, the target template not only modulates the sensory gain of neurons, but is also used to decide if the visual input matches the target (Duncan & Humphreys, 1989; Hout & Goldinger, 2015; Malcom & Henderson, 2010; Shiu & Pashler, 1984). Thus, while it is clear that the contents of the attentional template are critical for defining "task-relevance" at multiple stages of attentive processing, there is limited knowledge of what factors shape the "tuning" of the template. It has been largely assumed that the template is optimal when it perfectly matches the veridical target so that it can tune the most veridical sensory neurons and make the most accurate decision for a target-match. However, recent evidence suggests that the attentional template may actually be more optimal when "off-veridical" if it increases the psychological distance between targets and distractors (Navalpakkam & Itti, 2007; Becker, 2010; Scolari & Serences, 2009; Wolfe, 2000; Bauer, Joliceour, & Cowan, 1996; D'Zmura, 1991; Hodsoll, & Humphreys, 2001). In these studies, we extend those demonstrations to investigate the exact properties of the visual context that alter tuning properties of the target template.

One of the earliest studies to report "off-veridical" template representations found that shifts in the target representation in response to distractor context produced better target selection than a veridical template representation (Navalpakkam & Itti, 2007). Navalpakkam and Itti (2007) asked observers to search for a target line oriented 55° amongst 50° distractor lines during visual search “training” trials and then measured the target representation held in memory on separate “probe” trials. On probe trials, participants selected the target from five briefly presented oriented lines (80°, 60°, 55°, 50° and 30°). Notably, while the visual search "training" trials contained distractors that were linearly separable from the target (e.g., all were at the same orientation rotated counterclockwise from the target), the "probe" stimuli were sampled from both sides of the target (e.g., both counterclockwise and clockwise rotations of the target). Navalpakkahm and Itti (2007) found that the 60° stimulus was chosen more frequently than the 55° (true target) stimulus as the target on probe trials. This demonstrated that the target representation was shifted away from visual search distractors. In a second experiment, the same effect of target “shifting” was found using color stimuli, suggesting that shifted target representations occur across stimulus dimensions (see Figure 2.1). The authors argued that the shift reflected a bias in sensory gain towards neurons tuned to orientations more distant from the distractors (Figure 2.2A), in order to optimize the perceptual distinctiveness of the target from distractors (see also Hodsoll & Humphreys, 2001; Scolari, Byers & Serences, 2012).

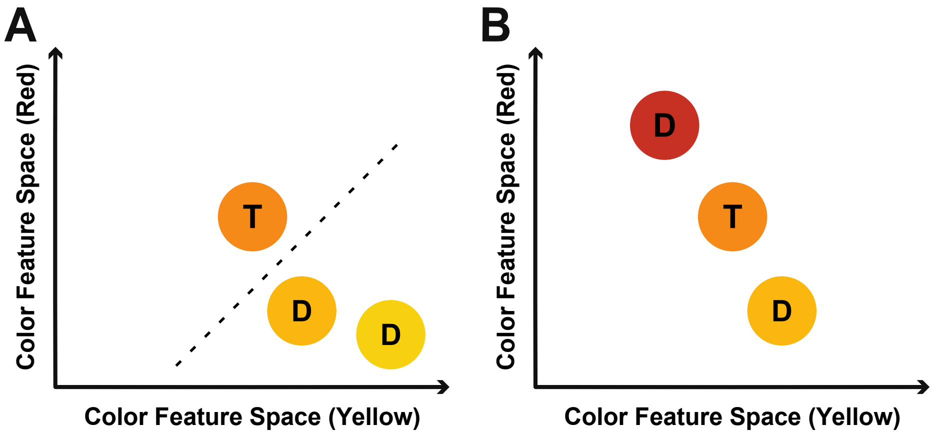

Figure 2.1. Illustration of linear separability between target and distractor stimuli. The target color is denoted with letter “T” and distractors with "D". A) A case where the orange target is linearly separable from "yellower" distractors. The linear operator is represented by dashed line. B) A case where the target is linearly nonseparable from distractors. (Adapted from Bauer, Jolicoeur & Cowan, 1998).

In addition to use of target "probe" trials, Scolari and Serences (2009; Experiment 2, 3) used an independent contrast sensitivity task to test for attentional biases in target features. They reasoned that contrast detection thresholds should be lowest for orientation-selective neurons with greater attentional gain. The results when distractors were similar to the target (i.e., 5° away) showed lower contrast detection thresholds for off-target features. Interestingly, both distractor orientations as well as target-exaggerated orientations had significantly lower thresholds, but there was an asymmetry early in training such that the exaggerated target features (i.e., orientations most distant from distractors) had the lowest thresholds (Scolari & Serences, 2009, Figure 4C). Furthermore, the off-target enhancement disappeared when the visual search distractor orientations were 90° from the target, suggesting that attentional shifting is unnecesary when distractors are uniform and very distinct from the target.

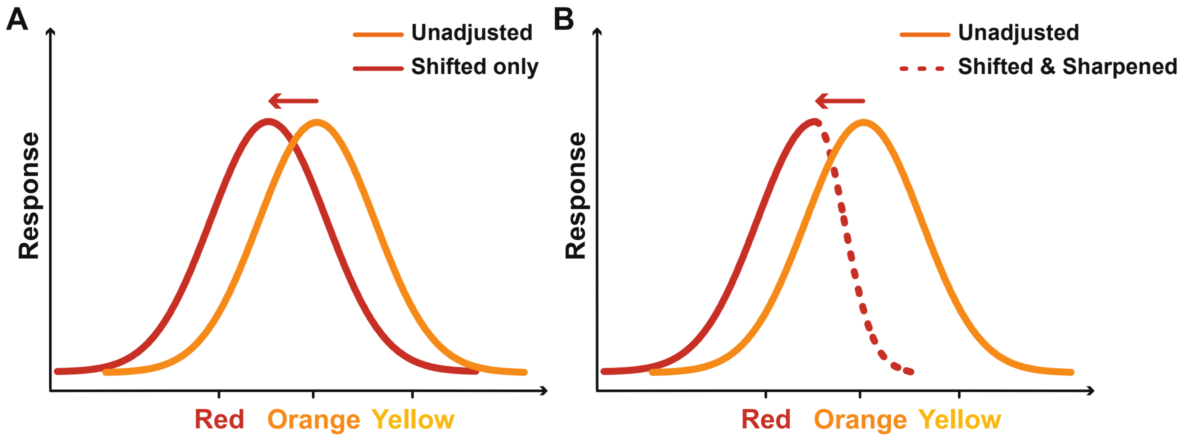

Figure 2.2. Examples of template adjustment to increase the distinctiveness between an orange target and yellow distractors. A) Shifting alone. B) A combination of shifting and asymmetrical sharpening. See texts for details.

Similar findings of shifted target representations have also been reported by other researchers using very different methods. For example, Becker and colleagues (2014) asked participants to search for a colored target (e.g., orange) amongst linearly separable distractors (e.g., yellow). Each search display was preceded by a cue display with task-irrelevant colored "cues" surrounding each possible target location. They found stronger attentional capture by red colored cues compared to orange ones, suggesting that attention was biased toward "redder" colors than the true target. These results led Becker and colleagues to develop the relational account of attentional guidance, which hypothesizes that target features are represented relative to distractors (e.g., the target is the "redder" or "bigger" object) rather than by specific features (Becker, 2010; Becker et al., 2014; Becker, Folk, & Remington, 2010). Although the proposed mechanism differs from Navalpakkam and Itti (2007) and Scolari and Serences (2009), they also conclude that the contents of the attentional template are adjusted to maximize the observer's ability to distinguish targets from expected distractors.

In addition to shifting the target representation, there is some evidence that the target template may also be asymmetrically sharpened when distractor competition is strong (Geng, DiQuattro & Helm, 2017). Sharpening has been observed in sensory neurons in response to attentional selection and has long been hypothesized to decrease the selectivity of task-irrelevant stimulus features (Series, Latham & Pouget, 2004; Lee et al., 1999; Ling, Jehee & Pestilli, 2016; Serences et al., 2009; Sompolinsky & Shapley, 1997; see also Scolari & Serences, 2009). In our previous study, the visual search display was composed of a single target and a distractor. The target color was fixed across the experiment; the distractor color varied continuously in similarity from the target color, but was always selected from one side of color space (i.e., target and distractors were linearly separable). Two groups of subjects saw the same distractors (ranging from 5º-60º along a color wheel), but the "high-similarity group" experienced a greater proportion of the most target-similar distractors and the "low-similarity group" saw the reverse distribution. In a separate template "probe" task, only the high similarity group had a target representation characterized by narrower tuning on the distractor side (i.e., asymmetrical sharpening) (Figure 2.2B); both groups had similar sized shifts in the central tendency of the target representation. This suggested that only the high-similarity group counteracted frequent pressure from highly competitive distractors by increasing the sharpness of the target template asymmetrically on the distractor side. The template "probe" task asked subjects for an explicit choice regarding the remembered target color and was therefore very different from those used in other studies in which the probe task targeted sensory processes (e.g., Navalpakkam & Itti, 2007; Soclari & Serences, 2009). This study provided evidence that expectations regarding the distractor context might shift and asymmetrically sharpen the attentional template, which may in turn affect visual search processing through sensory gain or decisional processes.

The aim of the current experiments is to determine if different distractor characteristics produce *shifting* vs. *sharpening* of the target template. The goal is to measure the "tuning" of the template as a memory representation based on expectations built from visual search trials, but is agnostic as to whether the representation affects sensory or decisional processes, or both. Specifically, we investigated two distractor features: linear separability and the strength of distractor competition. We hypothesize that when distractor colors are predictable and linearly separable from the target, the central tendency of the target representation will shift away from distractor values, but this will occur irrespective of exactly how similar the distractors are to the target. In contrast, we hypothesize that asymmetrical sharpening will occur in response to increasing competition from target-similar distractors. To test these hypotheses, we use a visual search “training” task to establish expectations for the distractor colors and a separate template “probe” task to measure the contents of the target template. Trials from the two tasks were interleaved. The separation of the visual search training trials and the template probe trials is essential for obtaining a measurement of the attentional template in memory that is uncontaminated by processes involved in active target selection from distractor competition.

Experiment 1

The goal of Experiment 1 was to test for the presence of shifting and asymmetrical sharpening in the target template due to the predictable distractor context. The distractor context was manipulated in visual search “training” task across two groups. In the “unidirectional” group, the distractors were all from *one direction* on the color wheel (e.g., bluer than the target color) and could be predicted from trial-to-trial. In the “bidirectional” group, the distractor set on each trial could be from *either direction* from the target color. It was therefore impossible to predict the directionality of distractor colors on a trial-by-trial basis. All distractors were highly similar to the target (5°-15° from the target) and therefore maxmized competittion for attention. The content of the target template was measured on separate template “probe” trials that calculated the likelihood of observers mistaking a range of color hues as the target color. Notably, because the probe trials were distinct from the visual search trials, our measurements of the template reflect information held in memory about the target feature.

Method

Participants. Forty students (12 males, 4 left handed, ages 18 - 26) from University of California, Davis participated in Experiment 1 in partial fulfillment of a course requirement. They were randomly assigned into the unidirectional or the bidirectional color group. We chose twenty participants for each group based on power calculations (.8 power, .05 two-tailed significance) using results from Experiment 2 in Geng, DiQuattro, and Helm (2017). Each participant was provided written informed consent in accordance with the local ethics clearance as approved by the National Institutes of Health. Each participant’s color vision was assessed by self-report and an online color blindness test (https://colormax.org/color-blind-test). All participants had normal or corrected-to-normal vision and all had normal color vision.

Apparatus. Participants were seated in a sound attenuated room 65cm away from a 27-in BenQ LCD monitor with a spatial resolution of 2560 x 1440 pixels and a refresh rate of 144hz. The operating system was Windows 7, and Matlab Psychtoolbox (Brainard, 1997; Pelli, 1997) was used to create all stimuli.

Design. The target and distractor colors were selected from a color wheel defined in LAB color space (a,b coordinates = 0, 0; luminance = 70; radius = 39). Two target colors (190°, 274°) were counterbalanced across subjects. Each subject was assigned a single target color throughout the experiment.

In the unidirectional group, the three distractors in each visual search training trial were different from each other and always 5°, 10°, and 15° away from the target color. The rotational direction (negative or positive) of those three distractors from the target color was counterbalanced across subjects: half of the subjects always saw negatively rotated distractors (-5°, -10°, and -15°) and half saw positively rotated distractors (5°, 10°, and 15°). These distractors were chosen to exceed the average just noticeable difference, yet be confusable with the target when presented in a competitive visual search context (Geng, DiQuattro & Helm, 2017). Because the two target colors and distractor color directions did not affect performance, *ps* > .2, data from these conditions were collapsed to maximize power. For descriptive simplicity, the distractors in the visual search training trials in both groups (i.e., "trained" distractor colors) will always be referred to as positive rotations from the target (i.e., 5°, 10°, 15°) and the non-target colors opposite to the distractor colors that appeared only in the template probe trials (i.e. "untrained" colors) will be labeled as negative rotations from the target (i.e., -5°, -10°, -15°).

In the bidirectional group, the visual search displays were identical to those used in the unidirectional group, but now the direction of the distractor sets (negative, positive) were randomly interleaved within a single subject: Half of the trials contained the three positive color distractors (i.e., 5°, 10°, 15°) and the other half contained the negative color distractors (i.e., -5°, -10°, -15°). An initial analysis was conducted to assess whether the specific target color affected performance, but there were no significant differences, *ps* > .3. Thus, all analyses collapse across the two target colors.

Subjects in both the unidirectional and bidirectional groups, saw the same colors during the template probe task. The colors included the target color (color 0°), and the three colors from each side of the target (i.e., -5°, -10°, -15°, 5°, 10° and 15°). Because the template probe task was identical across the two groups, we were able to assess the consequences of the specific visual search context on the target representation.

Procedure. Prior to the start of the experiment, an example of the target color was presented. The visual search training task (Figure 2.3A) began with the presentation of four circles (3° of visual angle in diameter) for 1000ms on a gray background (37.0 cd/m^2). The target color was always present and was located randomly at one of the 4 vertexes along an imaginary square (6° of horizontal and vertical visual angle from center to edge) while the distractors appeared at the other 3 vertices. In the unidirectional group, the three distractors were either all negative rotations (-5°, -10° and -15°) or positive rotations (5°, 10° and 15°) from the target color. The distractor set (negative or positive) was counterbalanced across subjects, so that each subject only saw one set of distractors. In the bidirectional group, the same distractors were used, but now the distractor set (negative or positive) was interleaved between trials, within each subject. Both groups saw the same stimuli, but individuals in the unidirectional group only saw one set of distractors while individuals in the bidirectional group saw both distractor sets. A number from 1-4 (1° of visual angle; white) was centrally located within each circle. Upon presentation of the display, participants searched for the predefined target-color circle and reported the number inside by pressing button ‘U’ for 1, ‘I’ for 2, ‘O’ for 3, or ‘P’ for 4 with their right hand. If no response was recorded within 2000ms, the trial automatically terminated. Auditory feedback was provided immediately following response or after 2000ms had elapsed (600hz tone for correct; 200hz tone for incorrect; no feedback for missing). A fixation cross (subtending .5° of visual angle; white) was centrally presented for 1000-1500ms before the next trial.

In the color template probe task (Figure 2.3B), each trial consisted of a centrally presented circle (3° of visual angle in diameter) for 500ms, after which a circular checkerboard mask (3° of visual angle) was displayed for 66ms. Participants reported whether the presented color was the target color (“yes” response, button ‘U’) or not (“no” response, button ‘I’) with their right hand. The ratio between target “yes” and “no” trials was 3:4. An uneven ratio was used to maximize the number of non-target color presentations. A "no" response bias, even if present, would not be selective for the analyses of interest based on differences in "yes" and "no" responses to each color presented in the template probe task. Participants were informed that a pseudo-feedback (400hz) tone would be given no matter what their response was in order to equate the presence of auditory events between the visual search and template task. A fixation cross was centrally presented for 1434ms-1934ms before the next trial began. The trial was terminated if no response was made within 2000ms.

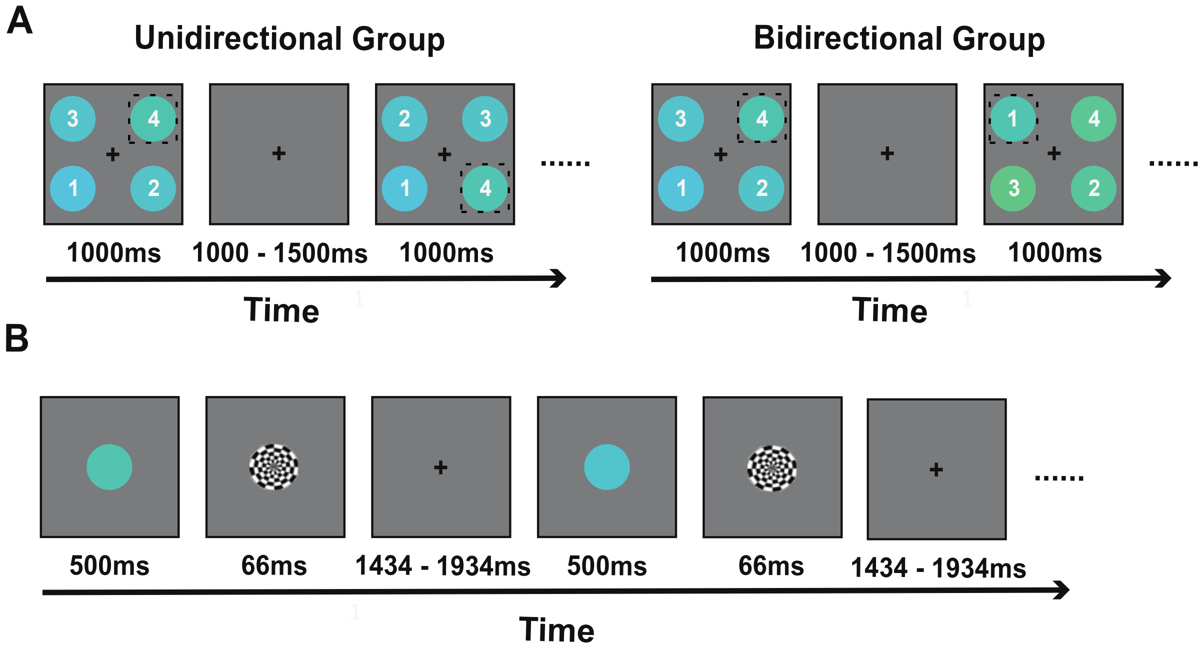

Figure 2.3. Example of visual search and template probe tasks for Experiment 1. Two trials for each task are illustrated. A) Visual search task: participants were instructed to locate the target color circle and report the number within. A high tone (600 hz) was given for correct responses, and a low tone (200 hz) for incorrect responses. The dashed squares illustrate the target but were not visible to the participants. B) Template probe task: participants were instructed to report if the centrally presented color circle was target color or not. A medium tone (400 hz) occurred on all trials regardless of responses to equate the presence of auditory feedback with the visual search task. Non-target color values are exaggerated for visual clarity in both figures (see methods for true values).

Prior to the beginning of the experiment, participants completed 32 practice trials composed of both visual search training and template probe tasks. Participants were instructed to fixate on the center cross throughout the whole experiment. The main experiment was composed of 320 visual search trials and 336 color probe trials. Trials were presented in four blocks, each containing alternating blocks of visual search training trials and template probe trials. Within each block, the first 4 alterations involved 10 visual search training trials followed by 7 template probe trials and the remaining 8 alterations had only 5 visual search training trials followed by 7 template probe trials. This design was created to maximize measurements of the target template on template probe trials between periodic visual search training. The use of independent probe trials is essential for measuring the contents of the attentional template as an ongoing memory representation of critical target features that is independent of concurrent visual search, which involves many processes beyond target representation, such as those necessary for resolving distractor competition.

Statistical Analyses. The visual search training task was used to establish expectations for the target color and the probe trials measured the contents of the attentional template independent of simultaneous distractor competition. Probe trials assessed the likelihood of each of seven colors being identified as the target color. “Target yes” responses on probe trials were false alarms when the color was a non-target, but a hit when it was the target color. While the response rate for each color is independent from other colors, we hypothesize that the *underlying source* of the response profile across colors comes from an underlying distribution – i.e., the “tuning” of the target template. Therefore, in order to estimate the underlying tuning function of the target representation, we used the density function of the split normal distribution to model the probability of “target yes” responses to each probe color (Figure 2.4A and 2.4B). The split normal distribution was selected because it allows for estimation of asymmetrical standard deviations around the central tendency but reduces to a normal distribution when the estimated standard deviations are equivalent (see below).

The split normal distribution is formed by merging two opposite halves of two probability density functions of a normal distribution at their common mode. Equation 1 gives the probability density function for estimating a split normal distribution (Johnson, Kotz & Balakrishnan, 1994). The distribution takes the left half of normal distribution with parameters (μ, σ_1) and the right half of a normal distribution with parameters (μ, σ_2), and scales them to a common value $f(\mu) = \frac{\sqrt{2\pi}}{\sigma_1 + \sigma_2}$ at the mode, μ. In a special case when $\sigma_1 = \sigma_2$, the split normal distribution reduces to a normal distribution.

$$h(x \mid \mu; \sigma_1; \sigma_2) = \begin{cases} \frac{\sqrt{2\pi}}{\sigma_1 + \sigma_2}\, \mathrm{e}^{-\frac{(x-\mu)^2}{\sigma_1{}^2}}, & if\ x < \mu; \\ \frac{\sqrt{2\pi}}{\sigma_1 + \sigma_2}\, \mathrm{e}^{-\frac{(x-\mu)^2}{\sigma_2{}^2}}, & otherwise. \end{cases} \qquad (1)$$

Because the response for each color in our probe task is independent, the probabilities of responding "yes" to all the colors do not sum to 1. We therefore introduced a subject-specific scaling parameter “a” that scales the distribution from each subject leading to equation 2. An individual who has a small value of “a” is more conservative in responding “yes”; conversely, an individual who has a large value of “a” is more liberal in responding “yes”.

$$f(x \mid a; \mu; \sigma_1; \sigma_2) = a\ h(x \mid \mu; \sigma_1; \sigma_2) \qquad (2)$$

Instead of using a more conventional method for parameter estimation (e.g. maximum likelihood estimation), all parameters were estimated using hierarchal Bayesian analysis (HBA). The hierarchical approach is particularly useful for this study given the small number of data points per subject because it captures commonalities across individuals and at the same time estimates each individual's parameter values (Gelman, et al., 2013). To perform HBA, we used the R package, Rstan (Stan Development Team, 2016).

Normal and half Cauchy distributions were used to set the hyper priors of the normal mean (μ), standard deviations (σ), and free parameter (a) (Equation 3). We used weakly informative prior distributions (Gelman et al., 2013), to avoid biasing the posterior distributions.

$$\begin{aligned} &\mu \sim \text{Normal}\ (0, 15) \\ &\sigma_1, \sigma_2 \sim \text{Cauchy}\ (0, 30) \qquad (3) \\ &a \sim \text{Cauchy}\ (0, 50) \end{aligned}$$

A total of 40000 samples were drawn after 20000 warming-up samples from 8 chains. We estimated individual and group parameters separately for each group ("uni-direction" and "bi-drection" group). Goodness of fit was visually inspected with the posterior predictive check method (Gelman et al., 2013).

The mode value (μ) reflects the central tendency of the target template. Non-zero values indicate that the point in color space over which the target template is centered. For the unidirectional group, a positive μ indicates a shift towards the visual search distractor colors and a negative value indicates a shift away from the visual search distractor colors. But for the bidirectional group, a non-zero μ value would not reflect distractor properties because the distractor colors came from the both sides of the target color. Thus, μ serves as the statistical analogue for the magnitude of template shifting. The sigma values (σ) reflect the dispersion of the target template. Therefore, σ_1 (subsequently referred as σ_{neg} in reference to the color stimulus space, see above) characterizes the width of the template over "negative" color values; and σ_2 (σ_{pos}) represents the width of the template over "positive" colors. Recall that negative colors were never seen as distractors during visual search in the unidirectional group, but appeared as distractors in the bidirectional group.

In addition to modeling the “target yes” responses with the split-normal distribution, we also directly compared the false alarm rates between the negative and positive non-target colors. This analysis is complementary to the analysis of in σ_{neg} and σ_{pos} from the split-normal distribution. However, in contrast to σ_{neg} and σ_{pos}, which are estimated in conjunction with μ, the raw false alarm rates are not related to estimations of central tendency and therefore are a more direct approximation of the likelihood of mistaking a non-target color as the target color. The “target yes” data are analyzed using ANOVA and posthoc analyses are always corrected for multiple comparisons using the Bonferonni method.

Finally, in addition to null hypothesis testing, we also computed Bayes factors (BF) (Rouder et al., 2009) for all student-t statistical analyses using BayesFactor package in r (Morey, Rouder & Jamil, 2015). The BF is a statistical index of the evidence the data provides for either the null or the alternative hypothesis. BF values in favor of the null hypothesis are denoted as BF_{01} and for the alternative as BF_{10}. It is important to note that these methods for estimating the underlying template likely reflect aggregate sensory and decisional mechanisms involved at various stages of processing (e.g., Smith & Ratcliff, 2009).

Results

The template probe trials asked subjects to indicate whether a particular colored stimulus was the target, or not. Although the proportion of "target yes" responses were independent for each color probed, we hypothesized that the responses reflect the "tuning" of the underlying target template. In order to recover the tuning profile of the template, the target probe data were first modeled with the split-normal distribution (see Methods above, Figure 2.4A and 2.4B), which estimates template tuning use estimated μ, σ_{neg} and σ_{pos} values. However, because σ_{neg} and σ_{pos} are estimated relative to μ, we conduct a second complementary analysis of the raw false alarm rates, which are an unbiased estimate of the likelihood of mistaking colors as the target.

Modeling the target template with the split normal distribution. To determine if there was a difference in the shift in central tendency of the template between groups, the μ values were compared using an independent sample t test. The difference was significant, *t*(38) = -5.29, *p* <.001, *d* = -1.67, BF_{10} = 2,814.47, indicating that the μ value for the unidirectional group was more negative than the bidirectional group. Additionally, the μ values from each group were compared against 0° (the veridical target feature). The μ values of both groups were significantly different from 0°, but only the unidirectional group's μ was negatively shifted1 (*M* = -3.64°, *sd* = 3.38°): *t*(19) = -4.82, *p* < .001, *d* =-1.08, BF_{10} = 240.52. The bidirectional group value was positively shifted (*M* = .94°, *sd* = 1.90°): *t*(19) = 2.22, *p* = .04, *d* = .50, BF_{10} = 1.69), although the evidence based on

---

[1] In order to determine whether or not the bidirectional probe trials changed the target representation over time, we compared the unidirectional group probe performance in the first half and second half of the experiment. A paired sample t test showed that the μ values did not differ between the first half and second half block, *t*(19) = -.71, *p* = .49, *d* = -.16, BF_{01} = 3.43. This indicates that the degree of template shifting in the two halves of the experiment was equivalent. We then conducted a two-way ANOVA with factors block and color direction on standard deviations. The results showed a significant main effect of color direction, *F*(1, 19) = 8.90, *p* = .008, η_p^2 = .32, a non-significant main effect of block, *F*(1, 19) = .04, *p* = .85, η_p^2 = .008, and a non-significant interaction *F*(1, 19) = .15, *p* = .70, η_p^2 = .002. This replicates the sharpening effect and shows no difference between the first and second halves of the experiment.

Cohen's d and the BF was relatively weak (cf. $BF_{10} = 240.52$ for the unidirectional group). The results[2] indicate that the unidirectional group shifted their target representation away from the distractor.

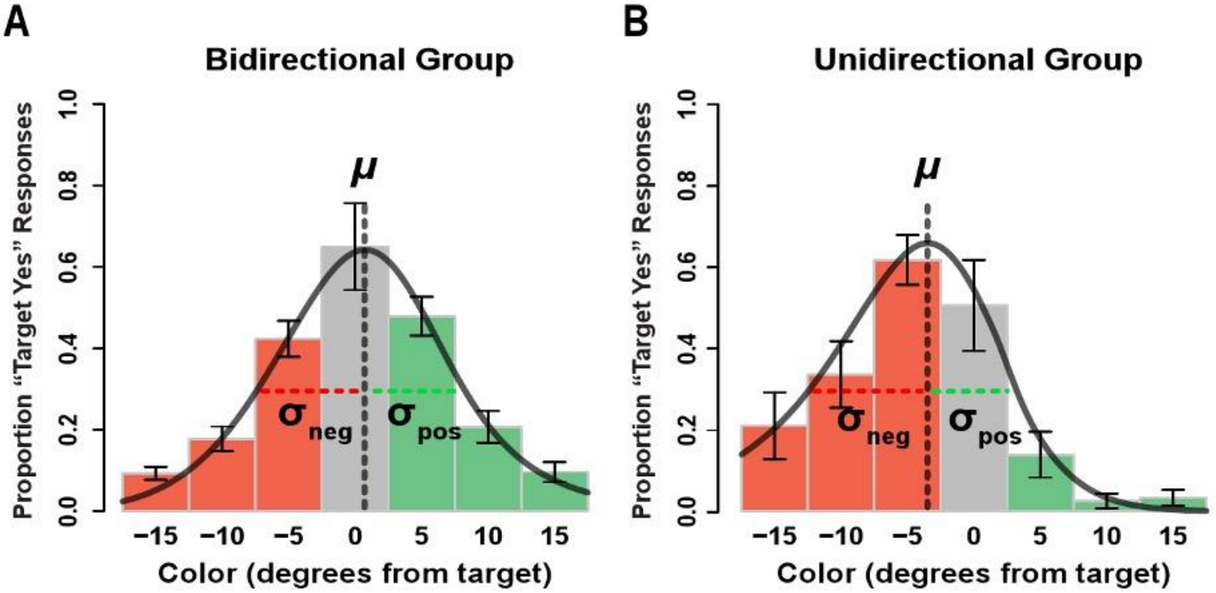

Figure 2.4. Group averages of "target yes" responses in Experiment 1. Black solid lines are split normal distribution fits. The center gray bar indicates proportion of "hits" in response to the true target color and other bars indicate "false alarms" to non-target colors. All error bars are SEM. A) The bidirectional group. Both negative and positive colors were distractors during visual search trials. B) The unidirectional group. Only positive colors (green bars) were seen as distractors during visual search trials.

---

[2] One might wonder if these results can be attributed to the fact that the unidirectional group experienced twice as many as 5°, 10° and 15° distractor set trials than the bidirectional group. To address this we compared performance from the first half of the experiment in the unidirectional group with performance across the whole experiment in the bidirectional group. Doing so equates the number of 5°, 10° and 15° distractors seen by observers in each group. An independent sample t test showed that the two groups had significantly different μ values, $t(19) = -5.38$, $p < .001$, $d = -1.70$, $BF_{10} = 3{,}592.45$, which is a replication of main result. Similarly, the two way ANOVA with group and color direction as factors on standard deviations showed exactly the same results as in the main text: Namely, there was a significant main effect of color direction, $F(1, 19) = 7.62$, $p = .009$, $\eta_p^2 = .17$, a non-significant main effect of group, $F(1, 19) = 1.42$, $p = .24$, $\eta_p^2 = .04$, and a marginally significant interaction $F(1, 19) = 3.67$, $p = .06$, $\eta_p^2 = .09$. Post hoc t tests found that the unidirectional group had a significantly larger σ_{neg} than σ_{pos} values, $t(19) = 2.96$, $p = .008$, $d = .66$, $BF_{10} = 6.13$. In contrast, there was no statistical difference between σ_{neg} and σ_{pos} in the bidirectional group, $t(19) = .69$, $p = .50$, $d = .15$, $BF_{01} = 3.48$.

Next, the σ values were entered into a 2 color direction (negative, positive) x 2 group (unidirectional, bidirectional) ANOVA. There was a significant main effect of color direction, $F(1, 38) = 7.29$, $p = .01$, $\eta_p^2 = .16$, a marginally significant main effect of group, $F(1, 38) = 3.23$, $p = .08$, $\eta_p^2 = .08$, and a marginally significant interaction, $F(1, 38) = 3.17$, $p = .08$, $\eta_p^2 = .07$. The main effect of color direction was due to larger σ_{neg} than σ_{pos} values overall. Although the interaction between groups was only marginally significant, our *priori* hypothesis was that there would be asymmetrical sharpening in the unidirectional group, but not the bidirectional group. We therefore additionally conducted simple effects t tests along with BF to compare σ values for color direction differences in each group. The paired sample t tests showed that the unidirectional group had a significantly larger σ_{neg} than σ_{pos} values, $t(19) = 3.01$, $p = .007$, $d = .67$, $BF_{10} = 6.71$. In contrast, there was no statistical difference between σ_{neg} and σ_{pos} in the bidirectional group, $t(19) = .69$, $p = .50$, $d = .15$, $BF_{01} = 3.48$. Thus, while the BF in the unidirectional group indicates that the data provides 6.71 times more evidence for the *alternative* hypothesis than the null hypothesis, the BF in the bidirectional group indicates that the data are 3.48 times more likely if the *null* hypothesis is true than the alternative. Together, these results are consistent with asymmetrical sharpening in the the unidirectional group, but not the bidirectionalal group; however, the results must be interpreted with caution given the marginally significant interaction in the ANOVA.

Analysis of false alarm rates. Unlike σ values which are influenced by estimates of μ, we turn next to the raw false alarm data as a more direct measurement of which non-target colors were mistaken as the target color. The false alarm rates of non-target colors during the identification task (Figure 2.5A) were entered into a 2X2 ANOVA to test for differences between color direction (negative, positive) and group (unidirectional, bidirectional). There was a significant main effect of color direction, $F(1, 38) = 23.55$, $p < .001$, $\eta_p^2 = .38$, a nonsignificant effect of group, $F(1, 38) = .07$, $p = .79$, $\eta_p^2 = .002$, as well as a significant interaction, $F(1, 38) = 38.07$, $p < .001$, $\eta_p^2 = .51$. Post-hoc t-tests, corrected for multiple comparisons, indicated the unidirectional group had significantly more false alarms to negative colors compared to positive colors, $t(19) = 8.09$, $p < .001$, $d = 1.81$, BF_{10} = 108,165.60, whereas the bidirectional group had similar false alarm rates for colors in both directions, $t(19) = -.96$, $p = 1$, $d = -.21$, $BF_{01} = 2.86$. Additionally, the unidirectional group had higher false alarm rates for negative colors than the bidirectional group, $t(38) = 3.99$, $p = .001$, $d = 1.26$, $BF_{10} = 86.77$, but the bidirectional group had higher false rates for positive colors, $t(38) = -5.53$, $p < .001$, $d = -1.75$, BF_{10} = 5,559.68). These results strongly support the hypothesis that asymmetrical sharpening occurs when highly similar visual search distractors that are linearly separable from the target and can be expected from trial-to-trial, but not when distractor sets from both sides of the target color alternate between trials.

Visual search performance. Having established that the target template in the unidirectional group was shifted and asymmetrically sharpened, we next assessed visual search performance. Recall that stimuli were identical in the unidirectional and bidirectional groups, except that only one of the two distractor color sets were used for a given participant in the unidirectional group whereas distractor sets were randomly interleaved trial-by-trial in the bidirectional group. Accuracy (Figure 2.5B) and reaction time (RT, Figure 2.5C) from the visual search trials were entered into between-groups t tests. Only RT data from correct trials were included in these analyses. The results show that the unidirectional group (*M* = 91%, *sd* = 6%) had significantly higher accuracy than the bidirectional group (*M* = 63%, *sd* = 12%), *t*(38) = 9.06, *p* < .001, *d* = 2.86, BF_{10} = 119,350,885. The unidirectional group (*M* = 841ms, *sd* = 154ms) also had significantly shorter RTs than the bidirectional group (*M* = 1021ms, *sd* = 137ms), *t*(38) = -3.90, *p* < .001, *d* = 1.23, BF_{10} = 69.17. The unidirectional group accuracy was on average more than 25% greater than the bidirectional group and RTs more than 150ms shorter. The big difference in performance indicates that being able to shift and sharpen the target representation away from expected distractors effectively increased the psychological distinctiveness of the target from distractors and enhanced performance substantially.

In addition, to compare performance between groups, we investigated the effect of repetition in distractor color set in the bidirectional group. If learned expectations contribute to changes in the attentional template and better visual search performance, we might expect chance repetitions to also produce smaller advantages. In other words, we expected that subjects would have better performance on “repeat” trials when distractors are the same as the N-1 trial than on “switch” trials, when the distractor set is opposite from the N-1 trial. A paired sample t test showed that the accuracy of distractor repeat trials (*M* = 67%, *sd* = 13%) was significantly higher than the accuracy of distractor switch trials (*M* = 61%, *sd* = 12%), *t*(19) = 4.03, *p* < .001, *d* = .90, BF_{10} = 48.78. Similarly, RT of distractor repeat trials (*M* = 943ms, *sd* = 133ms) was shorter than distractor switch trials (*M* = 1116ms, *sd* = 155ms), *t*(19) = -6.86, *p* < .001, *d* = -1.53, BF_{10} = 12,272.99. This suggests that repeated exposures to the same distractor set helps facilitate visual search and that learned expectations about distractor context over longer periods of time might build upon mechanisms of repetition priming.

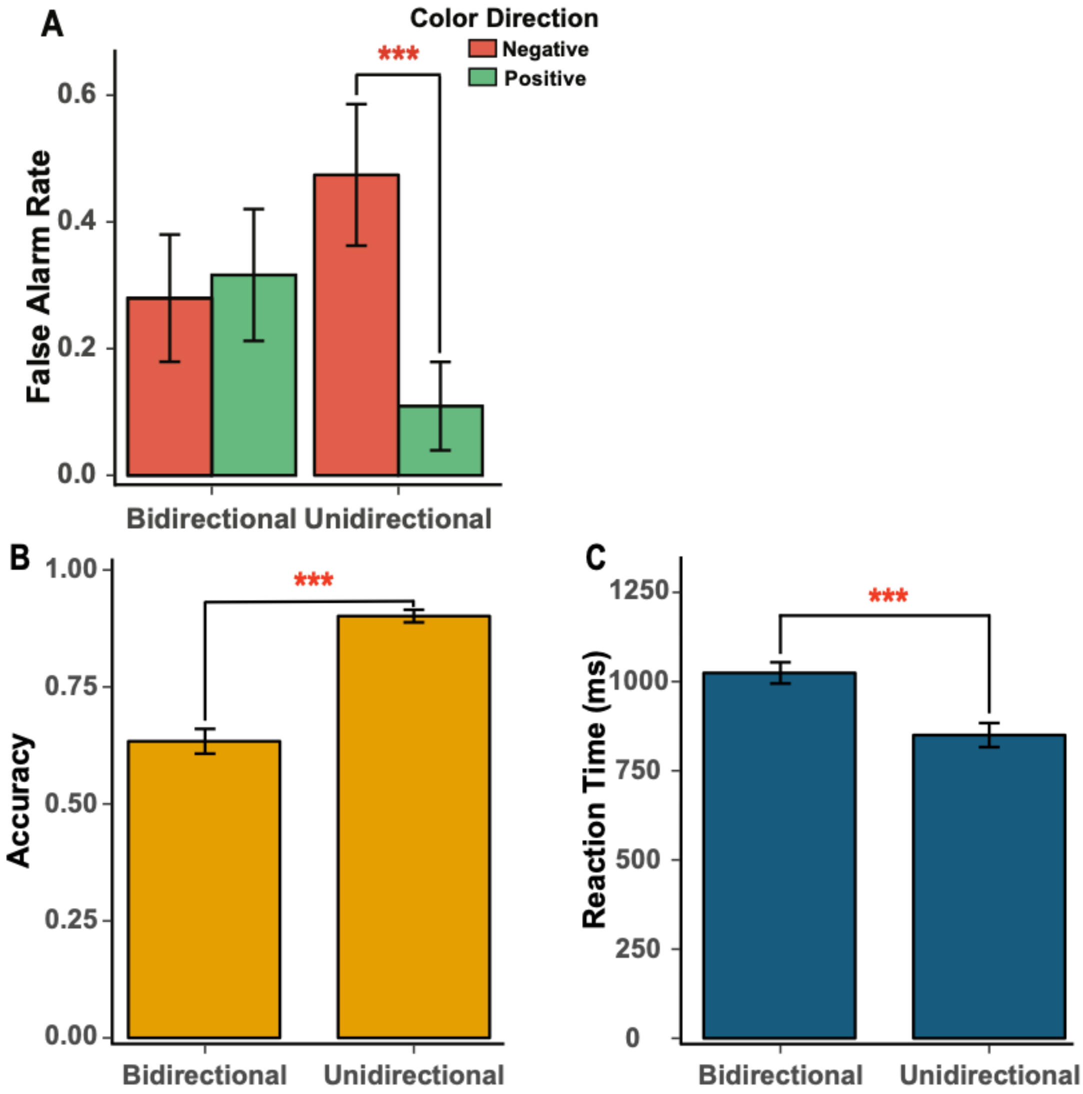

Figure 2.5. A) False alarm rates collapsed across color degree for each group and color direction in Experiment 1. B) Visual search accuracy for each group. C) Reaction times for each group in visual search task. All error bars are SEM.

Discussion

The goal of Experiment 1 was to test the hypotheses that the target representation held in the attentional template is shifted and asymmetrically sharpened away from distractors that are expected to be linearly separable and highly target-similar. Observers were either exposed to only a linearly separable distractor set during visual search “training” trials, or distractor sets from both sides of the target color that varied from tiral-to-trial. On separate “probe” trials that were identical between groups, we found evidence that the unilateral group shifted the central tendency of the target representation away from distractors and sharpened the boundary between the target and distractors. Additionally, performance on the visual search task was substantially better in the unidirectional group, suggesting that shifting and sharpening are attentional mechanisms that increase the psychological distance between targets and highly similar distractors and aid search efficiency. This establishes a clear link between the contents of the target template and visual search performance.

Experiment 2

Experiment 1 supported that hypothesis that the unidirectionality of target-similar distractors adjusted the shape of the target template. However, the experiment did not address whether shifting and sharpening are separable mechanisms that respond to different aspects of distractor expectations. To address this in Experiment 2, we manipulated the *strength of distractor competition*, defined by the target-to-distractor similarity across blocks while holding the linear separability of all distractors constant. We hypothesized that shifting would occur in response to the overall separability of the distractor set and therefore stay constant across blocks, but that sharpening would change with the strength in competitive pressure from distractors and increase over blocks.

Method

Participants. Twenty new UC Davis undergraduates (7 males, 3 left-handed, ages 19-27) participated in Experiment 2. Each provided written informed consent in accordance with the local ethics clearance as approved by the Nation Institutes of Health. Color vision was assessed through self-report and an online color blindness test (https://colormax.org/color-blind-test). All had normal or corrected-to-normal visual acuity and color vision.

Design. The experimental design was the same as the unidirectional group in Experiment 1, with the following exceptions: There were five distractor color sets manipulated over five sequential blocks (Figure 2.6). The first distractor color set in block 1 was composed of three identical gray distractors (average across LAB color space, 67.4 cd/m^2), which served as a baseline condition. Distractors in the remaining four blocks increased in similarity to the target: (60°, 55°, 50°) in block 2, (45°, 40°, 35°) in block 3, (30°, 25°, 20°) in block 4, and (15°, 10°, 5°) in block 5. As before, each of the three different distractor colors in each set were present in each visual search display. Distractor color (negative or positive rotations from the target color) was counterbalanced across subjects. As in Experiment 1, there were no spurious differences based on counterbalancing of target and distractor colors (*ps* > .39), so the data were collapsed in all subsequent analyses. Consistent with our labeling convention in Experiment 1, the distractors from the visual search trials (i.e., "trained" distractor colors) are always referred to as being “positive” rotations from the target (i.e., 5°, 10°, 15°) and the colors that appeared only in the template probe trials (i.e. "untrained" colors) are labeled as “negative” values from the target (i.e., -5°, -10°, -15°). The template probe task was identical to the one in the Experiment 1 and remained the same across five blocks. Recall that the colors in the probe task included the target color (color 0°), and the -5°, -10° -15, 5°, 10° and 15° color rotations from the target.

Procedure. The procedure of Experiment 2 was identical to Experiment 1, except for the additional factor of target-distractor similarity, which increased in 5 blocks over the experiment (Figure 2.6). The order of the 5 blocks was held constant moving from blocks with dissimilar distractors to those with greatest distractor similarity so as to avoid possible carry-over effects in learning about the strength of competition. The session began with 32 practice trials composed of both visual search and template probe trials. Each block contained 112 visual search training trials and 112 probe trials. Each block began with 4 alternations of 10 visual search training trials and 7 probe trials followed by 12 alternations of 6 visual search training and 7 probe trials. As in Experiment 1, this design was created to maximize the number of template probe trials with periodic visual search training.

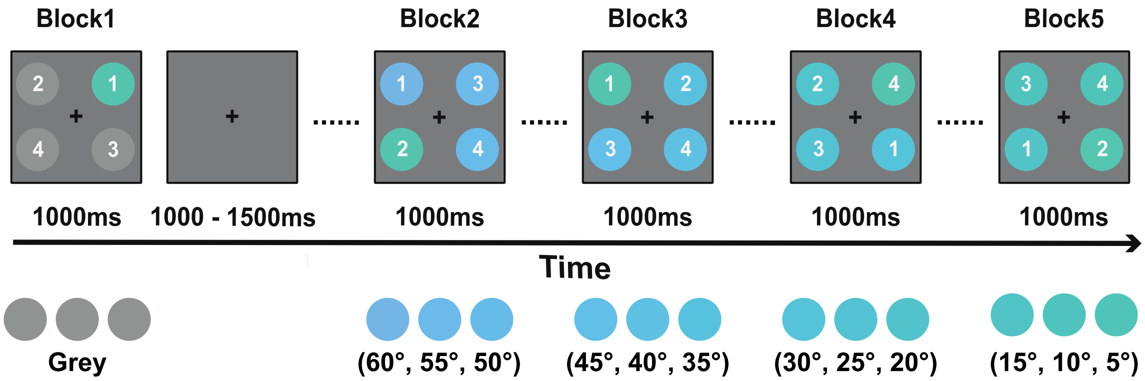

Figure 2.6. Visual search task design in Experiment 2. One visual search trial for each block is shown here to illustrate the increase in target-to-distractor similarity over blocks. The template probe task was identical to that in Experiment 1 (Figure 2.3B). See Methods for color values.

Results

Modeling the target template with the split normal distribution. Following the analysis strategy from Experiment 1, we fitted the likelihood of “target yes” responses with a split normal distribution for each person and block in order to estimate the central tendency and variance of the “tuning” of the target template (Figure 2.7). The μ values (Figure 2.8A) were then entered into a one-way ANOVA with the factor block (1-5). There was a significant main effect of block, $F(4, 76) = 6.65$, $p < .001$, $\eta_p^2 = .26$. We then measured the difference in μ values between two consecutive blocks using post-hoc t tests (Bonferroni corrected for multiple comparisons). Consistent with visual inspection of the data (Figure 2.8A), the only significant difference was between block 1 ($M = 0.42°$, $sd = 2.97°$) and block 2 ($M = -2.13°$, $sd = 3.10°$), $t(19) = 3.32$, $p = .01$, $d = .74$, $BF_{10} = 12.04$; all other *ts* < 1.54, *ps* > .56, *ds* < .34, $BF_{01} > 1.56$. Specifically, there was a negative shift in μ in block 2 when colored distractors were introduced and this shift was sustained in all remaining blocks, suggesting that the target template shifted as soon as linearly separable distractors were introduced and that the magnitude of the shift did not change with increases in distractor competition (i.e., distractor similarity) over blocks.

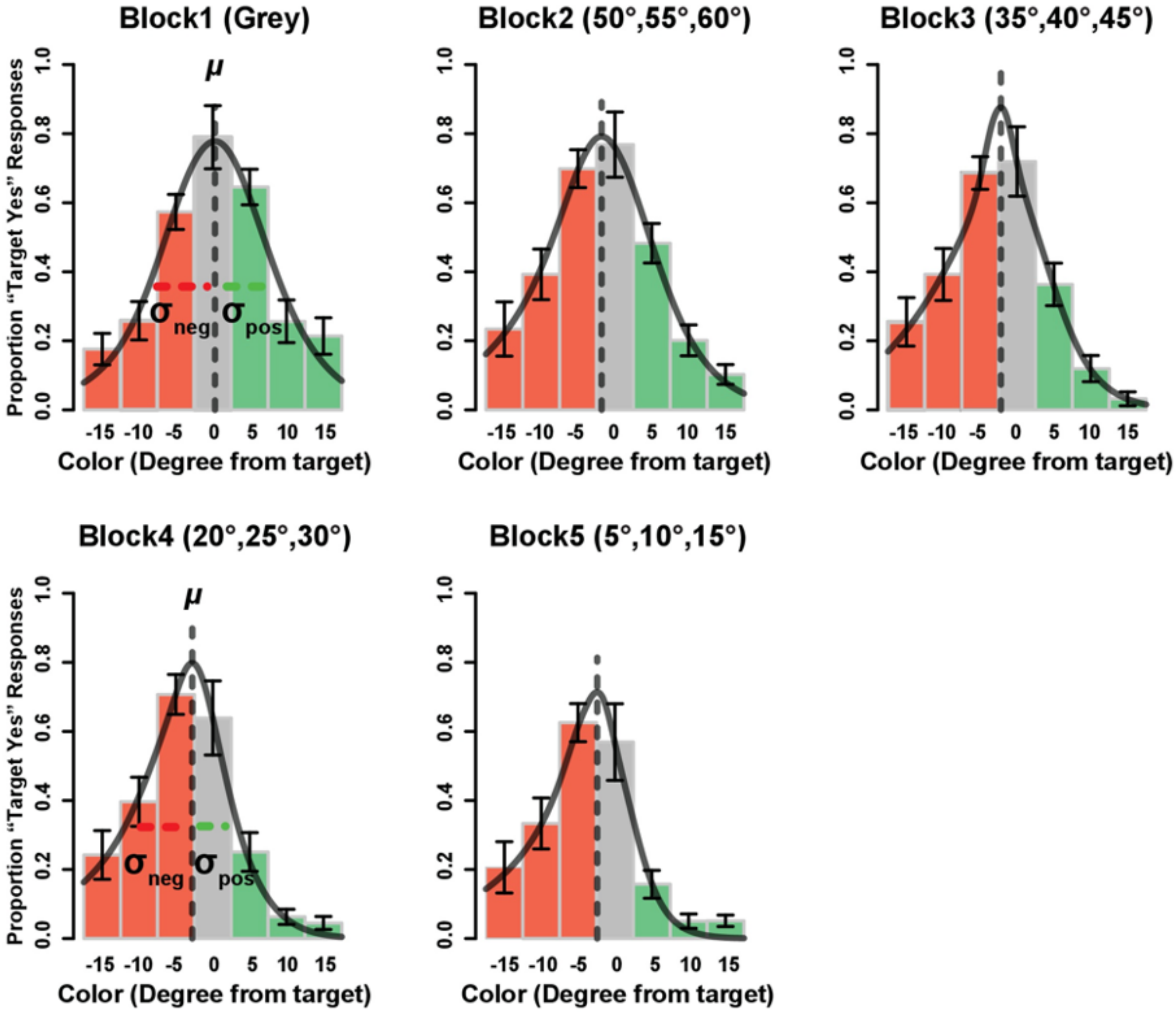

Figure 2.7. Group averages of "target yes" responses for each block in Experiment 2. Black solids lines are split normal distribution fits. The center gray bar indicates the true target color. All error bars are SEM.

Next, we examined changes in σ_{neg} and σ_{pos} as a function of block (Figure 2.8B). An ANOVA with block (1-5) and color direction (negative, positive) as factors yielded a significant main effect of block, $F(4, 76) = 5.16$, $p < .001$, $\eta_p^2 = .21$, a significant main effect of color direction, $F(1, 19) = 9.43$, $p = .006$, $\eta_p^2 = .33$, as well as a significant interaction, $F(4, 76) = 8.19$, $p < .001$, $\eta_p^2 = .30$. The interaction was due to a linear decrease in σ_{pos} over blocks, but no change in σ_{neg} over blocks (Figure 2.8B). To confirm this, slope values were calculated as a summary value of how σ changed over blocks. We found a significant negative slope for σ_{pos}, *t*(19) = -7.95, *p* < .001, *d* = -1.78, BF_{10} = 84,968.52, but a non-significant slope for σ_{neg}, *t*(19) = .36, *p* = .73, *d* = .08, BF_{01} = 4.06. These results demonstrate that the positive half of the target template was selectively sharpened over blocks to counteract competition from highly similar distractors, while the width of tuning over the negative half did not change. This indicates that asymmetrical template sharpening occurs selectively in response to distractor competition and not just distractor color directionality, but lateral shift in the target template occurs in response to color directionality and is insensitive to similarity.

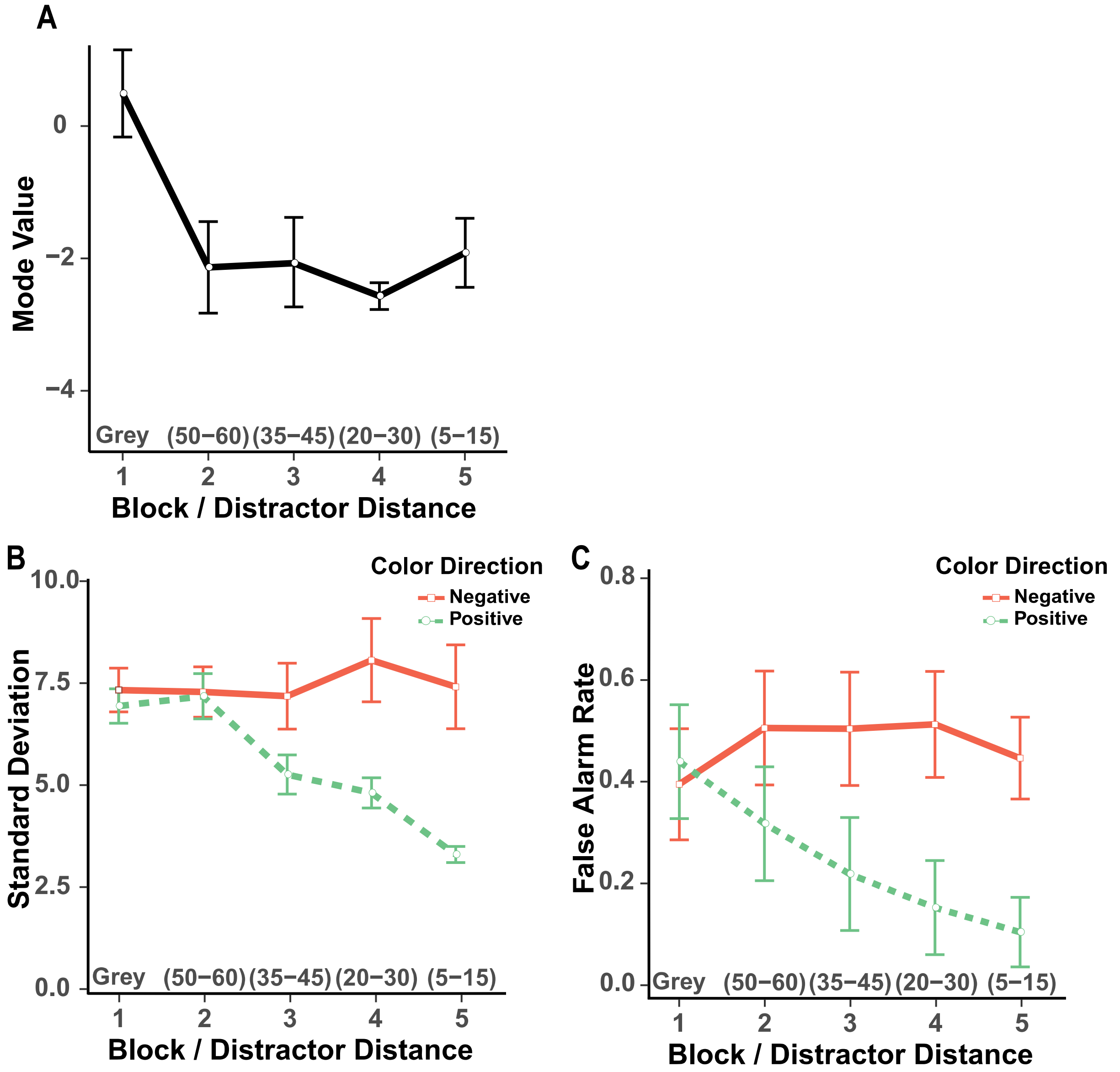

Figure 2.8. Model fits and false alarm rates from the template probe task in Experiment 2. A) Mode values estimated from the split normal distribution. B) Standard deviation of each color direction estimated from the split normal distribution. C) False alarm rates to negative and positive non-target color probes. All error bars are SEM.

Analysis of the false alarm rate. The raw false alarm rates for negative and positive non-target colors were entered into a 2 color direction (negative, positive) x 5 block (1-5) repeated measures ANOVA (Figure 2.8C). Recall that the raw false alarm rates are not related to estimations of central tendency and are a direct likelihood of mistaking a non-target color as the target. There was a significant main effect of color direction, *F*(1, 19)

= 20.29, $p < .001$, $\eta_p^2 = .52$, a significant main effect of block, $F(4, 76) = 9.66$, $p < .001$, $\eta_p^2 = .34$, and a significant interaction, $F(4, 76) = 9.57$, $p < .001$, $\eta_p^2 = .34$. Similar to the analyses of σneg and σpos, the interaction was due to a linear decrease in positive false alarm rates over blocks, but no change in negative false alarm rates over blocks (Figure 2.8C). To confirm this, slope values were calculated as a summary value of how false alarm rates changed over blocks. We found a significant negative slope for σ_{pos}, $t(19) = -7.63$, $p < .001$, $d = -1.71$, $BF_{10} = 48,801.63$, but a non-significant slope for σ_{neg}, $t(19) = .67$, $p = .51$, $d = .15$, $BF_{01} = 3.52$. These results were consistent with standard deviation results, suggesting asymmetrical template sharpening in response to distractor competition.

Visual search performance across blocks. The previous results demonstrate that the representation of the target color changed across blocks in response to the visual search context. Next, to understand how the increasingly asymmetrical template relates to search performance, we analyzed search accuracy (Figure 2.9A) and RT (Figure 2.9B) using two one-way ANOVAs with block as a within-subject factor. Both accuracy, $F(4, 76) = 23.95$, $p < .001$, $\eta_p^2 = .56$, and RT, $F(4, 76) = 50.87$, $p < .001$, $\eta_p^2 = .73$, were significant. The results were due to poorer performance in block 5 compared to any other block (Figure 2.9), post hoc t-tests comparing block 5 with all other blocks (accuracy: all *ts* < -4.88, *ps* < .005, *ds* < -1.00, (BF_{10})s > 270; RT: all *ts* > 8.14, *ps* < .001, *ds* > 1.82, (BF_{10})s > 118,707; RT was also longer in block 2 than block 3, $t(19) = 4.76$, $p = .001$, $d = 1.06$, $BF_{10} = 210.18$). Visual search performance was consistently at ceiling until block 5, when distractor competition was strongest. This suggests that changes in the target template were sufficient to maintain performance at ceiling over increases in distractor similarity for the first four blocks, but competition was sufficiently strong in block 5 that an increase in template sharpening was no longer able to fully exclude highly similar distractors.

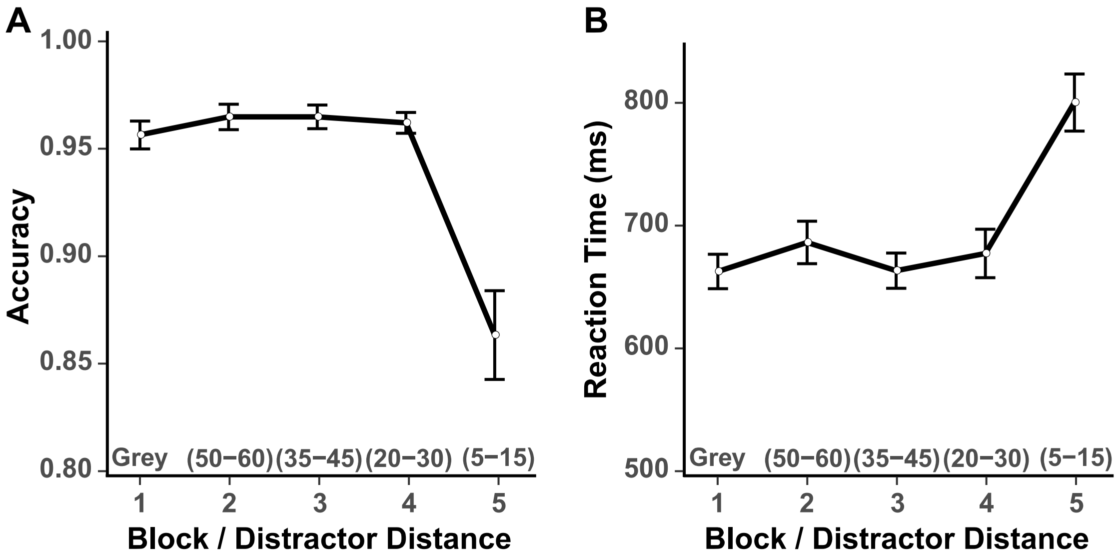

Figure 2.9. Experiment 2 A) visual search accuracy and B) reaction time. All error bars are SEM.

Discussion

The goal of Experiment 2 was to test whether the shifted central tendency and asymmetrical sharpening of target template identified in Experiment 1 were due to different distractor properties during visual search. The results demonstrated that the shift in central tendency occurred in response to the distractor set being linearly separable from the target, but was not sensitive to changes in target-to-distractor similarity. In contrast, asymmetrical sharpening, seen in the exclusion of positive (but not negative) non-target colors within the target template, was continuously updated as distractor similarity increased. This suggests that distractor competition dynamically sharpened the representational boundary between the target and the distractors in order to better exclude highly similar distractors. Together, the results suggest that shifting and sharpening of the target template occur in response to different distractor properties to maximize the ability to distinguish target from distractors during visual search.

Experiment 3

Experiment 2 provided evidence that shifting and sharpening are separate mechanisms to optimize the target template for visual search within predictable distractor contexts. However, it is possible that the continuous asymmetrical sharpening seen in Experiment 2 was not due to increases in distractor competition (as we concluded), but simply due to practice over time. In order to rule out this alternative hypothesis, Experiment 3 was identical to Experiment 2 (5 blocks of equal duration), but only the most dissimilar distractor set was used (identical to block 2 in Experiment 2).

Method

Participants. Twenty new UC Davis undergraduates (4 males, 1 left-handed, ages 18-27) participated in Experiment 2. Each provided written informed consent in accordance with the local ethics clearance as approved by the National Institutes of Health. Color vision was self-reported and assessed with an online color blindness test (https://colormax.org/color-blind-test). All had normal or corrected-to-normal visual acuity and color vision.

Design & Procedure. All stimuli and procedures were identical to Experiment 2, with one exception: The distractor set was identical in blocks 2-5 (Figure 2.10), (i.e., 60°, 55°, and 50° from the target color; identical to block 2 of Experiment 2). The two directions of distractors and two target colors were again counterbalanced across subjects and because there were no spurious differences (*ps* > .17), the data were collapsed in all subsequent analyses, with “negative” colors referring to colors that were not seen during visual search and “positive” colors referring to values seen as distractors during visual search. The template probe trials were identical to those in Experiment 2.

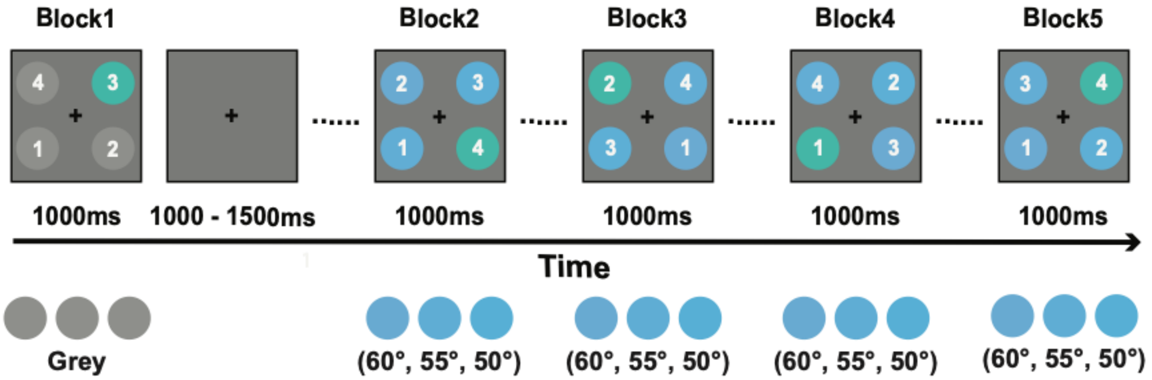

Figure 2.10. Visual search task design in Experiment 3. One visual search trial for each block is shown here to illustrate that the target-distractor similarity remained constant in blocks 2-5. The template probe task was identical to Experiment 1 (Figure 2.3B). See Methods for color values.

Results

Modeling the target template with the split normal distribution. Consistent with the previous experiments, the likelihood of “target yes” responses were fit by a split normal distribution for each person and each block (Figure 2.11). We found a significant main effect of block on μ values, $F(4, 76) = 3.08$, $p = .02$, $\eta_p^2 = .14$ (Figure 2.12A). We then measured the difference in μ values between two consecutive blocks using post-hoc t tests (Bonferroni corrected for multiple comparisons). The main effect was driven by a significant difference between block 1 ($M = -.32°$, $sd = 2.84°$) and block 2 ($M = -2.10°$, $sd = 2.91°$), $t(19) = 2.91$, $p = .04$, $d = .65$, $BF_{10} = 5.63$, which replicates Experiment 2. The central tendency of the target representation shifted away from visual search distractor colors once they appeared in block 2 following the all gray distractor control condition. Moreover, the μ values remained constant over block 2-5, suggesting that the magnitude of shift was not affected by practice over time.

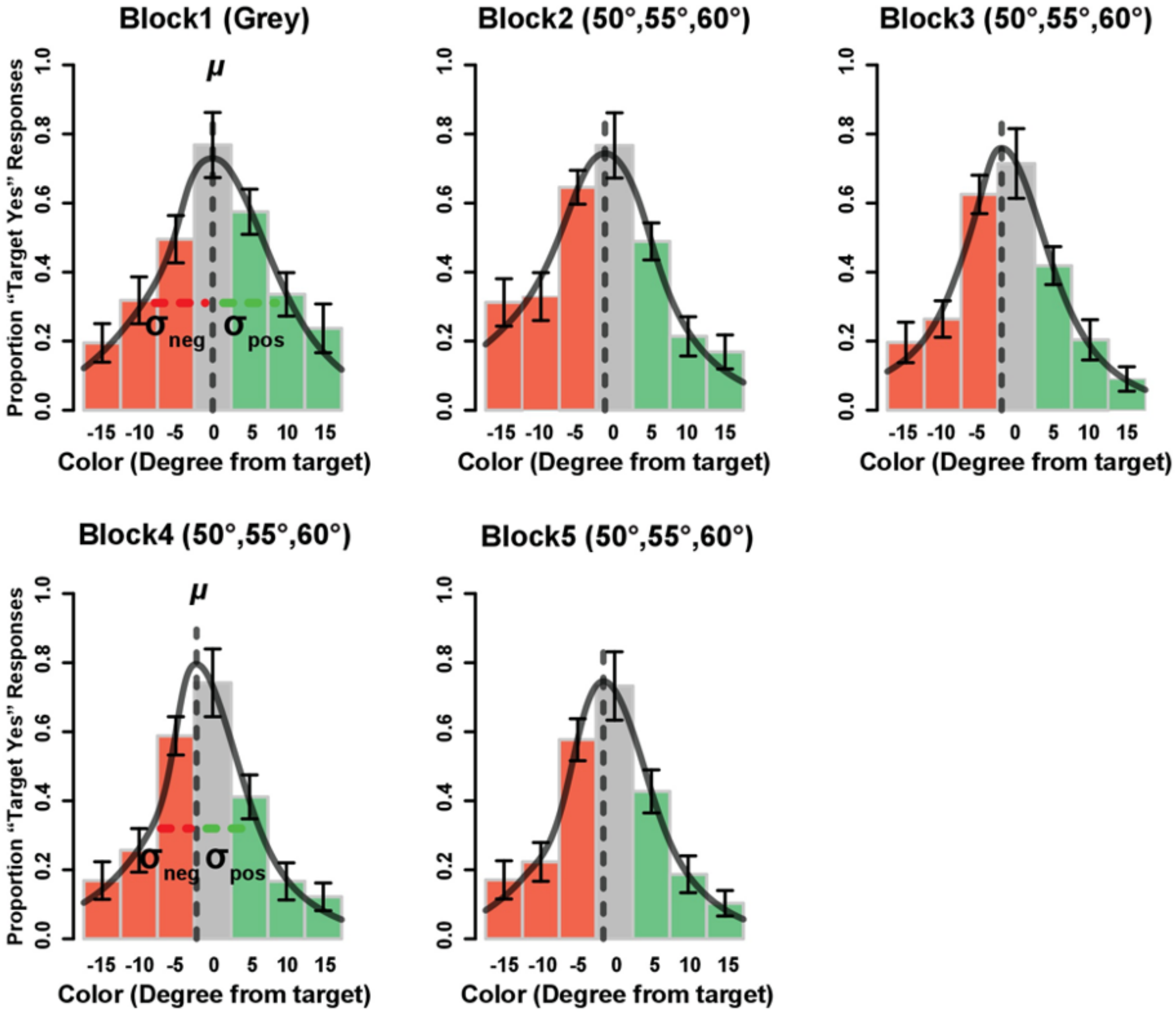

Figure 2.11. Group averages of "target yes" responses for each block in Experiment 3. Black solids lines are split normal distribution fits. The center gray bar indicates the true target color. All error bars are SEM.

Additionally, we conducted a two-way ANOVA with factors block (1-5) and experiment (Experiment 2, Experiment 3) to assess if there is between experiment differences for μ values. The results yielded a significant main effect of block, *F*(4, 152) =

9.38, $p < .001$, $\eta_p^2 = .20$, a non-significant main effect of experiment, $F(1, 38) = .005$, $p = .95$, $\eta_p^2 = 0$ and a non-significant interaction, $F(4, 152) = .50$, $p = .74$, $\eta_p^2 = .01$. The lack of between experiment differences suggest that the magnitude of shift was insensitive to specific distractor feature values, and only sensitive to the directionality of the entire distractor feature space.

Next, we analyzed σ_{neg} and σ_{pos} values as a function of block (Figure 2.12B). An ANOVA with color direction (negative, positive) and block (1-5) as factors yielded a non-significant effect of color direction, $F(1, 19) = .18$, $p = .68$, $\eta_p^2 = .009$, a significant main effect of block, $F(4, 76) = 10.13$, $p < .001$, $\eta_p^2 = .35$, and a non-significant interaction, $F(4, 76) = .80$, $p = .53$, $\eta_p^2 = .04$. The lack of a difference between σ_{neg} and σ_{pos} as a function of color direction suggests that asymmetries in template sharpness did not occur simply with practice. This result is evidence against the possibility that changes in σ asymmetry in Experiment 2 were due simply to practice effects.

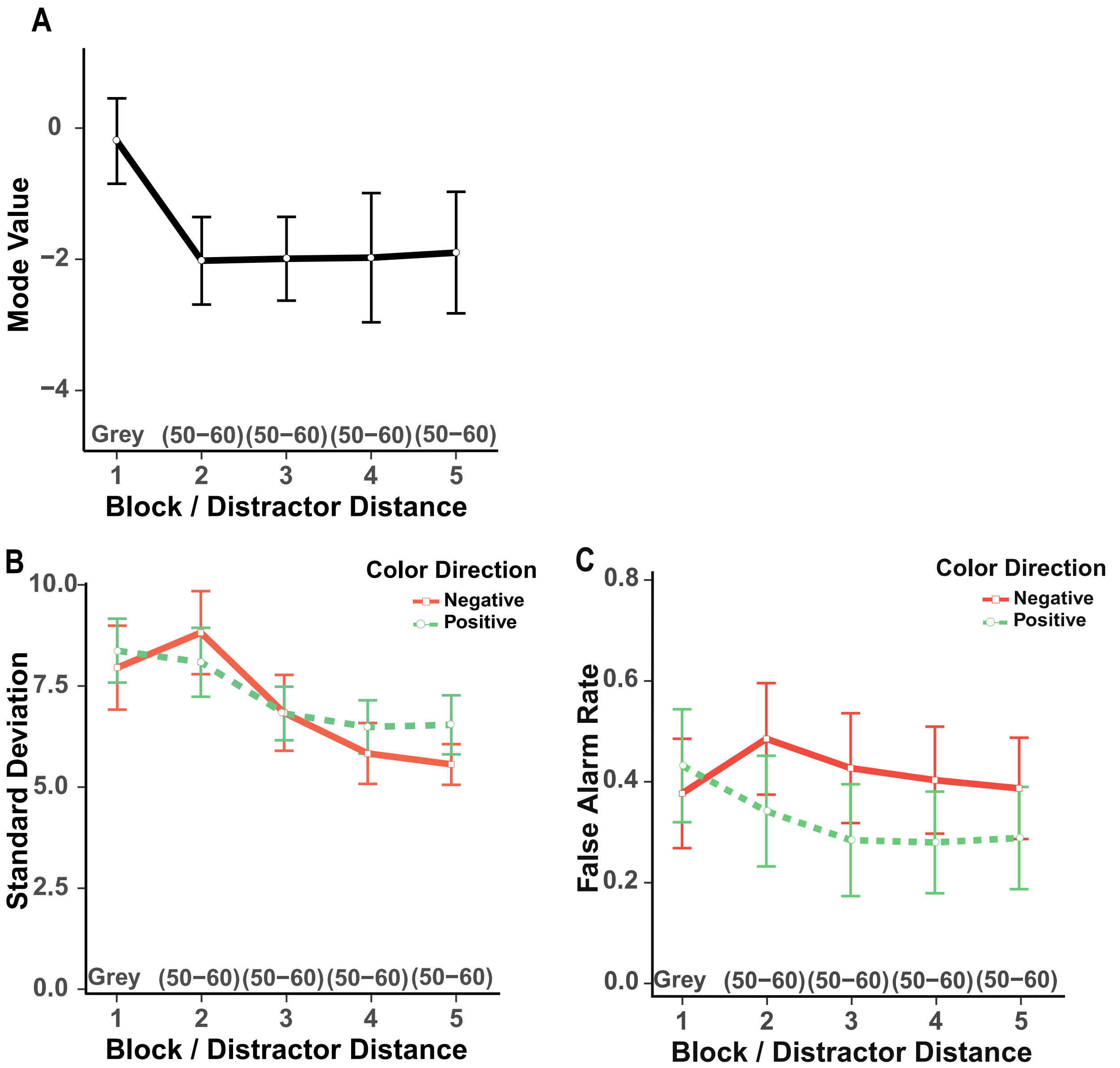

Figure 2.12. Model fits and false alarm rates from the template probe task in Experiment 3. A) Mode values estimated from the split normal distribution. B) Standard deviation of each color direction estimated from the split normal distribution. (C) False alarm rates to negative and positive non-target color probes. All error bars are SEM.

To quantify the apparent difference in results for σ_{neg} and σ_{pos} between experiments, we calculated slope of change in σ values over block for Experiments 2 and 3 (Figure 2.13A). Slope values were calculated as a summary index of how σ changed over blocks. The results yielded a significant main effect of color direction, $F(1, 38) = 4.93$,

p = .03, η_p^2 = .11, no main effect of experiment, F(1, 38) = 1.15, p = .29, η_p^2 = .03, but a significant interaction, F(1, 38) = 12.95, p < .001, η_p^2 = .25. Post hoc t-tests found that for the slope of σ_{pos} values was significantly more negative in Experiment 2 than Experiment 3, t(38) = -2.59, p = .01, d = -.82, BF_{10} = 3.95. However, the opposite pattern was found for the slope of σ_{neg}: the slope was more negative in Experiment 3 than 2, t(38) = -2.34, p = .02, d = -.74, BF_{10} = 2.52. This cross-over interaction indicates that the asymmetry in the width of template tuning found in Experiment 2 was due to the change in the strength of competition during visual search and not practice.

Analysis of the false alarm rate. Similar to Experiment 2, the false alarm rates collapsed across different negative and positive color degrees (Figure 2.12C) were entered into a 2X5 repeated measures ANOVA with factors color direction (negative, positive) and block (1 to 5). There was a significant main effect of block, F(4, 76) = 4.16, p = .004, η_p^2 = .18, a marginally significant main effect of color direction, F(1, 19) = 3.39, p = .08, η_p^2 = .15, and a significant interaction, F(4, 76) = 4.25, p = .003, η_p^2 = .18. The interaction was due to a significant difference between negative and positive colors in block 2 (t(19) = 2.94, p = .042, d = .66, BF_{10} = 5.93), but none others (all ts < 2.5, ps > .10, ds < .56, (BF_{10})s < 2.78). These results converge with those from modeling of the split-normal distribution and suggest that the asymmetry of the template tuning was not systematic and more importantly did not increase steadily over time, as it did in Experiment 2.

Next, to examine differences in asymmetrical sharpening between Experiments 2 and 3, the slope of false alarm rates over block were (Figure 2.13B) entered into a two-way ANOVA with factors color direction (negative, positive) and experiment (Experiment

2, Experiment 3). The results yielded a significant main effect of color direction, *F*(1, 38) = 20.17, $p < .001$, $\eta_p^2 = .35$, a non-significant main effect of experiment, *F*(1, 38) = 2.10, $p = .16$, $\eta_p^2 = .05$, and a significant interaction, *F*(1, 38) = 6.31, $p = .02$, $\eta_p^2 = .14$. Post hoc t-tests found that only the slope of the positive false alarm rates was different between Experiment 2 and Experiment 3, *t*(38) = -3.17, $p = .003$, $d = -1.00$, $BF_{10} = 12.70$, but not the slope of negative false alarm rates, *t*(38) = .95, $p = .35$, $d = .30$, $BF_{01} = 2.27$ (Figure 2.13B). Specifically, the slope of false alarm rates was more negative over positive distractors in Experiment 2, suggesting that the template tuning continued to sharpen with distractor similarity in Experiment 2, but not with just practice in Experiment 3. These results again support the conclusion that the asymmetrical sharpening effect found in Experiment 2 was due to the change in the strength of competition during visual search and not practice.

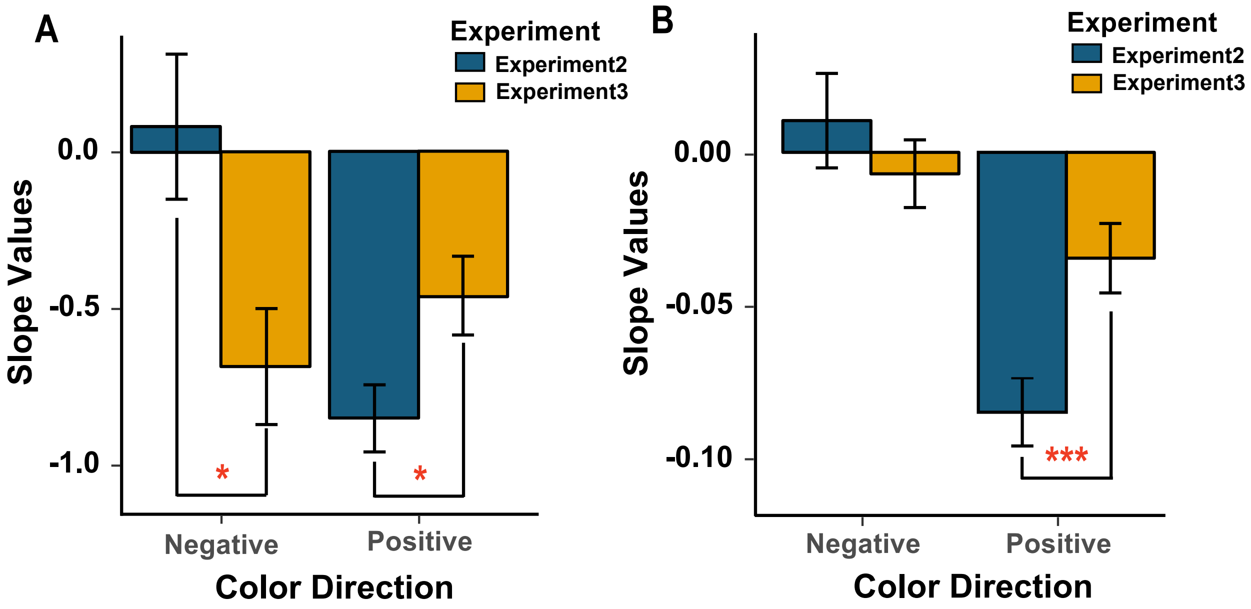

Figure 2.13. Comparison of slope values for model standard deviations and false alarm rates over block for Experiment 2 and 3. A) the slope values for standard deviations in each color direction and each experiment. B) the slope values for false alarm rates in each color direction and each experiment. All error bars are SEM.

Visual search performance across blocks. Visual search accuracy (Figure 2.14A) and RT (Figure 2.14B) were entered into two one-way ANOVAs using block (1-5) as the within subject variable. A significant effect was observed for RT, $F(4, 76) = 2.50$, $p = .05$, $\eta_p^2 = .11$, but not accuracy, $F(4, 76) = .44$, $p = .78$, $\eta_p^2 = .02$. RT was longer in block 2 (M = 682ms) than block 1(M = 661ms), $t(19) = 2.58$, $p_{\text{uncorrected}} = .02$, $p_{\text{corrected}} = .20$, $d = .58$, $BF_{10} = 3.08$. RT was also shorter in block 5 (664ms) than block 2, $t(19) = -2.53$, $p_{\text{uncorrected}} = .02$, $p_{\text{corrected}} = .20$, $d = -.57$, $BF_{10} = 2.84$, and block 4 (671ms), $t(19) = -3.01$, $p_{\text{uncorrected}} = .007$, $p_{\text{corrected}} = .07$, $d = -.67$, $BF_{10} = 6.74$. This indicated that visual search performance improved over blocks, in confirmation of expected practice effects that were independent of stimuli, and in contrast to the decrease in performance in block 5 in Experiment 2.

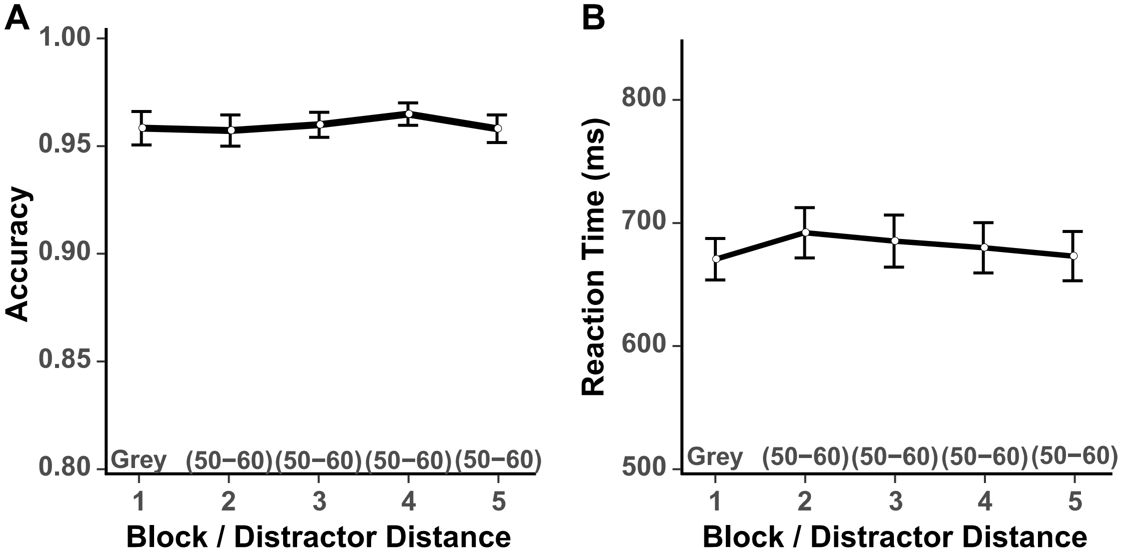

Figure 2.14. Experiment 3 A) visual search accuracy and B) reaction time. All error bars are SEM.

Discussion

The goal of Experiment 3 was to test if the asymmetries in template sharpening seen in Experiment 2 could be due to practice effects over time. However, there was no systematic increase in asymmetrical sharpening over blocks, suggesting that the effects seen in Experiment 2 were due to changes in distractor competition and not time. Moreover, direct analyses of data from the two experiments showed greater asymmetrical sharpening in Experiment 2, consistent with our conclusions that distractor competition, and not practice, is responsible for the degree of asymmetrical sharpening in template representations. Finally, also consistent with findings from Experiment 2, there was a shift in the template central tendency away from distractors that occurred early (block 2) and was sustained throughout the experiment. This suggests that shifts in template representations occur rapidly in response to the directionality of the distractor set, but not specific distractor values.

General Discussion

Theories of visual attention posit that individuals hold target relevant information in an "attentional template" during visual search (Bundesen, 1990; Bundesen, Habekost & Kyllingsbaek, 2005). Recent research has shown that the "tuning" of the attentional template is not always veridical, as previously assumed, and can be *shifted* away from distractors to enhance "off-target" features to increase the distinctiveness of the target representation from distractors (Becker, Folk & Remington, 2010; Becker et al., 2014; Navalpakkahm & Itti, 2007; Scolari, Byers & Serences, 2012; Scolari & Serences, 2009; Soto et al., 2008). It has also been suggested that the template may be asymmetrically sharpened to increase the precision of the boundary between target and distractors (Geng, DiQuattro & Helm, 2017). However, these previous studies have not explored whether different properties of the visual search distractors might independently contribute to template shifting or sharpening. The goal of the current experiments was to address this question. We hypothesized that *shifting* and asymmetrical *sharpening* would occur in response to different qualities of distractor pressure.

We tested this hypothesis in three experiments by separately manipulating distractor directionality (i.e., the overall linear separability of visual search distractors from the target) and the strength of distractor competition (i.e., the similarity of visual search distractors to the target). Importantly, in all experiments, visual search trials were used to “train” the template. The template was then measured by a separate "template probe" task in which participants classified colors as the target or a non-target. Using a separate probe task is necessary to measure the contents of the template, which are presumed to be held in memory (Giesbrecht, Sy, & Guerin, 2012; Woodman, Carlisle, & Reinhart, 2013; Myers et al., 2015), uncontaminated by attentional processes involved in selecting the target from concurrent distractors. This method was first used by Navalpakkam and Itti (2007) (see also Scolari & Serences, 2009) in order to test hypotheses of how expectations for a visual search display adjusts sensory gain.

However, because the attentional template is a memory representation of the target, it does not operate only on sensory processing. There is a long history of work showing that template contents impact processing by modulating sensory processing and by serving as the comparator against which target-match or mismatch decisions are made (Duncan & Humphreys, 1989; Hout & Goldinger, 2015; Wolfe, 2007; Malcom & Henderson, 2010; Smith & Ratcliff, 2009; Geng and Witkowski, under review; Shiu & Pashler, 1984). Therefore, the contents of the template should be expected to affect both sensory processing as well as decisional processes during visual search and our probe task. It is not possible, in our task, to dissociate the effect of the template contents on sensory and decisional processes, but this was not our goal. Instead, our goal was to get a direct measurement of the template without contamination from additional attentional mechanisms involved in target selection and concurrent distractor suppression. Importantly, the template probe task allowed us to do this by interrogating the template contents (in memory) independently from concurrent visual search, which involves additional mechanisms for target selection and distractor suppression.

There were three main findings. First, in all three experiments we found the central tendency of the target representation (i.e., the μ value estimated from modeling the split-normal distribution) was shifted away from the distractor colors. Importantly, the magnitude of this shift was insensitive to the levels of increased distractor competition in our experiments and practice over time. Thus, template shifting appears to occur in response to the entire distractor feature space, but not to specific feature values. This result may superficially appear to be at odds with findings from Scolari and Serences (2009) in which they did not find changes in the sensory template when distractors were very distant. However, their distractors were 90º rotations in orientation from the target and all three distractors were identical, possibly producing some target pop-out. Our distractors were variable, with the most extreme one being on 60º away in color space. It may be that our distractors were never sufficiently different from the target to render shifts in the template completely unnecessary. It remains an open question what specific conditions affect the magnitude of the shift in target representation.

Second, there was an asymmetrical sharpening in the width of the target template in response to the strength of distractor competition. This asymmetry was characterized by differences in the σ_{neg} and σ_{pos} parameters from split-normal distribution modeling as well as direct calculation of the false alarm rates to negative and positive non-target colors. In Experiment 2, we found that asymmetrical sharpening increased with distractor competition, suggesting that sharpening occurs to better exclude highly competitive distractors from erroneous target selection (see also, Geng, DiQuattro & Helm, 2017). Participants appeared to build a more asymmetrically precise template only when it was necessary to counteract pressure from competitive distractors. This gradual increase in sharpening suggests that there could be a potential carry over effect if we randomized distractor similarity in Experiment 2. Future work will be necessary to test how rapidly templates are updated in response to changes in distractor competition. Together, these results suggest that asymmetrical sharpening may be more effortful and is only used when necessary to increase the distance between the target and expected distractors; in contrast, shifting appears to occur even when distractor colors are easily distinguishable from the target. While our current results suggest that shifting and sharpening are sensitive to different distractor properties (set and similarity, respectively), it is not at all clear that these two profiles are due to one or more mechanisms. While we have suggested that they might be separate, others have shown that dynamical systems models can account for both (Simmering et al., 2006; Johnson et al., 2008). Further work is necessary to better understand the mechanisms underlaying shifting and sharpening of the template representation.

Third, the results suggest that shifting and sharpening the target template may increase the efficiency of visual search performance, although it is not possible to test causality between the template contents and visual search performance in these studies. This suggestion was particularly salient in Experiment 1 where exposure to highly similar distractors from only one side of target space during visual search produced relatively good search performance, but exposure to distractors from both sides of color space (at exactly the same degrees of similarity) produced substantially poorer performance. Interesting, this occurred despite the fact that on any single trial, the distractors were linearly separable from the target in both groups. The only difference was that the directionality of the distractor set was a between subject manipulation in the unidirectional group, but a within subject factor in the bidirectional group. The stimuli and procedures were otherwise identical, suggesting that the greater "difficulty" in the bidirectional group was due to an inability to shift the target representation (within the template) away from distractors, as the unidirectional group could. In Experiment 2, performance was sustained at a high level until the final block, when competition was the most severe. Perhaps continued sharpening protected performance against increasing distractor competition, but only to a degree. Together, the results suggest that changes in the target template are based on learned expectations of what the visual search context will look like in the next moment of time, not just what is currently available to the visual system. This pattern also highlights the difference between the contents of the attentional template, which is held over time, and the use of that template on any given trial to select the target from distractors. The template represents the psychological distance between the target and distractors, and therefore anticipates the visual search context.

Together these results suggest that attentional templates are not static recreations of target features, but are flexibly shaped to anticipate the quality of distractor competition. Specifically, this flexibility manifested in two ways: a shift in the central tendency of the target template away from linearly separable distractor features, and an asymmetrical sharpening to increase the precision of the target-to-distractor boundary (see Figure 2.2). One open question remains regarding the mechanisms that support these changes in representation. The optimal model of attentional gain suggests that template shifting increases signal-to-noise ratio by selectively increasing the gain of sensory neurons tuned to elements of the target that are most distant from distractors (Navalpakkam & Itti, 2007). Sharpening, instead, may result from decreasing the gain of sensory neurons tuned to distractor features (Reynolds & Heeger, 2009). Alternatively, the pattern we have seen may reflect a "higher level" memory representation that impacts visual search processes by modulating sensory gain as well as serving as the "template" against which decisional processes determine if a stimulus is a target match (Geng and Witkowski, under review; Smith & Ratcliff, 2009; Duncan & Humphreys, 1989; Hout & Goldinger, 2015; Malcom & Henderson, 2010). Although it is impossible to fully address the question of where in processing the template shift and sharpening measured in our task is encoded with the current behavioral data, the results suggest that more than one mechanism is used to adjust the target template in order to increase the representational distinctiveness of the target from expected distractors.

In conclusion, our experiments reveal that the target template is shaped by expectations regarding multiple distractor features. Expectations regarding the linear separability of the distractor set from the target produces a systematic shift in the target template away from distractors, but this adjustment is insensitive to the strength of distractor competition. In contrast, asymmetrical sharpening of the target template on the side of distractors is sensitive to strength of distractor competition. Both modulations of target template increase the psychological distinctiveness of targets from distractors and therefore facilitate better visual search performance.

References

Bauer, B., Jolicoeur P., Cowan, W. B. (1996). Visual search for colour targets that are or are linearly seperable from distractors. *Vision Research, 36*(10), 1439-1466. https://doi.org/10.1016/0042-6989(95)00207-3

Becker, S. I. (2010). The role of target–distractor relationships in guiding attention and the eyes in visual search. *Journal of Experimental Psychology: General*, *139*(2), 247–265. http://doi.org/10.1037/a0018808

Becker, S. I., Folk, C. L., & Remington R. W. (2010). The role of relational information in contingent capture. *Journal of Experimental Psychology: Human Perception and Performance*, *36*(6), 1460–1476, http://doi.org/10.1037/a0020370

Becker, S. I., Harris, A. M., Venini, D., & Retell, J. D. (2014). Visual search for color and shape: when is the gaze guided by feature relationships, when by feature values? *Journal of Experimental Psychology: Human Perception and Performance*, *40*(1), 264–291. http://doi.org/10.1037/a0033489

Bundesen, C. (1990). A theory of visual attention. *Psychological Review, 97*(4), 523 547. http://doi.org/10.1037/0033-295X.114.3.599

Bundesen, C., Habekost, T., & Kyllingsbæk, S. (2005). A neural theory of visual attention: bridging cognition and neurophysiology. *Psychological Review, 112*(2), 291–328. http://doi.org/10.1037/0033-295X.112.2.291

Brainard, D. H. (1997). The psychophysics toolbox. *Spatial Vision, 10*(4), 433–436. http://dx.doi.org/10.1163/156856897X00357

Desimone, R., & Duncan, J. (1995). Neural mechanisms of selective visual attention. *Annual Review of Neuroscience, 18*(1), 193–222. http://doi.org/10.1146/annurev.ne.18.030195.001205

Duncan, J., & Humphreys, G. W. (1989). Visual search and stimulus similarity. *Psychological Review, 96*(3), 433–458.

D’Zmura, M. (1991). Color in visual search. *Vision Research, 31*(6), 951-966.

Gelman, A., Carlin, J. B., Stern H. S., Dunson, D. B., Vehtari, A. & Rubin D. B. (2013). *Bayesian Data Analysis (Third Edition)*. CRC Press.

Geng, J. J., DiQuattro, N. E., & Helm, J. (2017). Distractor probability changes the shape of the attentional template*. Journal of Experimental Psychology: Human Perception and Performance, 43*(12), 1993-2007. http://dx.doi.org/10.1037/xhp0000430

Geng, J. J., & Witkowski, P. (under review). Template-to-distractor distinctiveness regulates visual search efficiency.

Giesbrecht, B., Sy, J. L., & Guerin, S. A. (2012). Both memory and attention systems contribute to visual search for targets cued by implicitly learned context. *Vision Research, 85*, 80-89. http://doi.org/10.1016/j.visres.2012.10.006

Hodsoll, J., & Humphreys G.W. (2001). Driving attention with the top down: the relative contribution of target templates to the linear separability effect in the size dimension. *Perception & Psychophysics, 63*(5), 918-926.

Hout, M. C., & Goldinger, S. D. (2015). Target templates: the precision of mental representations affects attentional guidance and decision-making in visual search. *Attention, Perception, Psychophy,. 77*(1), 128–149. doi:10.3758/s13414 014-0764-6.

Johnson N. L., Kotz S. & Balakrishnan N. (1994). *Continuous Univariate Distributions*, Volume 1. New York, NY: John Wiley & Sons.

Johnson J. S., Spencer J. P., & Schöner, G. (2008). Moving to higher ground: The dynamic field theory and the dynamics of visual cognition. *New ideas in psychology, 26*(2), 227-251. doi: 10.1016/j.newideapsych.2007.07.007.

Lee D. K., Itti L., Koch C., & Braun J. (1999). Attention activates winner-take-all competition among visual filters. *Nature Neuroscience, 2*(4), 375-381. http://doi.org/10.1038/7286

Ling S., Jehee J. F. M., & Pestilli F. (2016). A review of the mechanisms by which attentional feedback shapes visual selectivity. *Brain Structure and Function, 220*(3), 1237-1250. https://doi.org/10.1007/s00429-014-0818-5

Liu, T., Larsson, J., & Carrasco, M. (2007). Feature-based attention modulates orientation selective responses in human visual cortex. *Neuron, 55*(2), 313-323. doi:10.1016/j.neuron.2007.06.030

Malcolm, G. L., & Henderson, J. M. (2009). The effects of target template specificity on visual search in real-world scenes : Evidence from eye movements. *Journal of Vision, 9*(11), 1-13. doi:10.1167/9.11.8.

Morey, R.D., Rouder, J.N., & Jamil, T. (2015). Package 'BayesFactor'. URL <http://cran.r project.org/web/packages/BayesFactor/BayesFactor.pdf>.

Myers, N. E., Rohenkohl, G., Wyart, V., Woolrich, M. W., Nobre, A. C., Stokes, M. G. (2015). Testing sensory evidence against mnemonic templates. *Elife*, 4:e09000.

Navalpakkam, V., & Itti, L. (2007). Search goal tunes visual features optimally. *Neuron, 53*, 605–617. http://dx.doi.org/10.1016/j.neuron.2007.01.018

Reynolds, J. H., & Heeger, D. J. (2009). The normalization model of attention. *Neuron, 61*(2), 168–185. http://doi.org/10.1016/j.neuron.2009.01.002

Rouder J. N., Speckman P. L., Sun D., Morey R. D., & Iverson G. (2009). Bayesian t tests for accepting and rejecting the null hypothesis. *Psyhonomic Bulletin & Review, 16*(2), 225–237. https://doi.org/10.3758/PBR.16.2.225

Scolari M., Byers A., & Serences J. T. (2012). Optimal deployment of attentional gain during fine discriminations. *Journal of Neuroscience, 32*(22), 7723–7733. https://doi.org/10.1523/JNEUROSCI.5558-11.2012

Scolari, M., & Serences, J. T. (2009). Adaptive allocation of attentional gain. *Journal of Neuroscience, 29*(38), 11933-11942. http://doi.org/ 10.1523/JNEUROSCI.5642 08.2009

Serences J.T., Saproo S., Scolari M., Ho T., & Muftuler L.T. (2009). Estimating the influence of attention on population codes in human visual cortex using voxel based tuning functions. *NeuroImage, 44*(1), 223–231. http://doi.org/10.1016/j.neuroimage.2008.07.043

Series P., Latham P. E., Pouget A. (2004). Tuning curve sharpening for orientation selectivity: coding efficiency and the impact of correlations. *Nature Neuroscience, 7*(10), 1129-1135. http://doi.org/10.1038/nn1321

Shiu, L.-p., & Pashler, H. (1994). Negligible effect of spatial precuing on identification of single digits. *Journal of Experimental Psychology: Human Perception and Performance, 20*(5),1037-1054. http://dx.doi.org/10.1037/0096-1523.20.5.1037

Simmering, V. R., Spencer, J. P., & Schöner, G. (2006). Reference-related inhibition produces enhanced position discrimination and fast replusion near axes of symmetry. *Perception & Psychophysics, 68*(6), 1027-1046. doi: 10.3758/BF03193363.

Smith, P. L., & R. Ratcliff. (2009). An integrated theory of attention and decision making in visual signal detection*. Psychological Review, 116*(2), 283-317. http://dx.doi.org/10.1037/a0015156

Sompolinsky H., & Shapley R. (1997). New perspective on the mechanisms for orientation selectivity. *Current Opinion in Neurobiology, 7*(4), 514-522. https://doi.org/10.1016/S0959-4388(97)80031-1

Soto D., Hodsoll J., Rotshtein P., & Humphreys G.W. (2008). Automatic guidance of attention from working memory. *Trends in Cognitive Science, 12*(9), 342-348. https://doi.org/10.1016/j.tics.2008.05.007

Stan Development Team. (2017). Package 'RStan'. <https://cran.rproject.org/web/packages/rstan/rstan.pdf >.

Treue, S., & Martinez-Trujillo, J. C., (1999). Feature-based attention influences motion processing gain in macaque visual cortex. *Nature, 399*(6736), 575–579. http://doi.org/10.1038/21176

Wolfe, J. M. (2007). Guided Search 4.0: Current Progress with a model of visual search. In W. Gray (Ed.), *Integrated Models of Cognitive Systems*, (pp. 99-119). New York: Oxford.

Wolfe J. M. (2000). Visual Attention. In De Valois KK (Ed.), *Seeing*, (pp. 335-386). San Diego, CA: Academic Press.

Woodman, G. F., Carlisle N. B., & Reinhart R. M. (2013). Where do we store the memory representations that guide attention? *Journal of Vision, 13*(3), 1-17. http://doi.org/10.1167/13.3.1.

Chapter 3: Pattern Similarity in Frontoparietal Control Network Reflects an "off-veridical" Template that Optimizes Target-match Decisions during Visual Search

Abstract

Theories of attention hypothesize the existence of an "attentional" or "target" template that contains task-relevant information in memory when searching for an object. The target template contributes to visual search by directing visual attention towards potential targets and serving as a decisional boundary for target identification. However, debate still exists regarding how template information is stored in the human brain. Here, we conducted a pattern-based fMRI study to assess how template information is encoded to optimize target-match decisions during visual search. To ensure that match decisions reflect visual search demands, we used a visual search paradigm in which all distractors were linearly separable but highly similar to the target and were known to shift the target representation away from the distractor features (Yu & Geng, 2019). In a separate match-to-sample probe task, we measured the target representation used for match decisions across two resting state networks that have long been hypothesized to maintain and control target information: the frontoparietal control network (FPCN) and the visual network (VisN). Our results showed that lateral prefrontal cortex in FPCN maintained the context-dependent "off-veridical" template; in contrast, VisN encoded a veridical copy of the target feature during match decisions. By using behavioral drift diffusion modeling, we verified that the decision criterion during visual search and the probe task relied on a common biased target template. Taken together, our results suggest that sensory-

veridical information is transformed in lateral prefrontal cortex into an adaptive code of target-relevant information that optimizes decision processes during visual search.

Introduction

When looking for a target object (e.g., a tiger hiding in the grasslands), we engage in a continuous “look-identify” cycle in which we use target features in memory (e.g., orange color) to guide attention and make match decisions. The memory representation of the target is referred to as the “attentional” or “target” template (Duncan & Humphreys, 1989), and its contents determine the efficiency of visual search (Geng & Witkowski, 2019; Hout & Goldinger, 2015; Malcolm & Henderson, 2009, 2010). The template is a core construct within all models of attention, but controversy remains over how target information is encoded in the brain. One possible reason for disagreement is that most target stimuli have simple static features, allowing for sensory and control regions to maintain veridical representations that are hard to distinguish from each other. However, recent behavioral studies have shown that under certain circumstances, target representations are shifted to be more optimal when “off-veridical” (Becker, 2010; Navalpakkam & Itti, 2007; Scolari et al., 2012; Yu & Geng, 2019), and these biased templates can be measured separately during attentional guidance and attentional decisions (Wolfe, 2021; Yu et al., in press; Yu & Geng, under review). In this study, we use such a paradigm to ask if biased target templates can be measured in frontoparietal and/or visual regions during a target decision task. We hypothesized that the need for a flexible, off-veridical target representation will result in greater reliance on lateral frontal regions that are known to dynamically code task-relevance (Duncan, 2001).

Lateral prefrontal cortex has long been hypothesized by attention researchers to hold the target template because neurons there selectively encode task-relevant information and maintain it over time (Funahashi et al., 1989; Fuster & Alexander, 1971;

Miller et al., 1996). In one of the earliest demonstrations, Rainer et al., (1998) found that when shown an array of objects during a delayed-match-to-sample task, neurons in lateral prefrontal cortex maintained only the task relevant item over the subsequent delay period (Moore & Zirnsak, 2017; Squire et al., 2013). Since then, there have been many complementary studies in humans demonstrating that while task-relevant stimulus representations can be found widely throughout the brain (Christophel et al., 2017; Ester et al., 2015; Lee et al., 2013), the lateral prefrontal cortex specifically encodes the goal-relevant properties of the stimulus. For example, Long and Kuhl (2018) asked participants to make a judgment about a face stimulus based on a "goal cue" that indicated the dimension of relevance (gender or emotion). While decoding of stimulus properties in visual cortex was highly sensitive to sensory degradation following a visual mask, stimulus decoding within regions of the frontoparietal control network (FPCN; Schaefer et al., 2018) only occurred based on the goal-relevant stimulus dimension.

The data are consistent with the view that lateral prefrontal cortex encodes the contents of the task-based target template but guides attention and eye-movements through a functional network of oculomotor and sensory regions (Baldauf & Desimone, 2014; Bichot et al., 2015; Feredoes et al., 2011; Moore et al., 2003). Causal evidence for such network interactions was shown by Bichot et al. (2019) who found that silencing a region of ventrolateral prefrontal cortex impaired visual selectivity of visual search target features, suggesting this region maintains target templates that set attentional priority in sensory cortex. These studies are consistent with characterization of mid-lateral prefrontal cortex as being essential for control functions that selectively maintain information for visual search based on the current task demands (Badre & Nee, 2018; de la Vega et al., 2018; Duncan, 2001, 2013; Miller & D'Esposito, 2005; Panichello & Buschman, 2021).

Nevertheless, despite evidence implicating lateral prefrontal cortex in maintaining target representations, others have argued that low-level sensory regions may be better candidates for template storage because neurons in those regions are selectively tuned for different stimulus features (Harrison & Tong, 2009; Serences et al., 2009; Sreenivasan et al., 2014). However, many of these studies measured target representations during or just prior to target selection or comparison, leaving open the possibility that these measurements reflect "downstream" changes in sensory gain rather than the stable memory "source" of the target (Chelazzi et al., 1998; Desimone & Duncan, 1995; Reynolds & Heeger, 2009; Treisman & Gelade, 1980). Moreover, recent research has shown that information in target templates are not only used to modulate sensory processing but also used to determine target identity once an object has been selected (Bravo & Farid, 2016; Castelhano et al., 2008; Cunningham & Wolfe, 2014; Peltier & Becker, 2016; Rajsic & Woodman, 2020; Wolfe, 2021). This suggests that the target template contributes to attentional processes at multiple stages of processing and should be tuned to optimize target-to-distractor discriminability and minimize decision errors (Yu et al., in press).

To better understand how optimal template information is encoded, we conducted a visual search study with interleaved single-stimulus match-to-sample (probe) trials (Figure 1). The visual search task trained participants on the target feature relative to distractor features and the probe task asked participants to make target-match decisions. The separation of visual search and probe trials is essential for obtaining a measurement of target decisions without contamination from distractor processing and competition during active visual search given that target decisions more closely match the memory template (Yu et al., in press; Yu & Geng, under review). The task is based on previous work showing that difficult search for a target amongst linearly separable distractors (e.g., distractors are all “redder” than the orange target) induces a shift in the target template (e.g., becoming represented as yellower than the true target) (Bauer et al., 1996; Geng et al., 2017; Hodsoll & Humphreys, 2001; Scolari et al., 2012; Yu & Geng, 2019). Despite being off-veridical, the biased template is more optimal in this case because it prioritizes the ability to distinguish the target from distractors. The advantages in template-to-distractor distinctiveness have mostly been hypothesized to increase search efficiency by biasing sensory selection during attentional guidance (Becker, 2010; Navalpakkam & Itti, 2007; Scolari et al., 2012), but it has been recently shown in behavior to also facilitate target-match decisions (Yu et al., in press).

Here, we tested two non-mutually exclusive hypotheses concerning how the human brain encode the template information to optimize target-match decisions. Given the convergent findings from working memory, attentional control, and perceptual decision making, one hypothesis predicts that the off-veridical template representation would be stored and used to optimize target-match decisions in lateral prefrontal cortex within the frontoparietal network. Alternatively, a similar hypothesis could be made for visual cortex given evidence of working memory maintenance and target representations there during visual search (Chelazzi et al., 1998; Ester et al., 2009). We therefore identified a priori ROIs from frontoparietal control (FPCN) and visual (VisN) networks using a resting state network atlas defined from a large, independent sample of participants (Schaefer et al., 2018; Yeo et al., 2011). Evidence for a biased template even when there are no actual distractors present (on match-to-sample probe trials) would suggest that FPCN and VisN encode the target template as an adaptive memory of target characteristics in long-term memory to maximize the distinctiveness of target from distractors during visual search. Alternatively, if we find that the target representation is present, but veridical (i.e., centered around the true target value) on probe trials, it would suggest that the biased template is only invoked when it is actively used during visual search for attentional guidance. Furthermore, correspondence between pattern similarities in FPCN and VisN would suggest that a single template representation is used for target-match decisions; however, different patterns in FPCN and VisN would suggest that the readout of information from sensory cortex is transformed in order to optimize the efficiency of target decisions.

Results

PFC encodes an off-veridical template to optimize target decisions

The goal of the study was to test whether the frontoparietal control and/or visual network encodes an off-veridical target template learned from optimizing target-match decisions during visual search. To do this, twenty participants performed a difficult *visual search* task and a match-to-sample *probe* task based on our previous work (Yu & Geng, 2019) while being scanned (Figure 1B). The search target was presented once at the beginning of the experiment as a colored item (e.g., a green-blue circle). All distractors were highly similar to the target (5°, 10°, and 15° from the target) but also linearly separable from the target (e.g., all being bluer than the target color based on unidirectional rotation on a continuous color wheel) (Figure 1A). Upon presentation of the display, participants searched for the predefined target-color circle and reported the number inside by pressing 1-4 on a button box. The visual search trials were used to train participants' expectations for the target with respect to distractor colors (Becker, 2010; Navalpakkam & Itti, 2007; Yu & Geng, 2019). Overall performance was high (accuracy: *M* ± 95% CI = 88% ± 4%; RT: *M* ± 95% CI = 812ms ± 85ms) suggesting that participants had a target template that could be successfully distinguished from distractors (Supplemental Figure 1). The findings replicate our previous results using a similar paradigm (cf. data from Experiment 1, Yu & Geng, 2019).

On separate match-to-sample *probe* trials (Figure 1C), participants indicated whether or not a particular color stimulus (0°, ±5°, ±10° and ±15° from the target) (Figure 1A) was the target (Geng et al., 2017; Yu & Geng, 2019). Because each probe trial had only one stimulus presented at the center of the screen (Figure 1C), we were able to obtain a pure measurement of match decisions independent from rapid visual search cycles of target localization and identity decisions. Previous behavioral work has demonstrated that under these conditions, the target representation shifts "off-veridical" away from distractors such that targets with the relational (e.g., "greener") values (i.e., negative probe colors) were more likely to be selected and moreover, this bias was preserved stably in memory (Yu et al., in press). The data of primary interest for the fMRI analyses therefore included only the probe trials and are described in detail below.

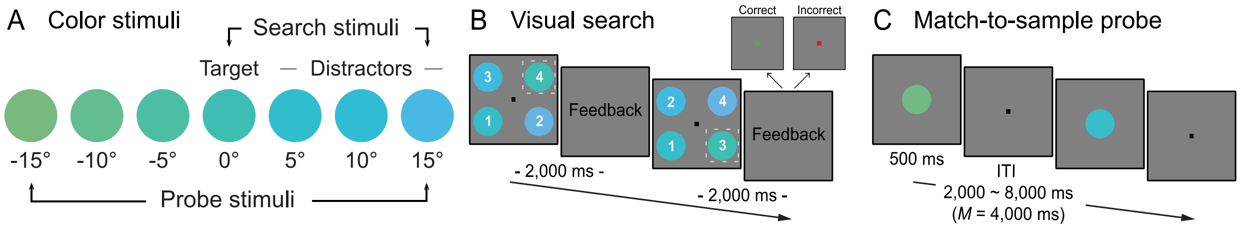

Figure 3.1. A) Color stimuli used in the fMRI experiment. The target color (0°) was a green-blue border color (Bae et al., 2015). The three distractors in visual search trials were all positive rotations (5°, 10° and 15°) from the target color. The probe colors included the target color (color 0°), and the three colors from each side of the target (i.e., −5°, −10°, −15°, 5°, 10° and 15°). B) Example of visual search trials in the fMRI experiment. Participants were instructed to locate the target color circle and report the number within. Feedback was provided immediately after responses (green fixation squares for correct; red squares for incorrect). The white dashed squares illustrate the target but were not visible to the participants. C) Example of match-to-sample probe trials in the fMRI experiment. Participants were instructed to report if the centrally presented color circle was target color or not. There was no feedback in the probe trials. Non-target color values are exaggerated for visual clarity in all figures.

Behavioral representational geometry

The mean proportion of "target yes" responses for each of the seven probe stimuli are shown in Figure 3.2A. The false alarm rates of non-target colors, as a measurement of which non-target colors were mistaken as the target color, were entered into a paired sample *t* test to test for differences between color directions (negative, positive). Participants had significantly more false alarms to the negative probe colors (*M* ± 95% CI = 44% ± 10%) compared to the positive ones (*M* ± 95% CI = 12% ± 7%), $t_{19} = 4.55$, $p = .0002$, $d = 1.02$, $BF_{10} = 139.58$. The behavioral results replicated previous findings (Navalpakkam & Itti, 2007; Scolari et al., 2012; Yu & Geng, 2019) that the target representation shifted away from distractors to enhance optimal off-target features that increase the template-to-distractor distinctiveness (Geng & Witkowski, 2019).

Next, we quantified the representational distance between each pair of probe stimuli by constructing a representational dissimilarity matrix (RDM) for each participant from their own data. This matrix, denoted (*B*)*,* reflected each individual's biased target template (see Figure 3.2B for group average RDM and Figure S3.2 in Supplemental Material for individual RDMs) and was created as a model for subsequent analyses of brain data. In addition to the biased RDM (*B*), we built a veridical RDM (*V*) (Figure 3.2E) to serve as an alternative baseline model of an unbiased target template (Figure 3.2D). To ensure that B and V capture distinct patterns, we performed a partial correlation analysis to regress out their shared covariance (Park et al., 2020). As expected, the partial biased model RDM (B') did not correlate with V (M ± 95% CI = -.03 ± .03, z_{19} = -2.28, p = .99), but did correlate strongly with B (M ± 95% CI = .55 ± .12, z_{19} = 3.92, p < .0001) (Figure 3.2C). In contrast, the partial base model RDM (V') had a high correlation with V (M ± 95% CI = .64 ± .08, z_{19} = 3.92, p < .0001) but only a weak one with B (M ± 95% CI = .06 ± .03, z_{19} = 2.91, p = .001) (Figure 3.2F).

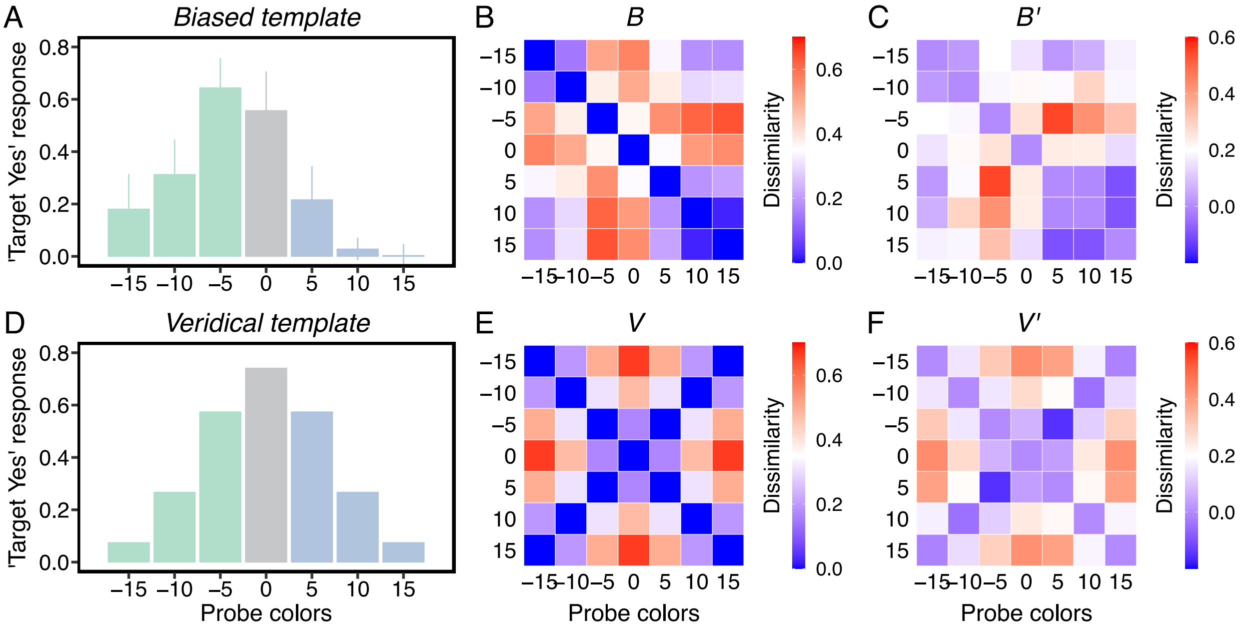

Figure 3.2. A) Group average of "target yes" responses. The center gray bar indicates proportion of "hits" in response to the true target color and other colored bars indicate "false alarms" to non-target colors. All error bars are 95% confidence intervals. B) The biased behavioral RDM averaged across participants (*B*). This RDM was generated by participants' own probe task performance and reflected the biased target representation in Figure A. See Supplemental Figure 3.2 for individual RDMs. C) To ensure the effects were specific to each of the model RDMs (*B* and *V*), we conducted a partial correlation analysis to regress out their covariance with the other. The partial biased matrix (*B′*) highly correlates with *B* but not with *V*. D) The veridical target template. This template is a theoretical template, which assumes the target template was normally distributed and centered at the target color. E) The veridical behavioral RDM (*V*). F) The partial base matrix (*V′*) has a strong correlation with *V* but extremely weak correlation with *B*.

Brain representational geometry

To test our primary hypotheses, we first test for representations of the target in our *a priori* anatomical ROIs based on FPCN and VisN networks defined through resting state data (Figure 3.3A): bilateral prefrontal-FPCN (PFC), parietal-FPCN (PAR) and central-VisN (VIS). The representational distances (one-sided Wilcoxon signed rank test; Holm-Bonferroni corrected from multiple comparisons across numbers of model RDMs, $N = 2$, and bilateral ROIs, $N = 8$) estimated in bilateral PFC were explained by the model RDM B' (left: M ± 95% CI = .12 ± .07, $z_{19} = 3.10$, $p = .007$; right: M ± 95% CI = .10 ± .06, $z_{19} = 3.02$, $p = .009$), but not by V' (left: M ± 95% CI = .02 ± .06, $z_{19} = .56$, $p = .89$; right: M ± 95% CI = .03 ± .06, $z_{19} = 1.16$, $p = .52$). In addition, the Kendall's τ_A rank correlations between the B' and V' model RDM and the brain RDM in bilateral PFC were compared using a one-sided paired samples Wilcoxon test to determine if the correlation with B' and V' differed from each other statistically. Significant differences were found in left PFC ($z_{19} = 1.72$, $p = .044$), but not in right PFC ($z_{19} = 1.12$, $p = .14$). Notably, while left PAR was significantly correlated with B' (M ± 95% CI = .09 ± .06, $z_{19} = 2.76$, $p = .025$), the right PAR pattern was only explained by B' at a reduced threshold (M ± 95% CI = .08 ± .07, $z_{19} = 2.17$, $p = .015$, uncorrected) (Figure 3.3B). The representations in bilateral PAR were not explained by V' (left: M ± 95% CI = .04 ± .05, $z_{19} = 1.23$, $p = .58$; right: M ± 95% CI = .04 ± .06, $z_{19} = 1.32$, $p = .61$). The Kendall's τ_A rank correlations with B' were not significantly higher than the correlations with V' in bilateral PAR (left: $z_{19} = .78$, $p = .23$; right: $z_{19} = .71$, $p = .25$). In contrast, the representations in bilateral VIS were explained by V' (left: M ± 95% CI = .10 ± .04, $z_{19} = 3.58$, $p = .001$; right: M ± 95% CI = .10 ± .05, $z_{19} = 3.21$, $p = .004$), but not by B' (left: M ± 95% CI = .03 ± .04, $z_{19} = 1.46$, $p = .62$; right: M ± 95% CI = .04 ± .05, $z_{19} = 1.46$, $p = .54$) (Figure 3.3B). The Kendall's τ_A rank correlations with *V′* were significantly higher than the correlations with *B′* in right VIS (z_{19} = 1.68, *p* = .048), but only marginally significantly in left PAR (z_{19} = 1.46, *p* = .077). To be sure that these findings were specifically related to our task, we further looked for brain-model pattern similarity within a control region in bilateral auditory cortex (AUD) defined by the same Schaefer atlas (Schaefer et al., 2018; Yeo et al., 2011). The pattern similarity in bilateral AUD was not explained by either template model RDM (z_{19} < 2.05, *ps* > .2) (Figure 3.3B).

The differences in PFC and VIS illustrate a "double dissociation" in which the prefrontal cortex matched the biased model better than the veridical one and the opposite pattern was found in the early visual cortex. The fact that the visual ROI encoded the veridical target, but the prefrontal cortex encoded the biased template during the same probe trial suggests that match decisions transformed veridical visual representations into a template space designed to improve target distinctiveness from visual search distractors. Furthermore, that this transform occurred on the probe trials when distractors were absent suggests that target decisions are based on a stable biased target representation stored in long-term memory (Wolfe, 2021; Yu et al., in press; Yu & Geng, under review).

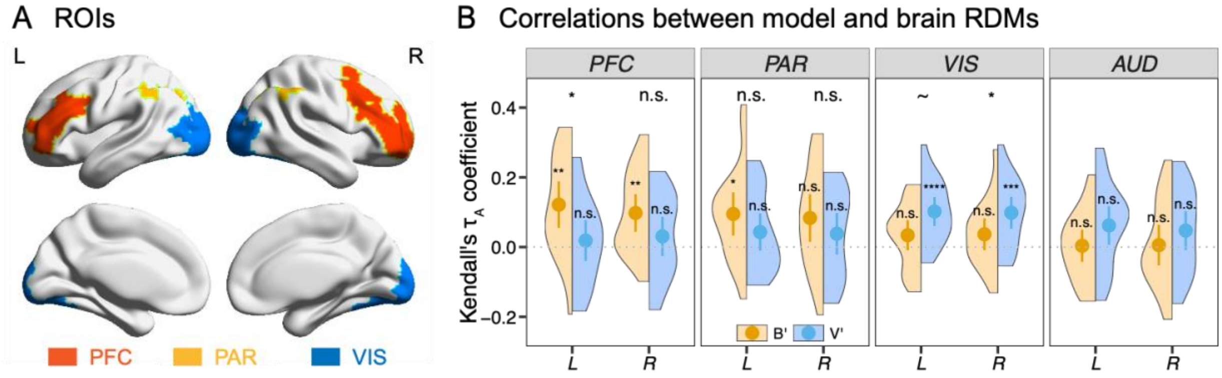

Figure 3.3. A) We assessed target representations in two resting-state networks defined from a large, independent sample of participants (Yeo et al., 2011): the frontoparietal control network

(FPCN) and the visual network (VisN). FPCN was divided into discontinuous prefrontal and parietal subregions, and VisN was separated into central (i.e., striate and extrastriate cortex) and peripheral subregions. All the cortical parcels corresponding to the prefrontal-FPCN (PFC), the parietal-FPCN (PAR) and the central-VisN (VIS) were selected as ROIs. B) Mean Kendall's τ_A rank correlations between the model RDMs (B' and V') and the brain RDM. The significance of the correlations was assessed by the one-sided Wilcoxon signed rank test. ****$p < .001$ (Holm-Bonferroni corrected from multiple comparisons across numbers of model RDMs, $N = 2$, and bilateral ROIs, $N = 8$), ***$p < .005$, **$p < .01$, *$p < .05$, ~$p < .1$, and n.s. > .1. All error bars are 95% confidence intervals.

Whole brain searchlight analysis

In order to capture all of the brain regions that possibly encode the target template, we conducted a whole brain searchlight analysis for each participant using their own biased RDM (*B*) (Figure S3.2 in Supplemental Material) and the baseline veridical RDM (*V*) (Figure 3.2E) as separate models. The group analysis with *B* identified five significant brain regions located in bilateral middle frontal gyrus (MFG) (left: [x, y, z] = [-32, 40, 14], $z_{19} = 5.43$; right: [x, y, z] = [34, 42, 32], $z_{19} = 4.66$), left superior parietal lobe (SPL) ([x, y, z] = [-38, -42, 32], $z_{19} = 4.58$), left percental gyrus (PrG) ([x, y, z] = [-46, -14, 48], $z_{19} = 5.92$), and right supplemental motor cortex (SMC) ([x, y, z] = [8, 20, 44], $z_{19} = 4.86$) (Figure 3.4A). The significant bilateral MFG result corresponds to the PFC ROI in FPCN from the previous hypothesis driven analysis. The group analysis with *V* also identified five significant brain regions located in bilateral occipital gyrus (OcG) (left: [x, y, z] = [-16, -96, 8], $z_{19} = 5.13$; right: [x, y, z] = [20, -90, 18], $z_{19} = 4.95$), replicating the hypothesis driven results above, and also left precentral gyrus (PrG) ([x, y, z] = [-46, 2, 36], $z_{19} = 4.76$), left postcentral gyrus (PoG) ([x, y, z] = [-40, -18, 50], $z_{19} = 4.85$), and left supplemental motor cortex ([x, y, z] = [-14, -2, 62], $z_{19} = 4.63$) (Figure 3.4B). Statistics and the MNI coordinates of the peak voxels in the five clusters are reported in Table 1. The significant results observed in motor regions, e.g., left PrG (contralateral to the right index and middle fingers that were used for button presses), were due to the actual motor response rather than response independent decision processes (see Supplemental Material button response RDM searchlight).

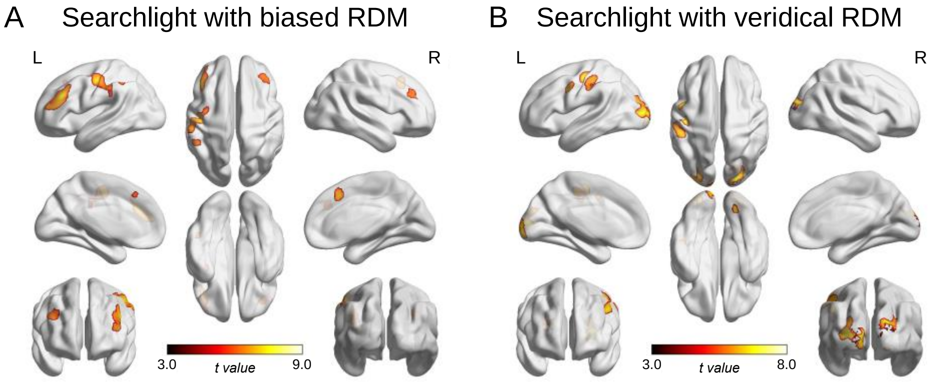

Figure 3.4. A) Brain maps showing the clusters identified in the whole brain searchlight analysis with the biased RDM (*B*). B) Brain maps showing the clusters identified in the whole brain searchlight analysis with the veridical RDM (*V*).

Table 1. Brain regions in which the neural activity pattern similarity was significantly correlated with the behavioral RDMs in the searchlight analysis.

Biased behavioral RDM						Veridical behavioral RDM					
Anatomical regions	x	y	z	# voxels	z value	Anatomical regions	x	y	z	# voxels	z value
L MFG	-32	40	14	1353	5.43	L OcG	-16	-96	8	1155	5.13
R MFG	34	42	32	364	4.66	R OcG	20	-90	18	1180	4.95
L SPL	-38	-42	32	184	4.58	L PoG	-40	-18	50	852	4.85
L PrG	-46	-14	48	951	5.92	L PrG	-46	2	36	287	4.76
R SMC	8	20	44	382	4.86	L SMC	-14	-2	62	186	4.63

Coordinates (x, y and z) are reported in MNI space

The biased decision template encoded in PFC was used during active visual search

We concluded from the fMRI results that visual cortex contained a veridical copy of the target template, but lateral prefrontal cortex encoded target decisions based on an off-veridical template in long-term memory biased by the search context. However, because the fMRI target identification task relied solely on probe trials, it is possible that the biased decision template we measured in PFC is different from that used during active visual search. Although it is not possible to isolate target-match decisions during visual search using fMRI given the rapid cycles of object selection and target-match evaluations before the target is found (Yu et al., in press), we tested for correspondence in decision processes on visual search and probe trials using drift diffusion modeling (DDM). We conducted an online behavioral study in which we applied DDM to characterize how accurately and quickly the target was selected from distractors during active visual search (Figure 3.5B, 3.5D) and how accurately and quickly the probe stimulus was identified as a target or non-target on probe trials (Figure 3.5C, 3.5E). Each visual search trial consisted of two bilaterally presented target and distractor circles (Figure 3.5A). *Standard* visual search trials always contained a positively 10° rotated distractor color and were used to set up expectations regarding the distractor context. On *critical* search trials, the distractors varied from the target color from +/- 30° in steps of 5°. *Critical* distractors, unlike *standard* distractors, could be positive or negative rotations from the target color and provided a way to assess how well each color matched the internal target template used for decision making during active visual search. The *probe* trials were identical to the fMRI experiment and asked participants to indicate whether a particular color stimulus (ranging from -30° – +30°) was the target (Figure 3.5A). A high correlation between individual drift rates on the *critical* search trials and drift rates from the *probe* trials would suggest that the two processes rely on a similar underlying decision criterion based on the target template.

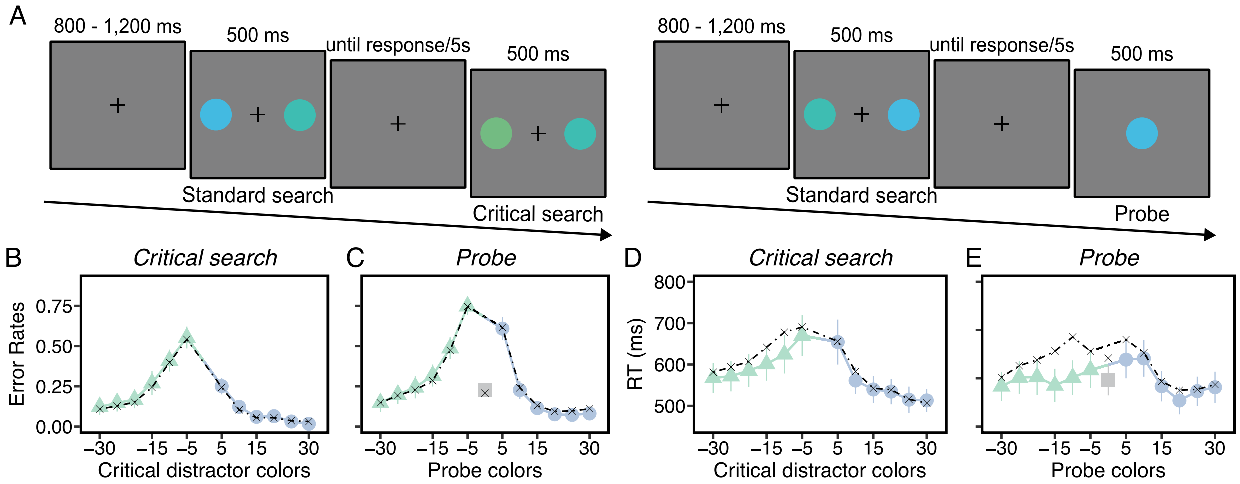

Figure 3.5. A) Example of *standard* and *critical* visual search trials, and *probe* trials. On search trials, participants were instructed to locate the target color circle and press a mouse button indicating its location. On probe trials, participants were instructed to report if the centrally presented color circle was the target color or not. No feedback was given on any of the trials. B) Error rates from the critical visual search trials. C) Error rates from the probe trials. D) RTs from the critical search trials. E) RTs from the probe trials. The black dashed lines represent the "fitted curves" for error rates and RT from the DDM for the best fit DDM parameters. All error bars are 95% confidence intervals.

Analysis of the drift rates

Figure 3.6A and 3.6B shows the group mean posterior estimates of the drift rates for the visual search and probe conditions, respectively. If the probe task taps into target information that is used during visual search decisions, we expected a positive correlation between these two metrics. Following the analysis strategy from the fMRI experiment, each participant's drift rates were converted to a dissimilarity matrix (Figure 3.6C and 3.6D). The significance of correlations between the search drift rate RDM and the probe drift rate RDM was evaluated by a permutation test by randomizing stimulus labels. There was a significantly positive correlation between the two RDMs, M ± 95% CI = .55 ± .04, p = .0004, highlighting the close relationship between the decision processes engaged during probe trial judgements of target color held in memory over time, and the decision processes engaged during active comparisons of the target template to search items during visual search.

Importantly, both drift rates showed the same biased pattern we observed in the fMRI experiment in FPCN. In particular, as shown in Figure 3.6A and 3.6B, the drift rate was negative at the -5° distractor in both critical search and probe trials; this indicates that the accumulation of evidence was slow, and moreover, that the "wrong" decision that the -5° stimulus was the target, was made more often than not on both visual search and probe trials. This pattern is consistent with the use of an off-veridical template to make target decisions during both visual search and probe trials. Also consistent with the notion that the biased template was created to increase target-to-distractor distinctiveness during visual search, the drift rates show that the "target no" response decision times were faster for the positive colors (M ± 95% CI = 551ms ± 29ms) that were seen as actual visual search distractors compared to the negative colors (M ± 95% CI = 602ms ± 36ms) ($t_{69} = -7.05$, $p < .0001$, $d = -.84$, $\mathrm{BF}_{10} > 1{,}000$) (Figure 3.5D). These results support those from the fMRI experiment and suggest that the decision processes during both visual search and probe trials relied upon a common biased target template in long-term memory that reflects a mechanism to increase the psychological distance between the target and distractors (Yu et al., in press; Geng & Witkowski, 2019).

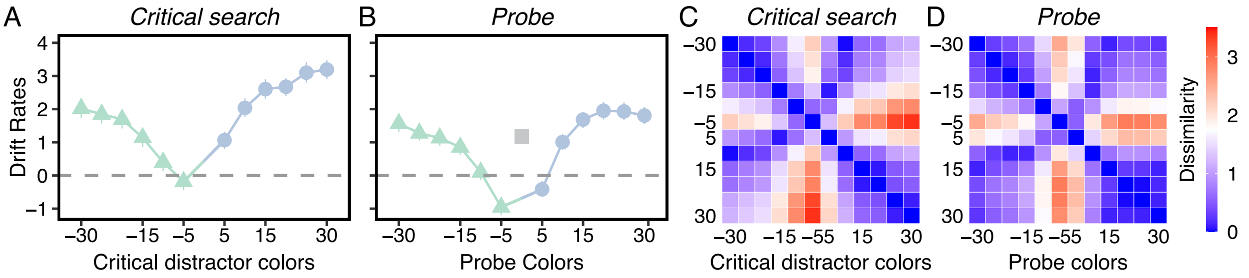

Figure 3.6. A) The drift rates for different critical search conditions. B) The drift rates for different probe color conditions. C) The search drift rate RDM averaged across participants. D) The probe drift rate RDM averaged across participants. All the error bars are the 95% confidence intervals.

Discussion

Models of attention all theorize the existence of an internal representation of target features in memory that is referred to as an attentional or target template (Bundesen, 1990; Duncan & Humphreys, 1989; Wolfe, 2021). It is commonly believed that lateral prefrontal cortex maintains template information to direct attention and eye-movements to possible targets through a functionally connected network of oculomotor and sensory regions (Baldauf & Desimone, 2014; Bichot et al., 2015; Feredoes et al., 2011; Moore et al., 2003). However, less is known about how template information might be used to optimize target-match decisions once a potential target has been selected. Here, using pattern-based fMRI methods and a perceptual decision-making task, we compared representations of target features across two resting-state networks. We targeted networks for which there is evidence of template maintenance, namely the frontoparietal control network and the visual cortical network (Schaefer et al., 2018; Yeo et al., 2011).

The argument for the importance of decision processes during visual search is based on the “look-identify” cycle inherent in visual search: Once a candidate object has been localized by attention, a decision must be made regarding the exact identity of the stimulus as a match or non-match to the target (Castelhano et al., 2008; Hout & Goldinger, 2015; Rajsic & Woodman, 2020). This decision component is a time-consuming part of the visual search cycle and must be accurate if visual search is to be ultimately successful. We previously showed that target-match decisions operated on more precise template information than attentional guidance, presumably because decisions need to be highly accurate whereas initial selection can be less precise (Yu, et al., in press; Yu & Geng, under review). Similarly, Rajsic & Woodman (2020) found that the benefit of weighting the target template over accessory memory representations in a dual-memory search task mainly lies in enhancing target recognition rather than more efficient localization of the target, again presumably because recognition serves to "gate keep" the outcome accuracy of object localization. Moreover, template information used during the decision stage more closely matched the precision of target information in long-term memory than guidance (Yu, et al., in press; Yu & Geng, under review). Together, these suggest that attentional decisions are better measurements of the underlying precision of the target template in memory than guidance.

In our current study, we successfully decoded the off-veridical template that maximized the target-to-distractor discrimination in PFC during a target identification probe task that isolated the match decisions from other processes of visual search. The results suggest that PFC engages in target decisions using templates that are held in long-term memory and shaped by the recent search context. This is consistent with previous research that frontoparietal regions dynamically change target representations depending on task contexts (Bracci et al., 2017; Ester et al., 2016; Lee et al., 2013; Long & Kuhl, 2018; Sarma et al., 2016; Swaminathan & Freedman, 2012). This information in lateral prefrontal cortex is then used to make target-match decisions, in addition to setting sensory priority to guide attention.

In contrast to the pattern in FPCN, our data indicates that stimulus responses in early visual cortex reflected the veridical target. The correlations between each brain region's responses and the two target RDMs (biased, veridical) illustrate a double dissociation that suggests that match decisions were based on a transformation of veridical target information in sensory cortex into a biased template space in service of improving decisions about target identity. This transformation suggests that improved visual search performance can be achieved by flexibly changing sensory readout, while leaving the sensory representations unchanged (Birman & Gardner, 2019).

In the online behavioral study, we found a close relationship between the target-match decisions in visual search and probe trials by applying DDM to accuracy and RT in the two tasks. This suggests that the decision process engaged during active visual search and the decision process engaged during probe trial judgments of target color rely on a similar underlying decision criterion based on an off-veridical template. The fact that the biased template was used to make decisions on probe trials when no distractors were actually present, indicates that experience with the target within a linearly separable context produces a change in the memory representation of the target used for making decisions about identity (Yu & Geng, 2019). This is consistent with the preferential decoding of the biased template in PFC, given that lateral prefrontal cortex adaptively encodes task relevant information in working memory (D'Esposito & Postle, 2015; Duncan, 2001; Lee et al., 2013; Miller et al., 1996; Riggall & Postle, 2012).

In conclusion, our findings provide evidence that the frontoparietal control network represents the target template as an adaptative memory of target features to optimally discriminate the target from distractors; in contrast, early visual cortex encodes veridical inputs, suggesting that decision processes about target identity are based on a transformation of veridical information when doing so increases target discrimination. This work strongly supports the role of lateral prefrontal cortex in flexibly controlling target relevant information in accordance with task goals to optimize decision processes during visual search.

Materials and methods

Participants

fMRI experiment

Twenty-one participants (self-reported 8 males and 13 females, all right-handed, aged between 19-30 years) participated in a 1.5h scanning session and received monetary compensation. Data from one participant were excluded from analyses due to excessive head motion larger than $4mm^3$, which resulted in a final group of twenty participants (self-reported 7 males, 13 females). This number far exceeded the estimated sample size of $N = 7$ (.95 power, .05 two-tailed significance) calculated with G*power (*http://www.gpower.hhu.de/*) based on behavioral data from our previous experiment that used similar stimuli and procedures (Yu & Geng, 2019; Experiment 1; unidirectional group). The behavioral effect we wished to detect was highly reliable, but we set our sample size at 20 due to expected noise associated with fMRI measurements. Each participant provided written informed consent in accordance with the local ethics clearance as approved by the National Institutes of Health. Each participant's color vision was assessed by self-report on an online color blindness questionnaire (*https://colormax.org/color-blind-test*). All participants had normal or corrected-to-normal vision and no history of neurological or psychiatric illness.

Online experiment

Seventy participants (self-reported 10 males and 60 females, 9 left-handed and 61 right-handed, aged 18-30 years) from University of California, Davis participated online in partial fulfillment of a course requirement. The sample size $N = 70$ (.85 power, .05 two-tailed significance) was determined based on a previous online study from which we adopted the experimental design (Yu, et al., in press; online Experiment 2). Eight participants were excluded from data analyses due to poor visual search performance (i.e., accuracy in standard visual search trials was below 75%). Data were collected until we obtained the target sample of 70 participants after exclusion criteria were applied. Each participant provided written informed consent in accordance with the local ethics clearance as approved by the National Institutes of Health. Each participant's color vision was assessed by self-report. All participants had normal or corrected-to-normal vision, and all had normal color vision.

Task and Stimuli

fMRI experiment

All stimuli were generated by a Dell computer and displayed on a 24" BOLDscreen LCD monitor with a spatial resolution of 1920 x 1200 pixels. The operating system was Windows 7, and Matlab Psychtoolbox (Brainard, 1997; Pelli, 1997) was used to create stimuli. The target and distractor colors were selected from a color wheel defined in CIELAB color space (a, b coordinates = 0, 0; luminance = 70). We used a green-blue boarder color (190°) and a blue-purple border color (274°) as the target colors to control for the potential color category effects on responses (Bae et al., 2015). The two target colors were counterbalanced across participants. Each participant was assigned a single target color throughout the experiment. Although the two target colors appeared to affect visual search RT differently ($t_{19} = -4.20$, $p < .001$), they did not impact accuracy ($p = .29$) nor performance on the probe task ($p = .72$). Data from these conditions were therefore collapsed to maximize power. The three distractors in each search trial were different from each other and always 5°, 10° and 15° positively rotated away from the target color. These distractors were chosen to exceed the average just noticeable difference, but still be confusable with the target when presented in a competitive search context (Geng et al., 2017; Yu & Geng, 2019). The colors in probe trials included the target color (0°), and three non-target colors from each side of the target (i.e., ±5°, ±10° and ±15°).

An example of the target color was presented at the beginning of the experiment. On *visual search* trials (Figure 3.1C), four circles (3° of visual angle in diameter) were presented for 1000ms on a gray background. The target color was always present and was randomly located at one of the four vertices along an imaginary square (6° of visual angle from center to edge); distractors appeared at the other three vertices. A number from 1-4 (1° of visual angle; white) was centrally located within each circle without duplication. Upon presentation of the search display, participants located the pre-defined target color circle and reported the number inside by pressing 1-4 on a button box with their right hand. Visual feedback was provided immediately following responses (the fixation square turned green for correct responses and red for incorrect responses). Each match-to-sample *probe* trial consisted of a centrally presented circle (3° of visual angle in diameter) for 500ms (Figure 3.1C). Participants reported whether the circle color was the target color: “yes” responses were indicated by a button press with the right index finger and “no” responses were indicated by a button press with the middle finger. Participants were informed that no feedback was provided on probe trials because there was no absolute “correct” or “incorrect” answer. If no response was made within 2000ms, both visual search and probe trials automatically terminated.

Prior to the start of the experiment, participants completed 48 practice trials composed of both search and probe trials. Participants were instructed to fixate on the center fixation square (.17° of visual angle from center to edge) throughout the experiment. The main experiment was composed of 320 visual search trials and 448 probe trials. Trials were presented in 8 blocks, each containing 2 alternating blocks of visual search trials and probe trials. Each alternating block contained 20 visual search trials followed by 28 probe trials. There was a 10s inter-trial interval when switching between visual search trials and probe trials. The probe trials in each scan had 24 repetitions of 0°, 16 repetitions of ±5°, 8 repetitions of ±10°, and 8 repetitions of ±15°. We used an uneven ratio (1:2) of veridical targets to non-target foils in order to maximize the number of non-target color presentations and to roughly equate the number of likely "yes" and "no" responses to avoid response biases, based on our previous findings (Yu & Geng, 2019).

Online experiment

The experiment was conducted entirely online through Testable (*https://www.testable.org/*). All stimuli were created in Illustrator, saved as PNG files, and uploaded to Testable.org. All stimuli were presented against a gray background (color hue = '#808080'). The two target colors (190° and 274°) were identical to the fMRI experiment and counterbalanced across participants. Because there were no spurious differences (*ps* > .35), the data were collapsed to maximize power in all subsequent analyses. There were three types of trials: 1) *standard* visual search trials to set up expectations for the distractor colors; 2) *critical* search trials to assess how target templates are used to identify targets during visual search; 3) *probe* trials to measure the target template independent of simultaneous distractor competition.

Each visual search trial (Figure 3.5A) consisted of two bilateral target and distractor circles (radius: 135 pixels) on the horizontal meridian (distance between the centers of the two circles: 400 pixels). The distractor color in the *standard* visual search trials was always positively 10° rotated from the target color. The *critical* distractor set was constructed in steps of 5° from the target color to +/-30° rotations from the target color, resulting in a total of 12 critical distractor colors. Each *probe* trial consisted of a centrally presented circle (radius: 135 pixels) (Figure 3.5A). The colors in probe trials included the target color (0°), and twelve non-target colors identical to the critical distractor set.

An example of the target color was presented at the beginning of the experiment. On search trials, participants were instructed to indicate whether the target color appeared on the left side by pressing the left arrow key or on the right side by pressing the right arrow key. On probe trials, participants were required to report whether the circle color was the target color by pressing the left arrow key for “yes” responses or the right arrow key for “no” responses. The stimuli in both trials appeared on the screen for 500ms and participants had up to 5s to make their responses. No feedback was given. After response, a central fixation cross was presented for 800-1200ms before the next trial started.

Participants completed 20 practice standard visual search trials with feedback before the main experiment started. Participants were instructed to fixate on the center cross when no stimuli were presented on the screen. The main experiment was composed of 108 standard visual search trials, 72 critical search trials and 108 probe trials. As in the fMRI experiment, we used an uneven ratio (1:2) of veridical targets to non-target foils to maximize the number of non-target color presentations and to roughly equate the number of likely "yes" and "no" responses. Trials were presented in 12 blocks. All blocks started with 9 standard visual search trials, after which 12 critical search trials presented in half of the blocks and 18 probe trials presented in the other half.

Regions of interest selection

We assessed target representations in two resting-state networks defined from a large, independent sample of participants (Yeo et al., 2011): the frontoparietal control network (FPCN) and the visual network (VisN) (Figure S3.3). The 400 brain parcels (Schaefer et al., 2018) were projected onto the high-resolution anatomical image of each participant using the FreeSurfer cortical parcellation scheme (*http://surfer.nmr.mgh.harvard.edu*). Each parcel was matched to one of the seven functional networks identified by Yeo et al., 2011. Next, we decomposed FPCN into separate prefrontal and parietal subregions and divided VisN into central (i.e., striate and extrastriate cortex) and peripheral subregions. All the cortical parcels corresponding to the prefrontal-FPCN (PFC), the parietal-FPCN (PAR), and the central-VisN (VIS) were selected as regions of interest (ROIs) for the representational similarity analysis (Figure 3.3A). Mean number of voxels in each ROI are reported in Table 2. None of the voxels from one ROI were contiguous with voxels from another ROIs. We also included the bilateral auditory cortex (AUD) in the somatomotor network as control regions. All ROIs were then coregistered to the functional data.

Table 2. Mean number of voxels in each region of interest selected from the Schaefer atlas.

Region of interest	Hemisphere	# of voxels
PFC	L	1270
	R	2163
PAR	L	502
	R	552
VIS	L	1547
	R	1600
AUD	L	486

	R	442

fMRI data acquisition and preprocessing

MRI scanning was performed on a 3-Tesla Siemens Skyra scanner with a 32-channel phased-array head coil at the imaging center at University of California, Davis. Functional data were collected using a T2-weighted echoplanar imaging (EPI) sequence. Each volume contained 60 axial slices (2.2mm thickness) parallel to the AC-PC line (TR, 1805ms; TE, 28ms). Each scan acquired 215 volumes (388s) and consisted of 40 visual search trials (fixed intertrial interval 2000ms) and 56 probe trials (jittered interstimulus interval with a mean of 4000ms). A total of 8 scans were acquired. A MPRAGE T1-weighted structural image (TR, 1800ms; TE, 2.97ms; $1 \times 1 \times 1 mm^3$ resolution; 208 slices) was acquired for visualizing the associated anatomy. fMRI data were analyzed using SPM12 (Wellcome Trust Centre for Neuroimaging). The structural image was coregistered to the mean of the EPI images. Data preprocessing included slice timing correction and spatial realignment. We fitted the time series of each voxel with a general linear model (GLM) with 8 regressors (1 visual search condition and 7 probe conditions). The GLM also included regressors for each scan and 6 motion parameters.

Representational similarity analysis

Behavioral representation of target templates

The primary question of interest was whether we could decode a biased target template that reflects individual decision biases in target identification based on visual search experiences. We hypothesized that this effect would be clearest in lateral prefrontal cortex given its adaptive coding of task relevance, but also tested parietal and visual regions known to be contain target representations (Bettencourt & Xu, 2016; Ester et al., 2009; Harrison & Tong, 2009). To do this, we performed representational similarity analysis (RSA) by extracting behavioral and neural representational geometries from each participant (Kriegeskorte et al., 2008; Nili et al., 2014). The behavioral target representation was measured by constructing a representational dissimilarity matrix (RDM) from the proportion of “target yes” responses in the probe trials (Figure 3.2A). The target-yes responses were false alarms when the probe color was a non-target color, and a hit when the color was a target color. The value in each cell of the RDM indicates the dissimilarity of the dependent measure between each pair of probe stimuli (Figure 3.2B). For example, if the proportion of target-yes responses to the -5° probe color was about the same as the 0° probe color, similarity would be high irrespective of the actual proportion of target-yes responses to the -5° and 0° probe color (Figure S3.2). We compared the brain RDM estimated from the patterns of neural activity in a *priori* ROIs with two candidate model RDMs. The model RDMs included (1) a biased RDM (B) constructed from each participants’ own probe performance (Figure 3.2B); (2) a veridical RDM (V) (Figure 3.2E), which assumed the target template was normally distributed and centered at the target color 0° (Figure 3.2D; $\sigma = 7$ and $\mu = 0$) (Yu & Geng, 2019; Experiment 1; bidirectional group).

Because the two model RDMs were significantly correlated with each other (M ± 95% CI = .36 ± .10, $z_{19} = 3.92$, $p < .0001$), we tested for an effect of B(V) while controlling for the shared covariance between B and V, using partial correlation (Park et al., 2020). Specifically, we measured the extent to which the brain RDM estimated in each ROI was explained by B'(V'). For example, B' indicates the Euclidean distances between each pair of stimuli in *B* while regressing out its correlation with the pairwise Euclidean distances in *V*: $B' = B - \mathrm{corr}(B, V) * V$ (Figure 3.2C). After regressing out the partial correlation, the model RDMs were independent from each other while preserving high correlation with their original matrices (i.e., *B'* does not correlate with *V* while it still highly correlates with *B*).

Neural representation of target templates

A 7×7 brain RDM for each ROI was constructed using the Euclidean distance based on the patterns of neural activity for each of the seven probe stimuli. We used *t*-statistics instead of regression estimates to down-weight response estimates from noisier voxels (Misaki et al., 2010; Walther et al., 2016). These *t* values were then normalized (mean response of each voxel across conditions = 0) to remove univariate differences between conditions. To ensure that the selected ROIs contained meaningful information regarding the template rather than rank noise, we performed a split half cross validation procedure. Specifically, we divided the imaging data into two independent splits of odd and even runs (four runs per split) and computed the representational distance between each pair of probe stimuli across the two splits. For example, the cross-validated distance between -5° and 0° was estimated as the Euclidean distance between the neural activity of -5° in one split and 0° in the other split. Because noise is independent between the two splits, the expected value of this distance is 0 if there is no systematic difference between the two conditions (Walther et al., 2016).

Next, we confirmed that the brain RDM of each ROI discriminated different probe stimuli with good sensitivity using the exemplar discriminability index (EDI) (Nili et al., 2020). EDI is defined as the mean of representational distances between different probe stimuli compared to the mean of the representational distances between the same probe stimuli (i.e., the average of the off diagonal vs. the average of the main diagonal). We confirmed that the EDI in all ROIs was positive (one sample *t* test, *ts* > 3, *ps* < .005), except for the control regions (*ps* > .10), suggesting that the different probe stimuli were discriminable in ROIs based on multivariate neural activity patterns.

The extent to which the brain RDM in each ROI was explained by the model RDMs was estimated with the Kendall's τ_A rank correlation. The computed Kendall's τ_A correlations were then subtracted from each participant's baseline value, which was estimated as the mean of permuted rank correlations by randomizing stimulus labels 5000 times. For the group level inference, the significance of correlations was tested with the non-parametric Wilcoxon signed-rank test across participants (Nili et al., 2014). The resulting *p* values were corrected for multiple comparisons across the numbers of bilateral ROIs (*N* = 8), as well as the numbers of model RDMs (*N* = 2). We reported results corrected for family-wise error (FWE) with the Holm-Bonferroni method at $p < 0.05$, but stronger effects were indicated with asterisks.

Searchlight-based RSA

In order to be as inclusive as possible in searching for regions of the brain that might encode the target representations overall, we conducted a searchlight analysis (radius of 8mm) within the whole brain using the RSA toolbox (Nili et al., 2014) and custom MATLAB code. We correlated the brain RDM at each searchlight location with each participant's model RDMs (*B* and *V*) using Kendall's τ_A rank correlation. The results formed a continuous statistical map that show how well the model RDMs explained the brain RDM at the local brain regions. These images were further normalized, smoothed using an 8-

mm full-width at half maximum (FWHM) Gaussian kernel and Fisher's z transformed to confirm the statistical assumption (normality) required for the second-level parametric tests. Each participant's statistical map was then submitted to a second-level one sample *t* test to find the voxels with correlation values greater than 0. The threshold for the resulting statistical maps were set at the cluster level $p < .05$, FWE corrected for multiple comparisons and a minimum number of voxels > 50.

Drift diffusion model

The main analysis of the online experiment consisted of modeling visual search performance from the critical trials and probe performance (error rates and RT; Figure 3.5B and 3.5D) using a drift diffusion model. The separation between the two decision boundaries (a) and the non-decision time (t) were estimated as fitted free parameters that were the same across color distractor values for each participant while the drift rate (ν) was estimated as a free parameter per color condition. Here, we were interested in how the drift rate (ν), which characterizes the accumulation of noisy evidence over time until one of two decision boundaries is reached, differed across conditions (Ratcliff & McKoon, 2008). Drift rates in the critical search trials represent how easily the target can be distinguished from the distractor. Drift rates in the probe trials indicate how easily the probe stimulus can be identified as the target from memory. Higher drift rates indicate stronger evidence, whereas lower drift rates suggest weaker evidence.

All parameters were estimated using a hierarchical Bayesian parameter estimation method (Ratcliff & Childers, 2015). To perform hierarchical DDM, we used the Python-based toolbox, HDDM (Wiecki et al., 2013). The HDDM model was fit to accuracy-coded data (i.e., the upper and lower boundaries correspond to correct and incorrect responses, and the starting point was fixed at 0.5). For each participant's data, we used Markov chain Monte Carlo (MCMC) sampling methods to estimate the posterior distribution of each parameter. Five chains were run with 10000 samples for each chain. The first 5000 warm-up samples were discarded as burn-in. Convergence was assessed by computing the Gelman-Rubin $\hat{R}$ statistic for each parameter. The range of $\hat{R}$ values across all group parameter estimates was between 0.99-1.10, suggesting that the samples of the different chains converged. Goodness of fit was visually inspected with the posterior predictive check method (Figure 3.5) (Wiecki et al., 2013).

Supplemental Material

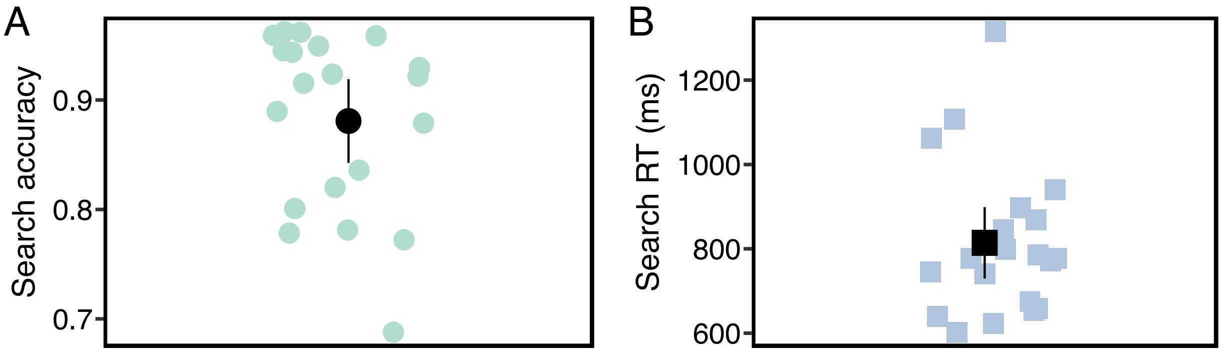

Figure S3.1. Visual search accuracy and RTs from the visual search trials. The colored dots represent individual data points, and the black ones indicate the mean values. All error bars are the 95% confidence intervals.

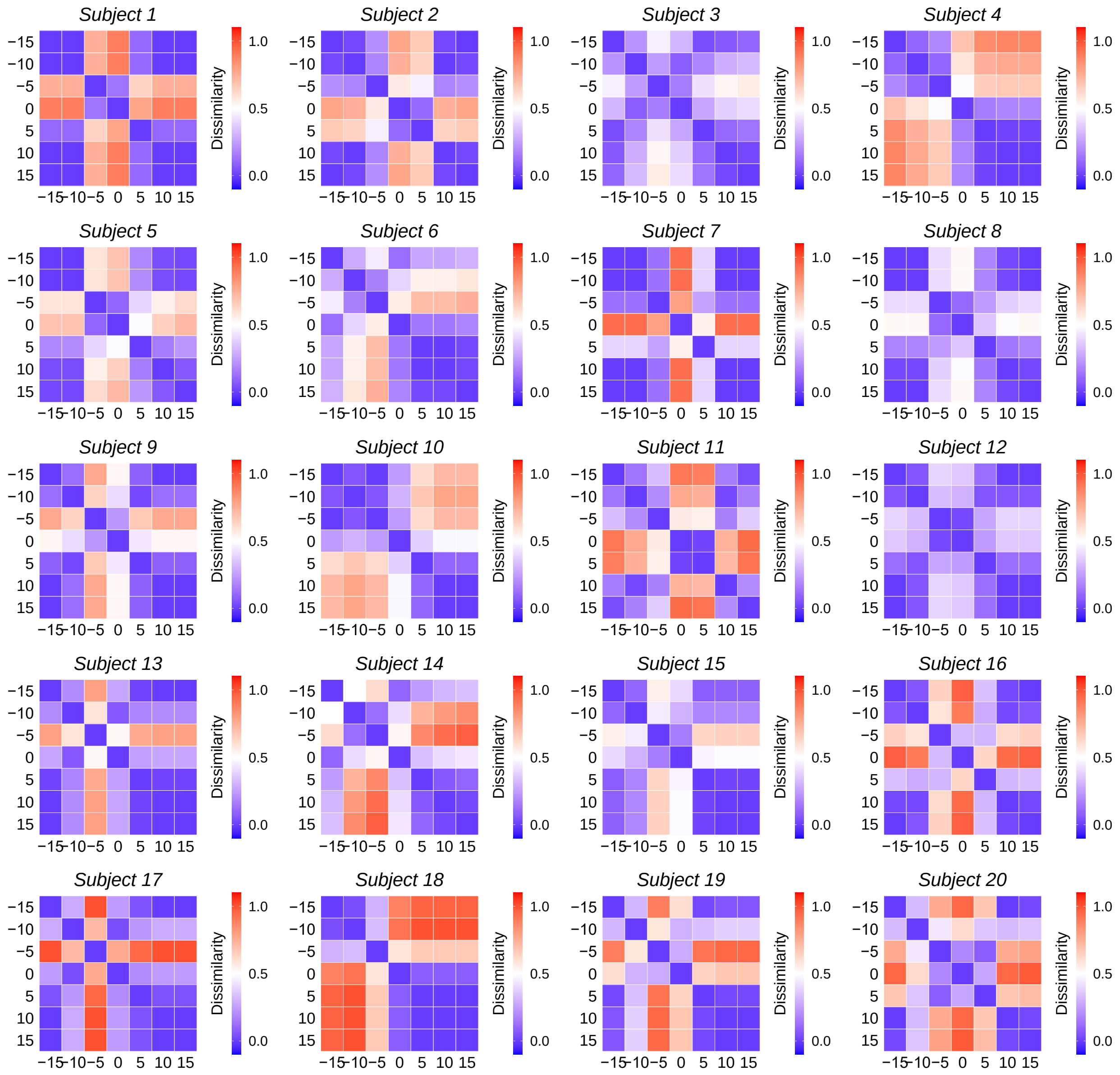

Figure S3.2. The individual biased behavioral RDM (*B*) generated by participants' own probe task performance.

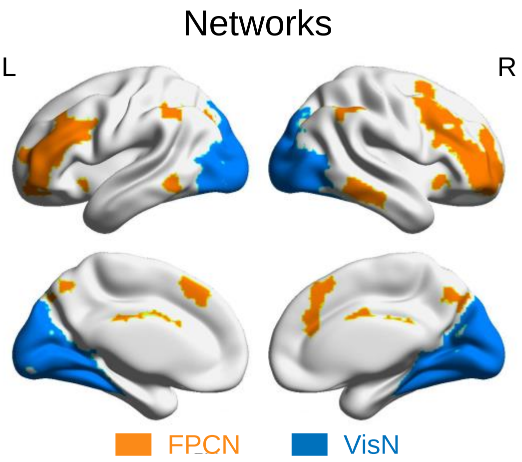

Figure S3.3. Two independently defined resting-state networks of a priori interest: frontoparietal control network (FPCN) and visual networks (VisN) (Yeo et al., 2011).

Button response RDM searchlight

The significant searchlight results observed in regions related to motor and somatosensory functions in the left hemisphere (contralateral to the right index and middle fingers that were used for button presses) raised the possibility that the selected ROIs were driven in part by the motor plan of making an index or middle finger button response, which corresponded to the yes/no target-match decision. Although the full *B′* and *V′* matrices cannot be explained by motor movements alone, to address this, we created a dissimilarity matrix that modeled the button responses *per se*, regardless of the actual probe stimulus. Specifically, each trial was labeled as either a “yes” trial or “no” trial based on the individual’s response. The group of “yes” and “no” trials were randomly split into two halves to create a response model RDM in which trials with the same response, irrespective of the actual stimulus, were maximally similar whereas trials with different responses were maximally dissimilar (Figure S3.4): the dissimilarity distance between the same responses was 0, and the distance between the different response types was 1. We then performed another whole brain searchlight for each participant using their individual button response RDM as the reference model. The group analysis identified only one significant region ($p < .001$, uncorrected) located in left PoG (Figure S3.4; [x, y, z] = [-44, -18, 58], $z_{19} = 3.53$, # of voxels = 92) in motor cortex contralateral to the right hand. 39 and 37 number of voxels in this cluster were overlapped with left PrG identified from the searchlight map with the biased and veridical RDM, respectively. The results support the notion that motor regions, e.g., left PrG, captured by the two RDMs of interest were involved in the actual motor response rather than response independent decision processes.

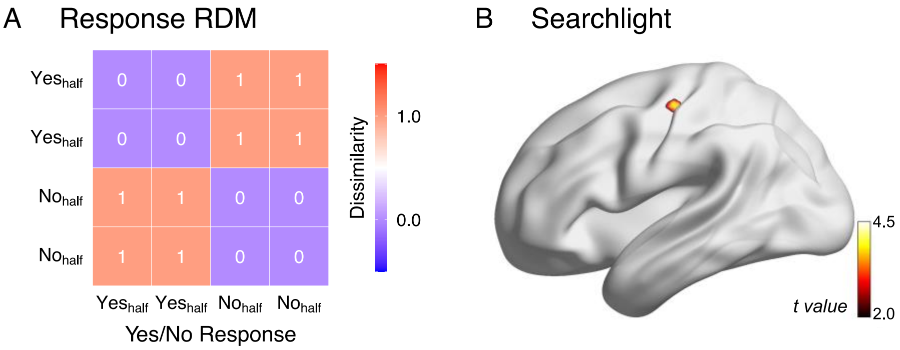

Figure S3.4. A) The button response behavioral RDM. B) Brain maps showing the clusters identified in the whole brain searchlight analysis, located in the left PoG.

References

Badre, D., & Nee, D. E. (2018). Frontal Cortex and the Hierarchical Control of Behavior. *Trends in Cognitive Sciences*, *22*(2), 170—188. https://doi.org/10.1016/j.tics.2017.11.005

Bae, G.-Y., Olkkonen, M., Allred, S. R., & Flombaum, J. I. (2015). Why some colors appear more memorable than others: A model combining categories and particulars in color working memory. *Journal of Experimental Psychology. General*, *144*(4), 744—763. https://doi.org/10.1037/xge0000076

Baldauf, D., & Desimone, R. (2014). *Neural Mechanisms of Object-Based Attention*. *344*, 5.

Bauer, B., Jolicoeur, P., & Cowan, W. B. (1996). Visual search for colour targets that are or are not linearly separable from distractors. *Vision Research*, *36*(10), 1439—1466. https://doi.org/10.1016/0042-6989(95)00207-3

Becker, S. I. (2010). The Role of Target–Distractor Relationships in Guiding Attention and the Eyes in Visual Search. *Journal of Experimental Psychology: General*, *139*(2), 247–265. https://doi.org/10.1037/a0018808

Bettencourt, K. C., & Xu, Y. (2016). Decoding the content of visual short-term memory under distraction in occipital and parietal areas. *Nature Neuroscience*, *19*(1), 150—157. https://doi.org/10.1038/nn.4174

Bichot, N. P., Heard, M. T., DeGennaro, E. M., & Desimone, R. (2015). A Source for Feature-Based Attention in the Prefrontal Cortex. *Neuron*, *88*(4), 832—844. https://doi.org/10.1016/j.neuron.2015.10.001

Bichot, N. P., Xu, R., Ghadooshahy, A., Williams, M. L., & Desimone, R. (2019). The role of prefrontal cortex in the control of feature attention in area V4. *Nature Communications*, *10*(1). https://doi.org/10.1038/s41467-019-13761-7

Birman, D., & Gardner, J. L. (2019). A flexible readout mechanism of human sensory representations. *Nature Communications*, *10*(1). https://doi.org/10.1038/s41467-019-11448-7

Bracci, S., Daniels, N., & Beeck, H. O. de. (2017). Task Context Overrules Object- and Category-Related Representational Content in the Human Parietal Cortex. *Cerebral Cortex (New York, NY)*, *27*(1), 310—321. https://doi.org/10.1093/cercor/bhw419

Brainard, D. H. (1997). The Psychophysics Toolbox. *Spatial Vision*, *10*(4), 433—436. https://doi.org/10.1163/156856897x00357

Bravo, M. J., & Farid, H. (2016). Observers change their target template based on expected context. *Attention, Perception, \textbackslash& Psychophysics*, *78*(3), 829—837. https://doi.org/10.3758/s13414-015-1051-x

Bundesen, C. (1990). A theory of visual attention. *Psychological Review*, *97*(4), 523—547. https://doi.org/10.1037/0033-295x.97.4.523

Castelhano, M. S., Pollatsek, A., & Cave, K. R. (2008). Typicality aids search for an unspecified target, but only in identification and not in attentional guidance. *Psychonomic Bulletin & Review*, *15*(4), 795–801. https://doi.org/10.3758/PBR.15.4.795

Chelazzi, L., Duncan, J., Miller, E. K., & Desimone, R. (1998). Responses of Neurons in Inferior Temporal Cortex During Memory-Guided Visual Search. *Journal of Neurophysiology*, *80*(6), 2918—2940. https://doi.org/10.1152/jn.1998.80.6.2918

Christophel, T. B., Klink, P. C., Spitzer, B., Roelfsema, P. R., & Haynes, J.-D. (2017). The Distributed Nature of Working Memory. *Trends in Cognitive Sciences*, *21*(2), 111–124. https://doi.org/10.1016/j.tics.2016.12.007

Cunningham, C. A., & Wolfe, J. M. (2014). The role of object categories in hybrid visual and memory search. *Journal of Experimental Psychology. General*, *143*(4), 1585—1599. https://doi.org/10.1037/a0036313

de la Vega, A., Yarkoni, T., Wager, T. D., & Banich, M. T. (2018). Large-scale Meta-analysis Suggests Low Regional Modularity in Lateral Frontal Cortex. *Cerebral Cortex*, *28*(10), 3414–3428. https://doi.org/10.1093/cercor/bhx204

Desimone, R., & Duncan, J. (1995). Neural Mechanisms of Selective Visual Attention. *Annual Review of Neuroscience*, *18*(1), 193—222. https://doi.org/10.1146/annurev.ne.18.030195.001205

D'Esposito, M., & Postle, B. R. (2015). The Cognitive Neuroscience of Working Memory. *Annual Review of Psychology*, *66*(1), 115—142. https://doi.org/10.1146/annurev-psych-010814-015031

Duncan, J. (2001). An adaptive coding model of neural function in prefrontal cortex. *Nature Reviews Neuroscience*, *2*(11), 820–829. https://doi.org/10.1038/35097575

Duncan, J. (2013). The Structure of Cognition: Attentional Episodes in Mind and Brain. *Neuron*, *80*(1), 35–50. https://doi.org/10.1016/j.neuron.2013.09.015

Duncan, J., & Humphreys, G. W. (1989). *Visual Search and Stimulus Similarity*. 26.

Ester, E. F., Serences, J. T., & Awh, E. (2009). Spatially Global Representations in Human Primary Visual Cortex during Working Memory Maintenance. *Journal of Neuroscience*, *29*(48), 15258—15265. https://doi.org/10.1523/jneurosci.4388-09.2009

Ester, E. F., Sprague, T. C., & Serences, J. T. (2015). Parietal and Frontal Cortex Encode Stimulus-Specific Mnemonic Representations during Visual Working Memory. *Neuron*, *87*(4), 893—905. https://doi.org/10.1016/j.neuron.2015.07.013

Ester, E. F., Sutterer, D. W., Serences, J. T., & Awh, E. (2016). Feature-Selective Attentional Modulations in Human Frontoparietal Cortex. *Journal of Neuroscience*, *36*(31), 8188—8199. https://doi.org/10.1523/jneurosci.3935-15.2016

Feredoes, E., Heinen, K., Weiskopf, N., Ruff, C., & Driver, J. (2011). Causal evidence for frontal involvement in memory target maintenance by posterior brain areas during distracter interference of visual working memory. *Proceedings of the National Academy of Sciences*, *108*(42), 17510—17515. https://doi.org/10.1073/pnas.1106439108

Funahashi, S., Bruce, C. J., & Goldman-Rakic, P. S. (1989). Mnemonic coding of visual space in the monkey's dorsolateral prefrontal cortex. *Journal of Neurophysiology*, *61*(2), 331—349. https://doi.org/10.1152/jn.1989.61.2.331

Fuster, J. M., & Alexander, G. E. (1971). Neuron Activity Related to Short-Term Memory. *Science*, *173*(3997), 652—654. https://doi.org/10.1126/science.173.3997.652

Geng, J. J., DiQuattro, N. E., & Helm, J. (2017). Distractor Probability Changes the Shape of the Attentional Template. *Journal of Experimental Psychology: Human*

Perception and Performance, *43*(12), 1993–2007. https://doi.org/10.1037/xhp0000430

Geng, J. J., & Witkowski, P. (2019). Template-to-distractor distinctiveness regulates visual search efficiency. *Current Opinion in Psychology*, *29*, 119—125. https://doi.org/10.1016/j.copsyc.2019.01.003

Harrison, S. A., & Tong, F. (2009). Decoding reveals the contents of visual working memory in early visual areas. *Nature*, *458*(7238), 632—635. https://doi.org/10.1038/nature07832

Hodsoll, J., & Humphreys, G. W. (2001). Driving attention with the top down: The relative contribution of target templates to the linear separability effect in the size dimension. *Perception \textbackslash& Psychophysics*, *63*(5), 918—926. https://doi.org/10.3758/bf03194447

Hout, M. C., & Goldinger, S. D. (2015). Target templates: The precision of mental representations affects attentional guidance and decision-making in visual search. *Attention, Perception \textbackslash& Psychophysics*, *77*(1), 128—149. https://doi.org/10.3758/s13414-014-0764-6

Kriegeskorte, N., Mur, M., & Bandettini, P. (2008). Representational Similarity Analysis – Connecting the Branches of Systems Neuroscience. *Frontiers in Systems Neuroscience*, *2*. https://doi.org/10.3389/neuro.06.004.2008

Lee, S.-H., Kravitz, D. J., & Baker, C. I. (2013). Goal-dependent dissociation of visual and prefrontal cortices during working memory. *Nature Neuroscience*, *16*(8), 997—999. https://doi.org/10.1038/nn.3452

Long, N. M., & Kuhl, B. A. (2018). Bottom-Up and Top-Down Factors Differentially Influence Stimulus Representations Across Large-Scale Attentional Networks. *The Journal of Neuroscience*, *38*(10), 2495—2504. https://doi.org/10.1523/jneurosci.2724-17.2018

Malcolm, G. L., & Henderson, J. M. (2009). The effects of target template specificity on visual search in real-world scenes: Evidence from eye movements. *Journal of Vision*, *9*(11), 8–8. https://doi.org/10.1167/9.11.8

Malcolm, G. L., & Henderson, J. M. (2010). Combining top-down processes to guide eye movements during real-world scene search. *Journal of Vision*, *10*(2), 4–4. https://doi.org/10.1167/10.2.4

Miller, B. T., & D'Esposito, M. (2005). Searching for "the Top" in Top-Down Control. *Neuron*, *48*(4), 535—538. https://doi.org/10.1016/j.neuron.2005.11.002

Miller, E. K., Erickson, C. A., & Desimone, R. (1996). Neural Mechanisms of Visual Working Memory in Prefrontal Cortex of the Macaque. *Journal of Neuroscience*, *16*(16), 5154—5167. https://doi.org/10.1523/jneurosci.16-16-05154.1996

Misaki, M., Kim, Y., Bandettini, P. A., & Kriegeskorte, N. (2010). Comparison of multivariate classifiers and response normalizations for pattern-information fMRI. *NeuroImage*, *53*(1), 103—118. https://doi.org/10.1016/j.neuroimage.2010.05.051

Moore, T., Armstrong, K. M., & Fallah, M. (2003). Visuomotor Origins of Covert Spatial Attention. *Neuron*, *40*(4), 671–683. https://doi.org/10.1016/S0896-6273(03)00716-5

Moore, T., & Zirnsak, M. (2017). Neural Mechanisms of Selective Visual Attention. *Annual Review of Psychology*, *68*(1), 47—72. https://doi.org/10.1146/annurev-psych-122414-033400

Navalpakkam, V., & Itti, L. (2007). Search Goal Tunes Visual Features Optimally. *Neuron*, *53*(4), 605—617. https://doi.org/10.1016/j.neuron.2007.01.018

Nili, H., Walther, A., Alink, A., & Kriegeskorte, N. (2020). Inferring exemplar discriminability in brain representations. *PLOS ONE*, *15*(6), e0232551. https://doi.org/10.1371/journal.pone.0232551

Nili, H., Wingfield, C., Walther, A., Su, L., Marslen-Wilson, W., & Kriegeskorte, N. (2014). A Toolbox for Representational Similarity Analysis. *PLoS Computational Biology*, *10*(4), e1003553. https://doi.org/10.1371/journal.pcbi.1003553

Panichello, M. F., & Buschman, T. J. (2021). Shared mechanisms underlie the control of working memory and attention. *Nature*, *592*(7855), 601–605. https://doi.org/10.1038/s41586-021-03390-w

Park, S. A., Miller, D. S., Nili, H., Ranganath, C., & Boorman, E. D. (2020). Map Making: Constructing, Combining, and Inferring on Abstract Cognitive Maps. *Neuron*, *107*(6), 1226-1238.e8. https://doi.org/10.1016/j.neuron.2020.06.030

Pelli, D. G. (1997). The VideoToolbox software for visual psychophysics: Transforming numbers into movies. *Spatial Vision*, *10*(4), 437—442. https://doi.org/10.1163/156856897x00366

Peltier, C., & Becker, M. W. (2016). Decision processes in visual search as a function of target prevalence. *Journal of Experimental Psychology: Human Perception and Performance*, *42*(9), 1466–1476. https://doi.org/10.1037/xhp0000248

Rainer, G., Asaad, W. F., & Miller, E. K. (1998). Selective representation of relevant information by neurons in the primate prefrontal cortex. *Nature*, *393*(6685), 577–579. https://doi.org/10.1038/31235

Rajsic, J., & Woodman, G. F. (2020). Do we remember templates better so that we can reject distractors better? *Attention, Perception, & Psychophysics*, *82*(1), 269–279. https://doi.org/10.3758/s13414-019-01721-8

Ratcliff, R., & Childers, R. (2015). Individual Differences and Fitting Methods for the Two-Choice Diffusion Model of Decision Making. *Decision (Washington, D.C.)*, *2015*.

Ratcliff, R., & McKoon, G. (2008). The Diffusion Decision Model: Theory and Data for Two-Choice Decision Tasks. *Neural Computation*, *20*(4), 873—922. https://doi.org/10.1162/neco.2008.12-06-420

Reynolds, J. H., & Heeger, D. J. (2009). The Normalization Model of Attention. *Neuron*, *61*(2), 168—185. https://doi.org/10.1016/j.neuron.2009.01.002

Riggall, A. C., & Postle, B. R. (2012). The Relationship between Working Memory Storage and Elevated Activity as Measured with Functional Magnetic Resonance Imaging. *The Journal of Neuroscience*, *32*(38), 12990—12998. https://doi.org/10.1523/jneurosci.1892-12.2012

Sarma, A., Masse, N. Y., Wang, X.-J., & Freedman, D. J. (2016). Task Specific versus Generalized Mnemonic Representations in Parietal and Prefrontal Cortices. *Nature Neuroscience*, *19*(1), 143—149. https://doi.org/10.1038/nn.4168

Schaefer, A., Kong, R., Gordon, E. M., Laumann, T. O., Zuo, X.-N., Holmes, A. J., Eickhoff, S. B., & Yeo, B. T. T. (2018). Local-Global Parcellation of the Human Cerebral Cortex from Intrinsic Functional Connectivity MRI. *Cerebral Cortex*, *28*(9), 3095—3114. https://doi.org/10.1093/cercor/bhx179

Scolari, M., Byers, A., & Serences, J. T. (2012). Optimal Deployment of Attentional Gain during Fine Discriminations. *The Journal of Neuroscience*, *32*(22), 7723—7733. https://doi.org/10.1523/jneurosci.5558-11.2012

Serences, J. T., Ester, E. F., Vogel, E. K., & Awh, E. (2009). Stimulus-Specific Delay Activity in Human Primary Visual Cortex. *Psychological Science*, *20*(2), 207—214. https://doi.org/10.1111/j.1467-9280.2009.02276.x

Squire, R. F., Noudoost, B., Schafer, R. J., & Moore, T. (2013). Prefrontal Contributions to Visual Selective Attention. *Annual Review of Neuroscience*, *36*(1), 451–466. https://doi.org/10.1146/annurev-neuro-062111-150439

Sreenivasan, K. K., Vytlacil, J., & D'Esposito, M. (2014). Distributed and Dynamic Storage of Working Memory Stimulus Information in Extrastriate Cortex. *Journal of Cognitive Neuroscience*, *26*(5), 1141—1153. https://doi.org/10.1162/jocn_a_00556

Swaminathan, S. K., & Freedman, D. J. (2012). Preferential encoding of visual categories in parietal cortex compared with prefrontal cortex. *Nature Neuroscience*, *15*(2), 315–320. https://doi.org/10.1038/nn.3016

Treisman, A. M., & Gelade, G. (1980). A feature-integration theory of attention. *Cognitive Psychology*, *12*(1), 97—136. https://doi.org/10.1016/0010-0285(80)90005-5

Walther, A., Nili, H., Ejaz, N., Alink, A., Kriegeskorte, N., & Diedrichsen, J. (2016). Reliability of dissimilarity measures for multi-voxel pattern analysis. *NeuroImage*, *137*, 188—200. https://doi.org/10.1016/j.neuroimage.2015.12.012

Wiecki, T. V., Sofer, I., & Frank, M. J. (2013). HDDM: Hierarchical Bayesian estimation of the Drift-Diffusion Model in Python. *Frontiers in Neuroinformatics*, *7*. https://doi.org/10.3389/fninf.2013.00014

Wolfe, J. M. (2021). Guided Search 6.0: An updated model of visual search. *Psychonomic Bulletin & Review*. https://doi.org/10.3758/s13423-020-01859-9

Yeo, B. T. T., Krienen, F. M., Sepulcre, J., Sabuncu, M. R., Lashkari, D., Hollinshead, M., Roffman, J. L., Smoller, J. W., Zöllei, L., Polimeni, J. R., Fischl, B., Liu, H., & Buckner, R. L. (2011). The organization of the human cerebral cortex estimated by intrinsic functional connectivity. *Journal of Neurophysiology*, *106*(3), 1125—1165. https://doi.org/10.1152/jn.00338.2011

Yu, X., & Geng, J. J. (2019). The Attentional Template Is Shifted and Asymmetrically Sharpened by Distractor Context. *Journal of Experimental Psychology: Human Perception and Performance*, *45*(3), 336–353. https://doi.org/10.1037/xhp0000609

Chapter 4: Attentional Guidance and Match Decisions Rely on Different Template Information during Visual Search

The following chapter consists of a manuscript that has been submitted for publication at *Psychological Science*

Abstract

When searching for a target object, we engage in a continuous “look-identify” cycle in which we use known features to guide attention towards potential targets and then to decide if it is indeed the target. Target information in memory (the target or attentional template) is typically characterized as a having a single, fixed, source. However, this notion is challenged by a recent debate over whether flexibility in the target template is “relational” (Becker, 2010) or “optimal” (Navalpakkam & Itti, 2007). Based on evidence from two studies in college students (*N*=30 Experiment 1; *N*=70 Experiment 2), we propose a resolution to this debate by proposing that the initial guidance of attention uses a coarse “relational” code, but subsequent decisions use an “optimal” code. Our results offer a novel perspective that template information differs in precision when guiding sensory selection and when making identity decisions during visual search (Wolfe, 2021).

Introduction

Imagine you are doing a field survey in India and the guide reminds you to be cautious of a tiger hiding in the grasslands. As you look around, the environment might be flooded with different types of animals, but there is a limit on how much information can be processed in any given moment. Therefore, we must hold a memory representation of the tiger, known as the “target” or “attentional” template, in mind while recursively locating and then inspecting candidate creatures within the same context until the target tiger is found (Malcolm & Henderson, 2010; Wolfe, 2021). Although the concept of a target template has been a staple of attention research for decades (Duncan & Humphreys, 1989; Eriksen, 1953; Green & Anderson, 1956), it has been largely assumed to contain a single, static, and veridical representation of what we are looking for. Recent studies have begun to challenge this notion by showing that template representations are dynamic and shift “off-veridical” when doing so increases the target-to-distractor distinctiveness (Geng & Witkowski, 2019). The goal of these studies is to go further and test the hypothesis that two versions of the search template are used at the guidance and decision stages of the “look-identify” cycle (Wolfe, 2021). While both can be off-veridical, we hypothesize that guidance operates on a more relational template whereas target decisions rely on a more optimal code.

Standard models of feature-based attention posit that the optimal template for a target contains highly specific information about the veridical features of the target (Treue & Trujillo, 1999), but studies in which the search target appears predictably amongst linearly separable distractors find that the target representation shifts “off-veridical” away from distractors (Bauer et al., 1996; Hodsoll & Humphreys, 2001; Scolari et al., 2012).

For example, search for an orange tiger amongst yellow grasslands results in an attentional bias towards color values that are “redder” than the actual orange of the tiger. Becker and colleagues (Becker, 2010; Martin & Becker, 2018) propose that this effect is due to observers using a “relational” rule to guide attention and first saccades towards the “reddest” object in the visual environment. In contrast, others argue that the bias is due to an “optimal shift” in the central tendency of the target tuning curve to more effectively discriminate the target from distractors (Geng et al., 2017; Navalpakkam & Itti, 2007; Scolari et al., 2012; Yu & Geng, 2019).

Even though the two positions may seem similar, they make very different predictions that have implications for understanding how target information is encoded and flexibly used during visual search. In particular, the two theories differ in predictions for how inclusive the template is of feature values that are opposite to the experienced distractors (i.e., the “negative” color values in Figure 4.1). The relational account predicts very broad inclusion of negative feature values because they all share the relational feature that defines the target from expected distractors (i.e., the “reddest”) (Figure 4.1A). There must be a boundary to relational inclusiveness, but this has not been established empirically. The optimal gain model instead predicts a shift in the central tendency towards a more negative value (i.e., being “slightly redder” than the orange target) but inclusion within the template of both negative and positive color values are scaled by distance from the shifted central value (Figure 4.1B). These differences can be visualized as the width of a response filter (Figure 4.1, left panel) or more generally as similarity matrices that capture the second-order pattern of expected responses (Figure 4.1, right panel).

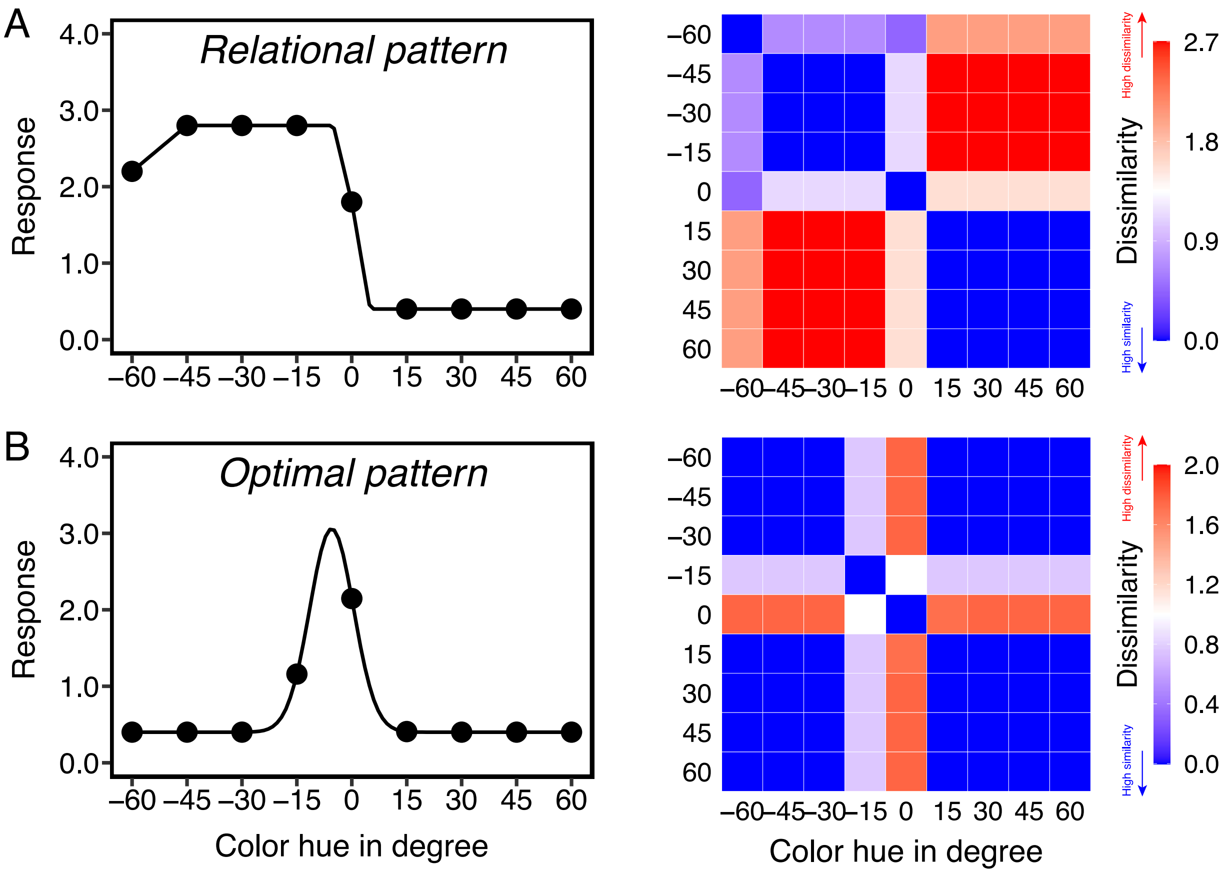

Figure 4.1. Simulated responses to colored stimuli in an experimental context in which the target color is depicted at 0° (e.g., orange) and expected distractors are positive rotations from the target (e.g., "yellower" hues). "Response" refers to any of several possible dependent variables, including the probability of a first saccade to an object or a decision that object is the target. Similarity matrix generated from the same data computed as the absolute difference between responses to each pair of stimuli. Similarity analyses are a particularly useful method to directly compare patterns of data across modalities with different units of measurement (e.g., manual responses, eye metrics, and model estimates) (Kriegeskorte et al., 2008). A) The relational account predicts higher attentional priority, and therefore a greater proportion of behavioral responses, to all features that fit the relational rule that distinguishes targets from distractors such as being the "reddest" object. This results in high similarity in expected responses to all stimuli with negative values, as illustrated by the dissimilarity matrix. C) The optimal gain model predicts a shift in the central tendency of the target representation with all other features are scaled by distance from the center value. This results in scaled similarity for both negative and positive feature values. See Methods (statistical analysis) for a detailed description of how simulated data points were estimated.

One possible explanation for why there appears to be evidence for two theories that ostensibly refer to the same "target template," is that they derive from studies using different methods. Some use RT or first saccade destinations as the metric of the template

(Martin & Becker, 2018), while others use a separate probe task to measure the learned target feature (Navalpakkam & Itti, 2007; Scolari & Serences, 2009; Yu & Geng, 2019). We hypothesize that these differences may tap into different stages of the look-identify cycle: the first saccade reflects early guidance of attention to the best match whereas the probe task requires binary decisions regarding target identity. This leads to an important question of whether attentional guidance and match decisions use the same or different template information during visual search. We hypothesize that guidance might rely on a coarser version of the template and match decisions require a more precise representation (Bravo & Farid, 2014; Martin & Becker, 2018; Rajsic & Woodman, 2020; Wolfe, 2021; Wu et al., 2013).

The template has long been hypothesized to guide attention and eye-movements to potential targets by modulating sensory gain (Desimone & Duncan, 1995; Reynolds & Heeger, 2009; Treisman & Gelade, 1980), but only more recently has it been explicitly postulated to operate on decision processes about the target match as well (Bravo & Farid, 2014; Geng & Witkowski, 2019; Wolfe, 2012). For example, Hout & Goldinger (2015) hypothesized that the target template serves a dual-function to guide attention to potentially relevant items and to compare visual inputs to the memory template for target verification or rejection (see also Rajsic & Woodman, 2020). While such studies have used eye metrics to measure the effect of the template at two time-points within the "look-identify" cycle, few have considered whether the information used during guidance and decisions is the same or different. One exception to this is a proposal by Wolfe (2021) that argues the search template can (and should) be divided into two: a "guiding" template in working memory that is used to direct attention to items that might be the target; and a “target” template in long term memory that is used to determine if a candidate object is, in fact, the target. The idea that there may be two active templates, one for guidance and one for target decisions is consistent with evidence that it is possible to hold one active template in working memory (to guide search) while holding one or more other target representations in a latent state within working memory or in long-term memory (Olivers et al., 2011; Woodman et al., 2013).

The aim of the current experiments is to test if attentional guidance and target match decisions rely on different information during visual search. Although we frame our hypothesis in terms of a single search template that has two informational formats during guidance versus decisions, the concept is compatible with Wolfe’s (2021) characterization of separate templates for guidance and the target memory. Using a visual search task for a target amongst linearly separable distractors, we test the hypothesis that early attentional guidance will be based on relational information (e.g., prioritizing the “reddest” object irrespective of its exact hue) whereas subsequent match decisions will be made against an “optimal” off-target feature (e.g., the slightly redder version of the orange target). If true, this would suggest that attentional guidance operates on a coarser code to weight sensory information and target match decisions use a more precise representation to determine identity. Our findings offer a novel perspective on how template information operates to guide attention and make identity decisions during visual search.

Experiment 1

The purpose of this experiment was to use eye-tracking to investigate whether distinct template information is used during the guidance and decision making stages of the “look-identify” visual search cycle. We use eye data as our main dependent measure of interest to test the hypothesis that guidance (first saccades) will be driven by the *relative* target feature (Figure 4.1A) but that match decisions (fixation dwell times) will be determined by *optimal* off-target feature tuning (Figure 4.1B).

Method

Participants. To determine the appropriate sample size for Experiment 1, we first conducted a pilot study with 7 subjects (data were not included in Experiment 1) using the similar methods and procedures. The smallest effect size of the two dependent measures of interest (in this case fixation dwell times, r = .55) was entered into G*power calculation (http://www.gpower.hhu.de/). The results estimated that N = 30 was necessary to detect significant effects (p = .05, two-tailed) with a power .9. Therefore, thirty subjects (10 males, 1 left-handed, ages from 18-23) from University of California, Davis participated in Experiment 1 in partial fulfillment of a course requirement. Each participant was provided written informed consent in accordance with the local ethics clearance as approved by the National Institutes of Health. Each participant’s color vision was assessed by self-report and an online color blindness test (https://colormax.org/color-blind-test). All participants had normal or corrected-to-normal vision and all had typical color vision.

Apparatus. Participants were seated in a sound attenuated room 60cm away from a ASUS MG279Q monitor with a spatial resolution of 1920 × 1200 pixels and a refresh rate of 60hz. The operating system was Windows 7, and Matlab Psychtoolbox (Brainard, 1997; Pelli, 1997) was used to create all stimuli. Eye movements were tracked using a video based eye-tracking system (Eyelink 1000, SR Research, Ontario, Canada) sampling from the right eye at 500 Hz.

Stimuli. All stimuli were presented against a gray background (luminance = 37.0 cd/m^2). The target (194°) and distractor colors were selected from a color wheel defined in CIELAB color space (a, b coordinates = 0, 0; luminance = 70; from Bae et al., 2015). We used a green-blue border color as the target color to control for the potential color category effects on responses (Bae et al., 2015). Experiment 1 included three types of trials: 1) *standard* visual search trials to set up expectations for the distractor colors; 2) *critical* search trials to assess how target templates are used during guidance and decision making stages of visual search; and 3) template *probe* trials to measure the template contents independent of simultaneous distractor competition.

Standard visual search trials (Figure 4.2) were composed of a target and five distractor circles (3°×3°), located equidistantly along an imaginary circle (diameters: 12°×12°). The locations of all six stimuli were randomly rotated 10 degrees clockwise or counterclockwise along the imaginary circle on every trial in order to prevent fixed expectations of where each stimulus would be located. The color of the five distractors were either all negatively or positively rotated 10 degrees from the target color. The rotational direction (positive or negative) was counterbalanced across subjects, so that each subject only saw one set of distractors (Yu & Geng, 2019). Because the directionality of the distractor colors did not affect performance (*ps* > .15, BF_{01} > 1.30), this factor was not included in subsequent analyses to maximize power. For descriptive simplicity, the distractors from the standard search trials (i.e., "trained" distractor colors) will always be referred to as positive rotations from the target. Each object contained either a left or right oriented line (1° of visual angle; black). Participants were asked to report the tilt of the line within the target circle.

Critical search displays (Figure 4.2) were identical to the standard search displays with only one exception: one of the regular circle distractors was replaced with a dodecagon shape (henceforth referred to as the "critical distractor") (Martin & Becker, 2018). We used a different shape for the critical distractor because we wished to use the true target color as a critical distractor in order to test how observers responded to it when the template shifts off-veridical. A different shape was used to avoid the presence of two target objects on a single trial. The critical distractor color was selected from a range of -60° to 60° from the target color, in steps of 15°. This resulted in a total of 9 possible critical distractor colors. Among the 9 colors, the -45° and 45° distractors were focal colors within the green and blue color categories, respectively. Thus, the ±60° distractors were beyond the blue-green color category boundary (Bae et al., 2015) and served to interrogate the boundary conditions of the relational and optimal theories.

Probe trials contained a color wheel (12° of visual angle radius; 2.1° of visual angle thickness) defined by the same LAB space coordinates was displayed (Figure 4.2). The inner colored circle presented at the center of the screen was an enlarged version of where the mouse was pointing at on the wheel. The color wheel was randomly rotated on each presentation.

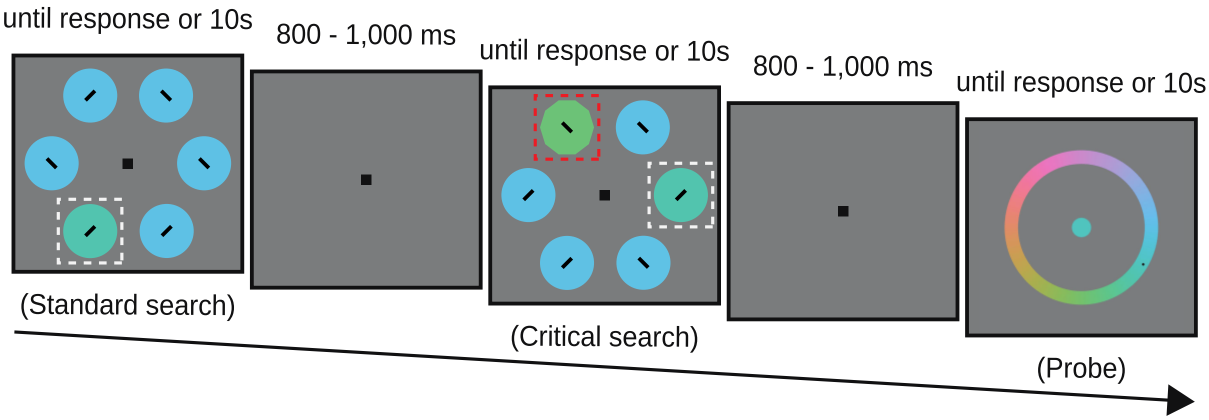

Figure 4.2. Example of *standard* and *critical* visual search trials and template *probe* trials in Experiment 1. *Standard* and *critical* visual search trials: Participants were instructed to locate the target color circle and report the line orientation within. A high tone (600 hz) was given for correct responses, and a low tone (200 hz) for incorrect responses. The dashed white squares illustrate the target and the red square illustrates the critical distractor, but were not visible to the participants. Template *probe* trials: participants were instructed to report the target color on the wheel by clicking on its location. The central dot illustrated the color over which the mouse dot hovered. No feedback was provided in the probe task.

Design. Participants completed 20 practice trials before the experiment started. The main experiment was composed of 324 standard visual search trials, 324 critical search trials and 60 template probe trials. Trials were presented in six blocks. The three types of trials were randomly interleaved within each block, with the constraint that there were no consecutive template probe trials. The locations of the target and distractors were randomly selected on each visual search trial. The target and critical distractor were equally likely to appear at all six possible locations, but the target and critical distractor were never adjacent to each other within a trial. Each search display contained an equal number of left or right oriented lines within the objects. The lines within the target and critical distractor were equally likely to be oriented to the left or right.

Procedure. The target color was presented to the participant before the experiment started. Participants were encouraged to make a fast and precise eye movement, and take their time to make the button press to ensure high accuracy of the manual response. A 9-point calibration was performed at the beginning of the experiment. To ensure that the eyes were fixated on the central square (.3°×.3°, black) at the onset of each search display, each trial began only after gaze was detected within a 1.5°×1.5° box around the fixation square for 200ms. Upon presentation of the display, participants searched for the predefined target-color circle and reported the line orientation inside by pressing the left or right mouse button with their right hand. The search display was presented until the manual response or up to 10s. Auditory feedback was provided immediately following the responses (600hz tone for correct; 200hz tone for incorrect).

In the probe trials, the color wheel remained on screen until the manual response or up to 10s. Participants were instructed to report the target color on the color wheel by clicking on its location with a mouse. No feedback was provided in the probe trials. A central fixation square was presented for 800-1000ms between trials.

Statistical analysis. The *standard* visual search trials were mainly used to establish expectations for the distractor colors. Overall search performance was high (accuracy: *M* = .97, *SD* = .02; RT: *M* = 1158ms, *SD* = 309ms) indicating that participants had a target representation that could be successfully distinguished from distractors. The data of primary interest therefore included only the *critical* search and *probe* trials; only data from these trials are described in subsequent analyses.

Trials with errors were excluded from the analyses; these included trials in which participants incorrectly identified the orientation of the line within the target color, or the total trial duration exceeded 3 standard deviations of that participant's mean reaction time. This resulted, in a loss of 4.8% of data (see Supplemental materials for full description of error rates and RT data). Furthermore, when the first saccade could not be assigned to a stimulus or when the eye movement never left the fixation region, the respective trials were excluded from the analyses, which led to a further loss of 5.2% data. Trials where the first saccade started more than 1000ms after the trial began were also removed, which accounted for .16% data.

The goal of Experiment 1 was to use eye data to directly compare the relational and optimal models of template shifting during visual search. Although sharing some similarities, the two models make qualitatively different predictions for how *critical distractors*, particularly those from the "negative" (i.e., untrained) direction of the target will be processed. The predictions from the two models, illustrated in Figure 4.1, were applied to both the proportion of first saccades on the critical distractors as well as fixation dwell times to decide that the stimulus is *not* the target. Specifically, if attention was tuned to the *relative* target feature, first saccades should be captured by all negative critical distractors more than the positive ones (Figure 4.1A). In contrast, the optimal gain theory predicts that first saccades should follow a Gaussian tuning curve with a peak over an *optimal* off-veridical feature (Figure 4.1B). We chose the following values for our simulation parameters based on the findings from our previous study (Yu & Geng, 2019): $\boldsymbol{\sigma} = 6$ (width of the gaussian tuning curves), and $\mu = -4$ (mean of the gaussian tuning curves).

In order to statistically compare our results against the theoretical models, we chose to convert each dependent measure of interest (first saccades and fixation dwell times) into a normalized space based on response similarity. Representational similarity analysis (RSA) is commonly used in brain imaging studies to convert data from very different units including brain, behavior, and computational models into a common space for comparison (Kriegeskorte et al., 2008; Nili et al., 2014). Using RSA in this study has several advantages: first, all dependent measures can be compared against both theoretical models without unit conversion or adjustments based on model specific parameters; second, the overall pattern of the data can be established without the need to directly compare single data points (e.g., using a series of t-tests); and third, similarity matrices are "parameter free" and the fit of the data to the theoretical models is determined by a simple correlation between the two patterns.

The primary analysis consisted of converting first saccade and dwell time data from critical search trials into representational dissimilarity matrices (RDM). The value in each cell of the RDM indicates the dissimilarity (inverse of similarity) of the dependent measures between a pair of stimulus conditions (Figure 4.3B and 4.3D). For example, if the proportion of first saccades to the -15° critical distractor was about the same as the -30° distractor, similarity would be high irrespective of the actual proportion of first saccades to the -15° and -30° distractors. The diagonal entries are dissimilarity values between identical conditions and are 0, by definition. Once similarity matrices were computed for the first saccades and fixation dwell times, the primary analysis involved correlating each eye data RDM with each of the two theoretical RDMs to determine which of the two models better describe the data. The two theoretical RDMs were not significantly correlated (*r* = -0.1, *p* = .56). Thus, any correlation between the eye data RDMs and each theoretical matrix cannot be explained by partial correlations with the other.

The significance of correlations between the eye data and theoretical RDMs was evaluated by permutation tests. The null distribution for the correlation was estimated by randomly rearranging the stimulus labels of one of the two RDMs of interests for each participant. Then, we correlated this randomized similarity matrix with another RDM of interest, and computed the spearman correlations between those two RDMs. This step was repeated 10,000 times for each set of data and used to create a null distribution of permuted correlations. The *p* value of the true correlation was calculated as the rank order of the true correlation in the permuted null distribution. For example, if the real correlation is larger than any of the permuted values within the null distribution, then the *p* value is estimated as $p < .0001$. We rejected the null hypothesis if the real correlation was larger than the top 500th permuted correlation ($p < .05$).

Results

Analysis of the first saccades that went to the critical distractors. The proportion of first saccades to each critical distractor (Figure 4.3A) were converted to a representational dissimilarity matrix (RDM) (Figure 4.3B) for comparison against the relational (Figure 4.1A) and optimal model matrices (Figure 4.1B) using a permutation test by randomizing stimulus labels (see Methods). The first saccade RDM had a significantly positive correlation with the relational RDM (r_{rel} = .71, p_{rel} = .0001), but not the optimal RDM (r_{opt} = .003, p_{opt} = .44). In addition, the r values from these correlations were compared against each other using a permutation test and found to be significantly different, $p(r_{\text{rel}} > r_{\text{opt}}) = .0001$, confirming that the first saccade RDM was more strongly correlated with the relational RDM than with the optimal RDM. These results strongly support the hypothesis that early attentional guidance, indexed by the first saccade, was tuned to the *relative* feature of the target, in replication of Becker and colleagues (Becker, 2010; Martin & Becker, 2018). However, while all negative critical distractors had a high likelihood of capturing attention, the proportion of first saccades to negative distractors did gradually decrease as color similarity decreased, suggesting the strength of capture was weakly modified by color similarity (Figure 4.3A).

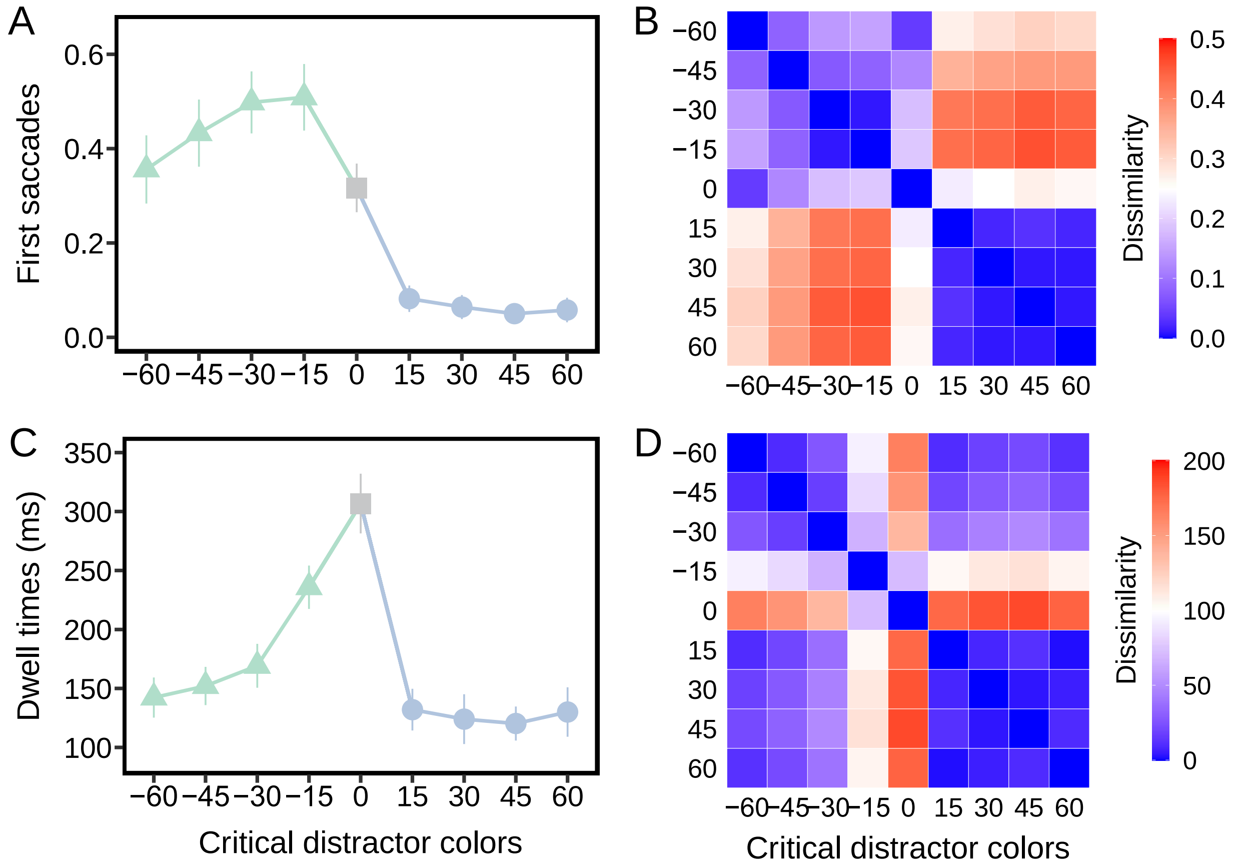

Figure 4.3. A) The proportion of first saccades to the critical distractors. B) The first saccade RDM averaged across participants. C) The fixation dwell times on the critical distractors. D) The fixation dwell time RDM averaged across participants. All error bars are the 95% confidence intervals.

Analysis of the fixation dwell times on the critical distractors. We next compared the RDM (Figure 4.3D) converted from the mean fixation dwell times (Figure 4.3C) against each of the two theoretical model RDMs. The dwell time RDM was significantly correlated with the optimal RDM ($r_{opt} = .67$, $p_{opt} = .004$), but not with the relational RDM ($r_{rel} = .04$, $p_{rel} = .28$). Additionally, the correlation between the dwell time RDM and the optimal RDM was stronger than between the dwell time RDM and the relational RDM, $p(r_{opt} > r_{rel}) = .0001$. These results demonstrate that the target match decisions, occurring once an object was fixated, followed the optimal tuning mode (Navalpakkam & Itti, 2007; Yu & Geng, 2019). These results were replicated in a second experiment that used a finer grained measurement for near target (±5°) critical distractors (see Supplemental materials Experiment 1b). It should be noted that the modulation of color similarity on the fixation dwell times, as presented in Figure 4.3C, was asymmetrical between the positive and negative directions. The negative distractors appeared to be more difficult to reject as non-targets than the corresponding positive ones, suggesting that the match decisions were more difficult overall in the negative direction, hinting at a contribution from the relational model.

Analysis of the probe performance. The probe task measured the contents of the target template, which are presumed to be held in memory (Giesbrecht et al., 2013; Woodman et al., 2013), uncontaminated by many processes involved in concurrent visual search, such as those necessary for resolving target selection and distractor suppression. The relative click distance from the true target color was divided into 5° bins (Figure 4.4A) and then converted to an RDM (Figure 4.4B). As expected, there was a significantly positive correlation between the probe RDM and the optimal RDM (r_{opt} = .80, p_{opt} = .004), but a non-significant correlation between the probe RDM and the relational RDM (r_{rel} = -.05, p_{rel} = .48). The comparison between the r values confirmed that the probe RDM was more strongly correlated with the optimal RDM than with the relational RDM, $p(r_{\text{opt}} > r_{\text{rel}})$ = .0001. This replicated previous findings (Geng et al., 2017; Navalpakkam & Itti, 2007; Scolari & Serences, 2009; Yu & Geng, 2019) that the target representation was shifted away from distractors to enhance optimal off-target features to increase the template-to-distractors distinctiveness (Geng & Witkowski, 2019).

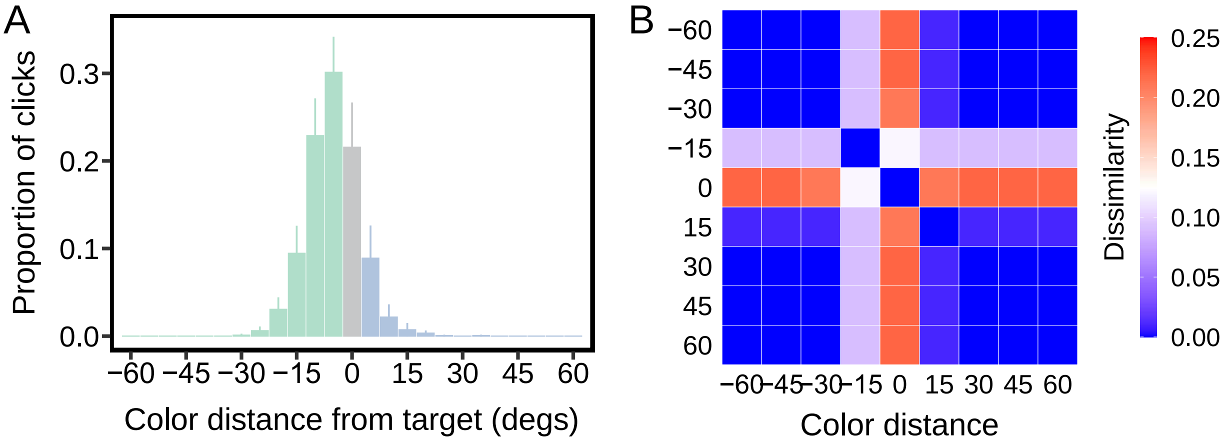

Figure 4.4. A) Group averages of relative click distance from the veridical target color in the template probe task. Raw data were divided into 5° bins. All error bars are the 95% confidence intervals. B) The probe RDM averaged across participants.

Experiment 2

We concluded from Experiment 1 that attentional guidance and target match decisions rely on a relational and an optimal code, respectively. However, dwell times, which were used to infer decision processes may not have been a pure measurement of target decisions since they were terminated based on a final “non-target” decision that could also rely on shape information. Furthermore, while first saccades are routinely considered reflection of guiding templates, fixation dwell times are a less standard measurement of decision processes. To address this in Experiment 2, we applied the drift diffusion model (DDM) to visual search performance to characterize how accurately and quickly the target was discriminated from distractors. To do this, we modified the search paradigm to include only one target and one distractor, which were always the same shape. Additionally, in order to test the relationship between long-term memory representations of the target and the drift rates, we again included the independent continuous memory probe task. Finding a correlation between the long-term memory of the target color and the target match decision (drift rates) would suggest that the target template held in long-term memory is used to generate target match decisions (Wolfe, 2021).

Method

Participants. To determine the sample size for Experiment 2, we first conducted a pilot study with 25 subjects (data were not included in Experiment 2) using the similar methods and procedures. The effect size for the correlation between drift rates and probe responses (r = .377) was entered into G*power calculation and estimated that N = 69 necessary to detect significant effects (p = .05, two-tailed) with a power .9. We opted for a sample size of 70 to allow counterbalancing of the distractor colors in the standard visual search trials. Data were collected online until we obtained a sample of 70 participants after exclusion criteria (accuracy in the standard search was below 75%) were applied. 40 participants were excluded from data analysis. A large number of outliers was expected due to the fact that the experiment was conducted online and we did not provide any feedback (see Procedures for detailed information). 70 participants (16 males, 6 left-handed, ages from 18 - 31) from University of California, Davis participated online in Experiment 2 in partial fulfillment of a course requirement. Each participant was provided written informed consent in accordance with the local ethics clearance as approved by the National Institutes of Health. Each participant's color vision was assessed by self-report. All participants had normal or corrected-to-normal vision and all had normal color vision.

Stimuli. The experiment was conducted entirely online through Testable (https://www.testable.org/). All stimuli were created in Illustrator, saved as PNG files and uploaded to Testable.org. Although we expected colors to vary when viewed on different monitors, the relationship between the target and distractors was expected to present across participants. Variability was expected to disadvantage our ability to detect the hypothesized optimal pattern in the data since the optimal pattern requires greater precision in distinguishing colors. All stimuli were presented against a gray background (color hue = '#808080'). The target and distractor color (10°) in the *standard* visual search trials were identical to Experiment 1. Each search trial (Figure 4.5) consisted of two bilaterally presented target and distractor circles (radius: 135 pixels) at the center of the screen (distance between the centers of the two circles: 400 pixels). The two directions of distractors were again counterbalanced between subjects and because there were no spurious differences ($ps > .45$, $BF_{01} > 3.2$), the data were collapsed in all subsequent analyses. The *critical* distractor set was constructed in steps of 5° from the target color to 60° positive or negative rotations from the target color, resulting in a total of 24 distractor colors.

The color wheel in the *probe* trials (Figure 4.5) was divided into 72 bins (5° per bin) and each bin had a number attached. Participants reported the number of the color wedge that best matched the target color in memory. There was a total of six possible rotations of the color wheel.

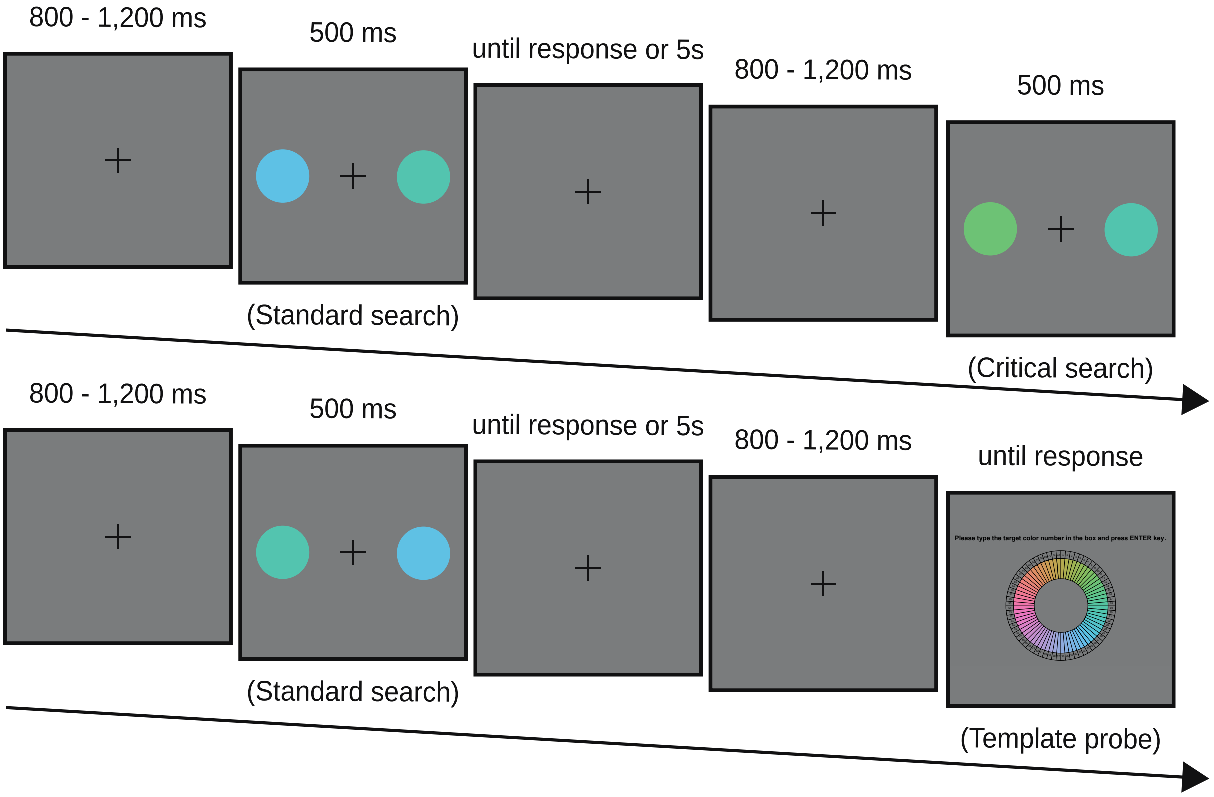

Figure 4.5. Example of *standard* and *critical* visual search trials, and template *probe* trials in Experiment 2. Participants were instructed to locate the target color circle and press the respective mouse button. On probe trials, participants typed the number corresponding to the estimated target color bin. There was no feedback given on any of the trials.

Design. Participants completed 20 practice standard visual search trials with feedback before the main experiment started. The main experiment was composed of 144 standard visual search trials, 144 critical search trials and 12 template probe trials. The three types of trials were presented in 12 blocks and randomly interleaved within each block, with the limitations that the probe trials only appeared after the standard search trials, and that there were no consecutive probe trials.

Procedure. An example of the target color was presented prior to the beginning of the experiment. On search trials, participants were instructed to indicate whether the target color appeared at the left side by pressing the left mouse button or at the right side by pressing the right mouse button. The stimuli appeared on the screen for 500ms and participants had up to 5s to make their responses. On probe trials, participants were required to type the number of the color wedge that best matched the target color in memory in a response box at the bottom of the screen. The color wheel would remain on the screen until response. Because Experiment 2 used a 2AFC design to measure the decision process through the pattern of choices and response times, we did not provide any feedback in the critical search trials to keep the responses unbiased from feedback. In order to equate the absence of feedback, no feedback was given in the other two types of trials as well. After responses, a central fixation cross was presented for 800-1200ms before the next trial started. Participants were instructed to fixate on the center cross when no stimuli were presented on the screen.

Statistical analysis. Consistent with Experiment 1, the goal of the standard search trials was to set up expectations for the distractor colors. Overall performance was significantly higher than chance (accuracy: *M* = .89, *SD* = .07; RT: *M* = 583ms, *SD* = 106ms), suggesting that these participants held an effective target representation. Trials were excluded when search RTs were below 200 or above 2500ms, or when the responses in the probe task were outside of the blue-green color range, which accounted for a total of 2% of the data.

The main analysis consisted of modeling visual search performance (error rates and RT; Figure 4.6) from the critical trials using a drift diffusion model (DDM). The separation between the two decision boundaries (a) and the non-decision time (t) were estimated as fitted free parameters that were the same across color distractor values for each subject while the drift rate (v) was estimated as a free parameter per distractor condition. There was no theoretical reason to believe the decision boundary and non-decision time should vary between critical distractors (see Supplemental materials). Instead, we were interested in how the drift rate (v), which characterizes the accumulation of noisy evidence over time until one of two decision boundaries is reached, differed across conditions (Ratcliff & McKoon, 2008). Drift rates in this experiment represent how easily the target can be distinguished from the distractor: Higher drift rates indicate stronger evidence, whereas lower drift rates suggest weaker evidence.

All parameters were estimated using a hierarchical Bayesian parameter estimation method. The hierarchical approach is particularly useful for this study given the small number of choices and RT values measured per subject (due to constraints in online experimentation) because it captures commonalities across individuals and at the same time estimates each individual’s parameter values (Ratcliff & Childers, 2015). To perform hierarchical DDM, we used the Python-based toolbox, HDDM (Wiecki et al., 2013). The HDDM model was fit to accuracy-coded data (i.e., the upper and lower boundaries correspond to correct and incorrect responses, and the starting point was fixed at 0.5).

For each participant's data, we used Markov chain Monte Carlo (MCMC) sampling methods to estimate the posterior distribution of each parameter. Each chain was run with 10000 samples, with the first 5000 warm-up samples discarded as burn-in. A total of 5 chains were run. Convergence was assessed by computing the Gelman-Rubin $\hat{R}$ statistic for each parameter. If the samples of the different chains converged, the $\hat{R}$ statistic should be close to 1. The range of $\hat{R}$ values across all group parameter estimates was between 0.99-1.10, suggesting satisfactory convergence. Goodness of fit was visually inspected with the posterior predictive check method (Figure 4.6).

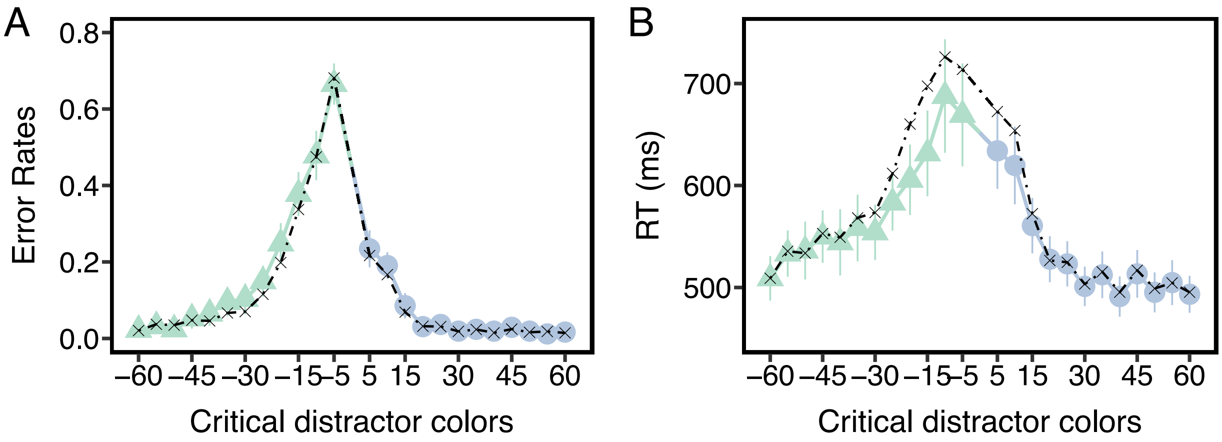

Figure 4.6. Error rates and RTs from the critical visual search trials. The black dashed lines represent the "fitted curves" for error rates and RT from the DDM for the best fit DDM parameters. The model fits illustrate the fact that the DDM captured the pattern of RT and accuracy well, rendering interpretation of the drift rates reasonable. All error bars are the 95% confidence intervals.

Results

Analysis of the drift rates. Figure 4.7A shows the group mean posterior estimates of the drift rates for each search condition. Following the analysis strategy from Experiment 1, each subject's drift rates were converted to a dissimilarity matrix (Figure 4.7B) for comparison against the relational and optimal model matrices (Figure 4.1) using a permutation test by randomizing stimulus labels. The theoretical RDMs were upsampled to match the number of conditions in the drift rate RDM. The two theoretical RDMs were only weakly correlated (r = .12, p = .05). The drift rate RDM was significantly correlated with both theoretical RDMs (optimal: r_{opt} = .77, p_{opt} = .0001; relational: r_{rel} = .22, p_{rel} = .005), but the correlation with the optimal RDM was significantly greater than the relational RDM ($p(r_{\text{opt}} > r_{\text{rel}})$ = .0001). As shown in Figure 4.7A, the drift rates for positive critical distractors were larger than that for negative distractors overall but there was a monotonic increase in drift rates for both negative and positive distractors as they became more dissimilar from the target. Interestingly, the nadir was at the -5° distractor and the drift rate was negative. This indicates that the accumulation of evidence was slow and the "wrong" decision was made more often than not. These results support the conclusion that the target match decisions were strongly modulated by the similarity to the optimal off-target feature centered over -5°, but there was also an overall directional bias. The blend of both models in these data are not unexpected given the dependent variable here involves accuracy and RT data, which would include combined effects of covert attentional guidance and decision processes, but it is noteworthy that the optimal model explained significantly more variance in the results.

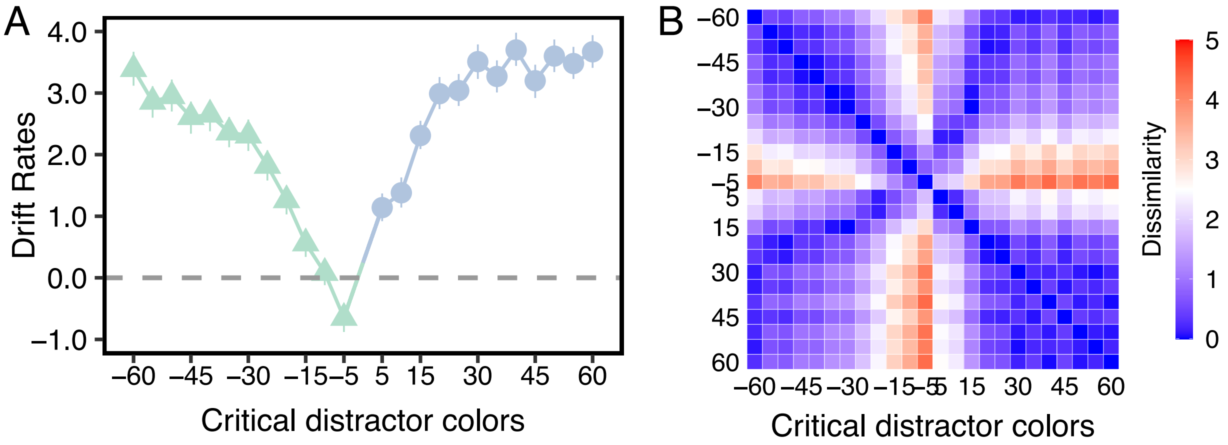

Figure 4.7. A) The drift rates for different critical search conditions. All the error bars are the 95% confidence intervals. B) The drift rate RDM averaged across participants.

Analysis of the probe task. The color wheel was composed of 72 color wedges sampling color hue in steps of 5°. Therefore, the relative click distance from the veridical target color was divided into 5° bins (Figure 4.8A) and then converted to an RDM (Figure 4.8B). The probe RDM was significantly correlated with both theoretical model matrices, $r_{\text{opt}} = .56$, $p_{\text{opt}} = .0001$, $r_{\text{rel}} = .11$, $p_{\text{rel}} = .001$. The comparison between the r values from these correlations confirmed that the probe RDM was more strongly correlated with the optimal RDM than with the relational RDM, $p(r_{\text{opt}} > r_{\text{rel}}) = .0001$. These results converged with Experiment 1, suggesting that the target representation was shifted away from distractors to enhance optimal off-target features.

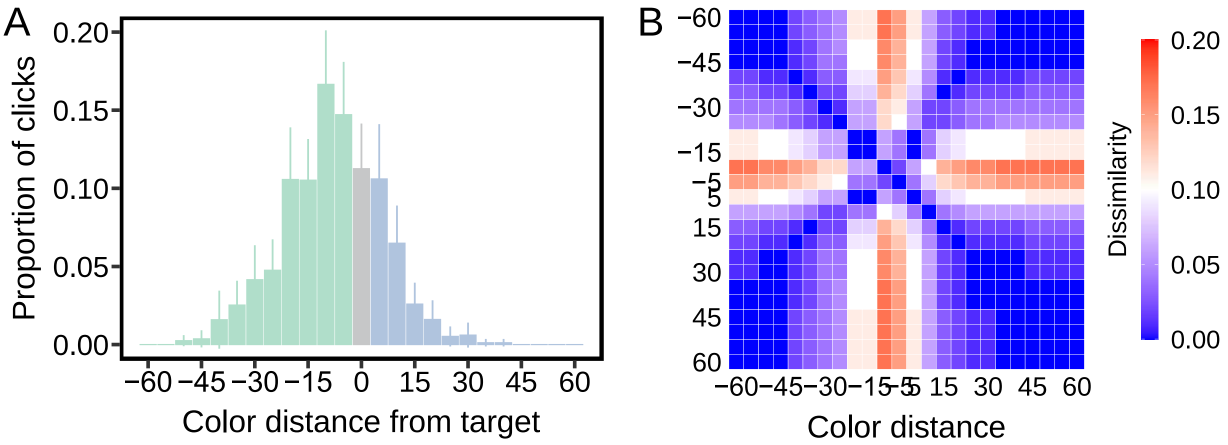

Figure 4.8. A) Group averages of relative click distance from the veridical target color in color wheel probe task. All error bars are the 95% confidence intervals. B) The probe RDM averaged across participants.

Correlation between performance on the memory probe and search tasks. Next, we conducted a correlation analysis on individual differences between how well the probe data match the optimal RDM and drift rates. A positive correlation between these two metrics would suggest that individuals whose responses on the probe task were closer to the optimal model also made faster and more accurate decisions about which of the two objects was the target during visual search. First, the correlation between each subject's probe matrix and the optimal RDM from above was used as a measurement of how well their target templates fit the optimally tuned template. Second, new drift rate parameters were estimated for each subject with data collapsed across color directions (negative, positive) in order to reduce the feature space (cf. a drift rate parameter per distractor color). The resulting correlation values were then correlated with their drift rate parameter from visual search. We found that participants who had more optimally tuned templates showed faster drift rates, reflecting an easier discrimination of target from distractors, with both negative and positive distractors (negative: r = .28, p = .02, BF_{10} = 3.50; positive: r = .35, p = .003, BF_{10} = 14.70). These results highlight the underlying relationship between the target decision processes and the target color held in long-term memory over time.

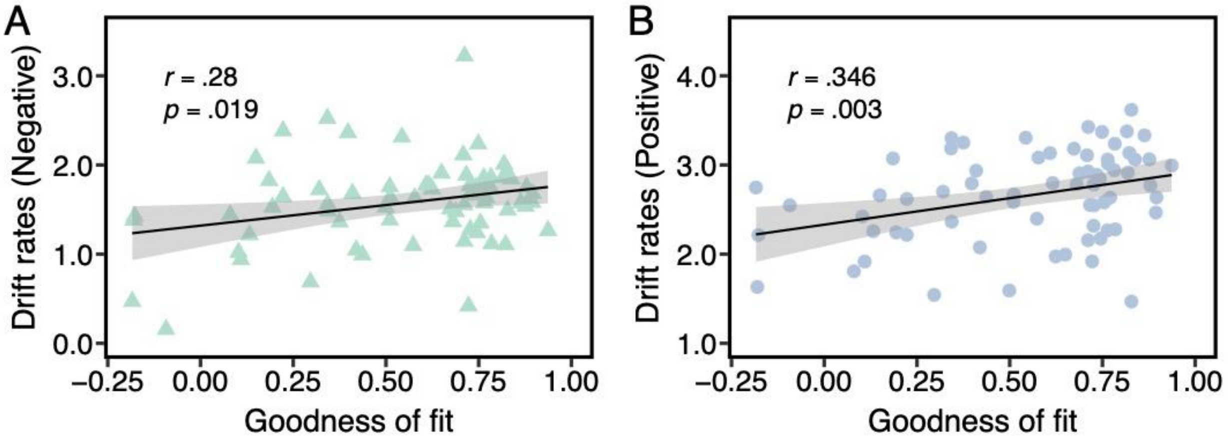

Figure 4.9. The relationship between the goodness of fit of each participant's template to the optimally tuned template and the drift rates during visual search.

Discussion

The purpose of these experiments was to test hypotheses of how template information is used during guidance and decision stages of visual search. Using a visual search task for a target amongst linearly separable distractors, the results demonstrate that early attentional guidance was a coarse process mainly based on “relational” sensory information, whereas subsequent match decisions were compared against a more precisely tuned template centered on an “optimal” off-target feature. Although previous studies have found evidence for coarse guidance (Kerzel, 2019; Martin & Becker, 2018) and precise decisions (Rajsic & Woodman, 2020) separately, our experiments provide direct evidence that the informational content of a single target object is used differently on these two subprocesses of visual search.

There is a long history of work showing that the contents of the template can bias the deployment of attention and saccades towards potential targets (Chelazzi et al., 1998; Olivers et al., 2011; Soto et al., 2008). Recent research has shown that the template may not be precisely centered over the specific target feature, as previously assumed, but instead be shifted to increase the distinctiveness of the target from distractors (Hodsoll & Humphreys, 2001; Navalpakkam & Itti, 2007; Scolari & Serences, 2009). In line with Becker and colleagues’ relational account (Becker, 2010; Martin & Becker, 2018), the eye data in Experiment 1 showed that all negative critical distractors that were relational matches captured attention and first saccades more strongly than positive distractors. Thus, attention appears to be initially guided by the relative feature of the target, not specific feature values. This coarse representation of the target might be well suited for rapid stimulus prioritization under noisy sensory conditions, e.g., when many stimuli are in peripheral vision where color and spatial acuity are poor (Hulleman, 2010; Hulleman & Olivers, 2017; Rosenholtz, 2017).

Once one item is selected, however, a decision must be made regarding the exact identity of the stimulus as a match or non-match to the target. Unlike attentional guidance, the importance of this decision process on visual search has only been explored more recently (Hout & Goldinger, 2015; Malcolm & Henderson, 2010; Rajsic & Woodman, 2020). In the current study, we used fixation dwell times (Experiment 1) and the DDM drift rates (Experiment 2) as measurements of target-match decisions. The optimal model fit both dwell times and drift rates, indicating that the decision process operates on an optimally shifted and precisely tuned template. The precision appears necessary for accurate decisions to be made and the shift increases the target-to-distractor discriminability to speed decisions.

It should be pointed out that although the first saccades were better described by the relational model and the dwell times and drift rates were better described by the optimal model, both sets of data showed hints of the other pattern. Therefore, it is possible that guidance and decision are influenced by both relational and optimal tuning, but the relative bias towards one or the other is weighted by the pressure to perform fast guidance or precise decisions. These results raise an open question about whether guidance and decisions during the visual search cycle operate using two discrete representations or a single, flexible template that is weighted by the exact computation required at each stage of visual search.

Both ideas, that of separate templates and that of flexible weighting of a single template source are present in the literature. For example, Wolfe and colleagues suggest that there is a “guiding” template in working memory and a separate “target” template in long term memory to guide search when there is a large (>100) number of potential targets (Cunningham & Wolfe, 2014; Wolfe, 2021). Our results are compatible with this framework, and further suggest that the target template in long-term memory serves as the template on which match decisions are made. Participants who established more optimally tuned target templates in long-term memory had higher drift rates, suggesting that decisions during visual search are directly related to the off-veridical target representation in memory (Geng & Witkowski, 2019; Lleras et al., 2020). This finding is consistent with the characterization of target templates held in long-term memory in Guided Search 6.0 (Wolfe, 2021), in which a potential target in working memory selected by the guiding template is compared against a target template held in long-term memory through a drift diffusion process.

Our findings also recall the literature surrounding questions about how active representations are used in working and long-term memory to guide attention during visual search. Our results are consistent with the finding that stable search targets are stored in long-term memory, and that this information can be used for target match decisions (Carlisle et al., 2011; Woodman et al., 2013). We do not have a position at this time on whether relational guidance is based on an active working memory template that is separate from the optimal memory representation of the target, or whether relational guidance reflects a coarser manifestation of the same target template in memory. The former is a possibility given that one target representation can be held in active working memory while the other is held as an accessory or latent item in working or long-term memory (Olivers et al., 2011; Woodman et al., 2013). The latter is also a possibility given findings that there are versions of a single target representation in multiple brain regions, with the exact computation done on the target information being dependent on the stage of processing (Lee et al., 2013; Long & Kuhl, 2018). Another possibility is that participants simply set different criterions on a single template for each stage of processing: a liberal criterion to broadly capture all potential targets in the visual field (possibly also accounting for acuity degradations in peripheral vision), and then a more conservative criterion for more precise decisions. Future work is necessary to determine the exact mechanisms by which guidance and decisions operate on different information patterns. Finally, the current findings were based on the special case of search for a target amongst linearly separable distractors. Real-world search targets, however, are infrequently linearly separable from distractors. The generalizability of our findings should be further investigated under more typical conditions to determine if the differences in the precision of guidance and decision are a general property of visual search.

Taken together, our findings suggest that the target template operates distinctively during guidance and decision stages of visual search. Early attentional guidance is a coarse process to weight sensory information, but later match decisions depend on a more precise representation of the target to efficiently determine identity. To return to our example of searching for a tiger in the grasslands, our results suggest that out in the field, guidance is coarse and will select anything that might be a tiger. In contrast, once attention has selected an object, an optimal target template is more useful for deciding if the object is indeed a tiger, or not. Although we are not able to fully address whether the information source for the two stages of processing is identical or separate with only the current behavioral data, the results offer a resolution to the debate in the literature over how template information is shifted in response to expected distractor features.

Supplemental Material

Experiment 1: Error rates and RT

The eye data were the dependent measure of primary interest in Experiment 1. The error rates and RT were expected to reflect a combination of guidance, decisions, and other factors due to the long and complex trial structure (e.g., involving multiple eye movements, emphasis on accuracy). Nevertheless, we entered error rates and RT into a one-way ANOVA with repeated measures to assess the effects of critical distractors on visual search performance. Only RT data from correct trials were included in these analyses. There was a significant main effect of distractors on both error rates ($F(8, 232) = 2.47$, $p = .01$, $\eta_p^2 = 0.08$, $BF_{10} = 1.61$) and RT ($F(8, 232) = 18.72$, $p < .001$, $\eta_p^2 = .39$, $BF_{10} = 2.87$). The small effect size ($\eta_p^2 = 0.08$) and ceiling performance made the error rates uninteresting (Figure S4.1A). Post-hoc t tests, corrected for multiple comparisons, only focused on RT measures (Figure S4.1B). The results indicated that search RT (M = 1576ms) were longest in the presence of the -15° critical distractor, $ts > 3.68$, $ps < .008$, $ds > .67$, $(BF_{10})s > 34.84$. Interestingly, an unilateral “Mexican hat” surround suppression effect emerged at the 15° distractor ($ts > 6$, $ps < .0001$, $ds > 1.10$, $(BF_{10})s > 11{,}993$), which was closest to the 10° distractors in the standard visual search trials (Fang et al., 2019; Störmer & Alvarez, 2014).

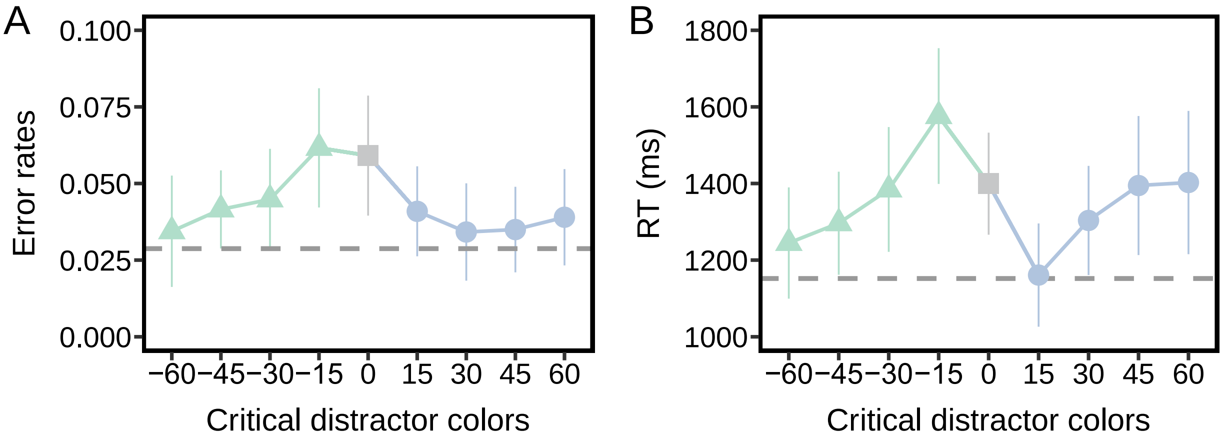

Figure S4.1. Error rates and RTs from the critical visual search trials. The dash lines indicated the search performance in the standard trials. All error bars are the 95% confidence intervals.

Experiment 1B

In Experiment 1, our probe results suggested that the central tendency of the target template shifted ~5° in the negative direction, compared to the true target color. In order to capture a finer grained measurement of visual search performance for near target colors, we conducted a new experiment that included ±5° critical distractors.

Method

Participants. Twelve participants (4 males, 0 left-handed, ages from 18-24) from University of California, Davis participated in Experiment 3 in partial fulfillment of a course requirement. Each participant was provided written informed consent in accordance with the local ethics clearance as approved by the National Institutes of Health. Each participant's color vision was assessed by self-report and an online color blindness test (https://colormax.org/color-blind-test). All participants had normal or corrected-to-normal vision and all had normal color vision.

Stimuli, Design & Procedure. All stimuli and procedures were identical to Experiment 1, with one exception: the critical distractor color set was composed of -45°, -30°, -15°, -5°, 0°, 5°, 15°, 30° and 45°. The two directions of distractors were again counterbalanced between subjects and because there were no spurious differences ($ps > .4$, $BF_{01} > 1.7$), the data were collapsed in all subsequent analyses. Overall, 11.36% of trials were removed from data analysis by the same criteria in Experiment 1.

Results

Analysis of the first saccades that went to the critical distractors. Following the analysis strategy from Experiment 1, we converted each subject's probability of first saccades (Figure S4.2A) to a dissimilarity matrix (Figure S4.2B), and compared it against the relational and optimal model matrices. The first saccade RDM had a significantly positive correlation with the relational RDM ($r_{\text{rel}} = .80$, $p_{\text{rel}} = .0003$), but not the optimal RDM ($r_{\text{opt}} = -.03$, $p_{\text{opt}} = .55$). In addition, the r values were compared against each other using a permutation test and found to be significant, $p(r_{\text{rel}} > r_{\text{opt}}) = .0001$, confirming that the first saccade RDM was more strongly correlated with the relational RDM than with the optimal RDM. These results replicate those from Experiment 1.

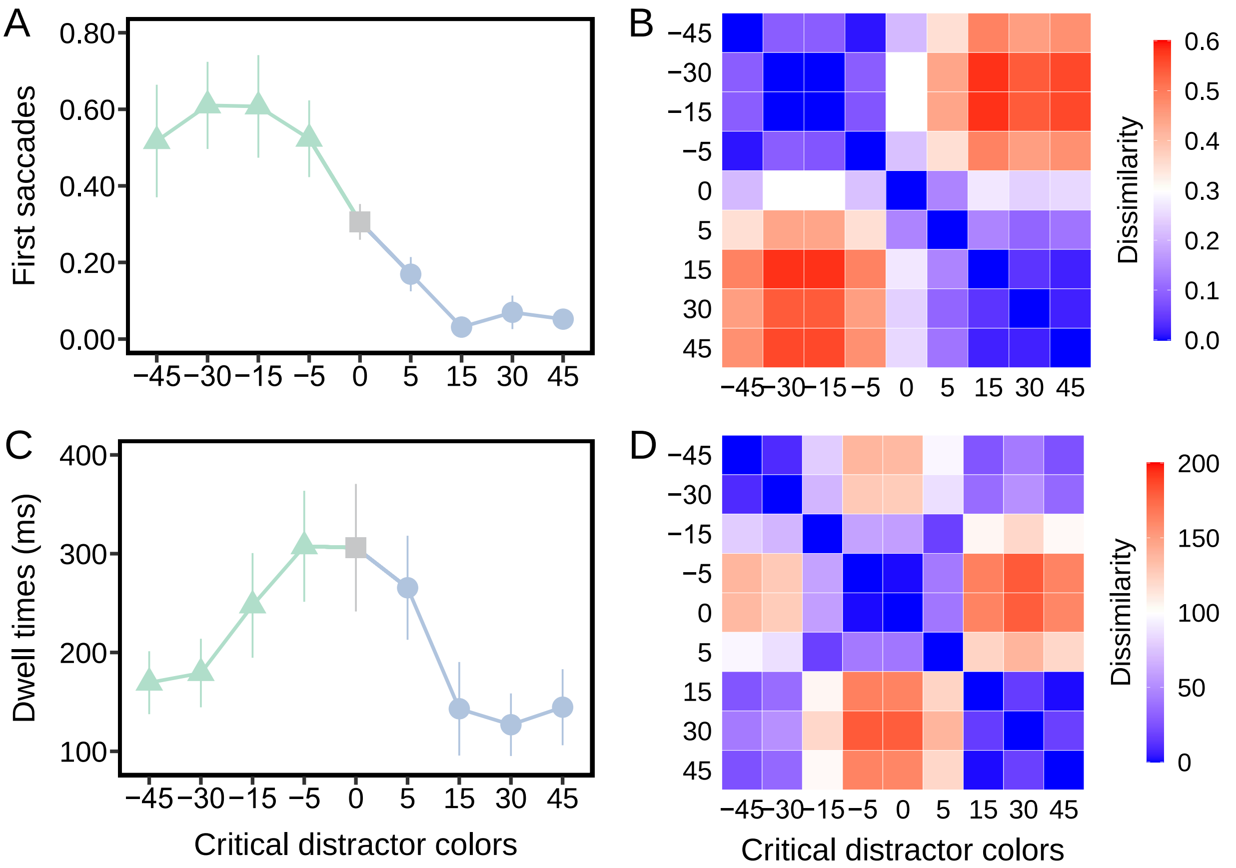

Figure S4.2. A) The probability of first saccades captured by critical distractors. B) The first saccade RDM averaged across participants. C) The fixation dwell times on the critical distractors. D) The fixation dwell time RDM averaged across participants. All error bars are the 95% confidence intervals.

Analysis of the fixation dwell times on the critical distractors. The dwell time RDM (Figure S4.2D) was only significantly correlated with the optimal RDM (r_{opt} = .46, p_{opt} = .008), but not with the relational RDM (r_{rel} = -.02, p_{rel} = .52). The comparison between the r values confirmed that the dwell time RDM was more strongly correlated with the optimal RDM than with the relational RDM, $p(r_{\text{opt}} > r_{\text{rel}})$ = .0001. These results again replicated those from Experiment 1, suggesting that the match decisions strongly reflected optimal tuning.

Although the fixation dwell times on the -5° distractor did not differ from it on the 0° distractor (Figure S4.2A; $t(11)$ = -.09, p = .92, BF_{01} = 3.47), the central tendency of the dwell time distribution was shifted negatively from 0° (the true target feature). This result argues against the possibility that the “tuning” of the fixation dwell times was actually veridical. It is also possible that the non-significant difference could be due to the fact that the rejection of near target distractors (i.e., ±5°, 0°) was influenced by shape discrimination, not color. In other words, ~306ms (mean fixation dwell times on the 0° distractor) might be the minimum time required to discriminate the dodecagon shape distractor from the circle shape target, when the two stimuli had similar colors. The potential confounding effect of shape discrimination on target non-match decisions was addressed in Experiment 2.

Experiment 2: DDM general parameters

Table S1. Summary statistics for each group level parameter's posterior

	mean	std	2.5q	25q	50q	75q	97.5q	mc err
a	1.28	0.03	1.22	1.26	1.28	1.30	1.34	0.0011
t	0.32	0.006	0.31	0.31	0.32	0.32	0.33	0.0001
v(-5)	-0.65	0.11	-0.88	-0.72	-0.65	-0.57	-0.43	0.0038
v(-10)	0.08	0.11	-0.12	0.01	0.08	0.16	0.31	0.0042
v(-15)	0.56	0.11	0.34	0.48	0.57	0.64	0.80	0.0039
v(-20)	1.26	0.11	1.03	1.18	1.26	1.34	1.50	0.0048
v(-25)	1.82	0.12	1.58	1.73	1.81	1.89	2.07	0.0049
v(-30)	2.31	0.12	2.06	2.23	2.32	2.40	2.57	0.0049
v(-35)	2.36	0.12	2.12	2.27	2.36	2.45	2.61	0.0045
v(-40)	2.65	0.13	2.38	2.55	2.65	2.74	2.89	0.0047
v(-45)	2.61	0.13	2.34	2.52	2.6	2.69	2.86	0.0047
v(-50)	2.95	0.13	2.70	2.86	2.94	3.04	3.22	0.0047
v(-55)	2.86	0.13	2.60	2.77	2.85	2.95	3.11	0.0046
v(-60)	3.39	0.13	3.12	3.30	3.39	3.49	3.67	0.0056
v(5)	1.14	0.11	0.92	1.06	1.14	1.23	1.37	0.0038
v(10)	1.38	0.12	1.14	1.30	1.39	1.46	1.63	0.0043
v(15)	2.31	0.12	2.09	2.21	2.31	2.39	2.55	0.0048
v(20)	2.99	0.13	2.74	2.90	2.99	3.08	3.26	0.0055
v(25)	3.04	0.12	2.79	2.96	3.04	3.13	3.31	0.0048
v(30)	3.51	0.14	3.23	3.41	3.51	3.60	3.79	0.0060
v(35)	3.27	0.13	3.01	3.18	3.26	3.35	3.53	0.0053
v(40)	3.70	0.13	3.44	3.61	3.70	3.80	3.98	0.0054
v(45)	3.20	0.13	2.92	3.10	3.20	3.29	3.46	0.0049
v(50)	3.60	0.13	3.34	3.50	3.60	3.69	3.87	0.0056
v(55)	3.48	0.13	3.23	3.40	3.48	3.57	3.75	0.0056
v(60)	3.67	0.13	3.41	3.58	3.68	3.76	3.94	0.0053

References

Bae, G.-Y., Olkkonen, M., Allred, S. R., & Flombaum, J. I. (2015). Why some colors appear more memorable than others: A model combining categories and particulars in color working memory. *Journal of Experimental Psychology. General*, *144*(4), 744—763. https://doi.org/10.1037/xge0000076

Bauer, B., Jolicoeur, P., & Cowan, W. B. (1996). Visual search for colour targets that are or are not linearly separable from distractors. *Vision Research*, *36*(10), 1439—1466. https://doi.org/10.1016/0042-6989(95)00207-3

Becker, S. I. (2010). The Role of Target–Distractor Relationships in Guiding Attention and the Eyes in Visual Search. *Journal of Experimental Psychology: General*, *139*(2), 247–265. https://doi.org/10.1037/a0018808

Brainard, D. H. (1997). The Psychophysics Toolbox. *Spatial Vision*, *10*(4), 433—436. https://doi.org/10.1163/156856897x00357

Bravo, M. J., & Farid, H. (2014). Informative cues can slow search: The cost of matching a specific template. *Attention, Perception, \textbackslash& Psychophysics*, *76*(1), 32—39. https://doi.org/10.3758/s13414-013-0532-z

Carlisle, N. B., Arita, J. T., Pardo, D., & Woodman, G. F. (2011). Attentional Templates in Visual Working Memory. *Journal of Neuroscience*, *31*(25), 9315–9322. https://doi.org/10.1523/JNEUROSCI.1097-11.2011

Chelazzi, L., Duncan, J., Miller, E. K., & Desimone, R. (1998). Responses of Neurons in Inferior Temporal Cortex During Memory-Guided Visual Search. *Journal of Neurophysiology*, *80*(6), 2918—2940. https://doi.org/10.1152/jn.1998.80.6.2918

Cunningham, C. A., & Wolfe, J. M. (2014). The role of object categories in hybrid visual and memory search. *Journal of Experimental Psychology. General*, *143*(4), 1585—1599. https://doi.org/10.1037/a0036313

Desimone, R., & Duncan, J. (1995). Neural Mechanisms of Selective Visual Attention. *Annual Review of Neuroscience*, *18*(1), 193—222. https://doi.org/10.1146/annurev.ne.18.030195.001205

Duncan, J., & Humphreys, G. W. (1989). *Visual Search and Stimulus Similarity*. 26.

Eriksen, C. W. (1953). Object location in a complex perceptual field. *Journal of Experimental Psychology*, *45*(2), 126–132. https://doi.org/10.1037/h0058018

Geng, J. J., DiQuattro, N. E., & Helm, J. (2017). Distractor Probability Changes the Shape of the Attentional Template. *Journal of Experimental Psychology: Human Perception and Performance*, *43*(12), 1993–2007. https://doi.org/10.1037/xhp0000430

Geng, J. J., & Witkowski, P. (2019). Template-to-distractor distinctiveness regulates visual search efficiency. *Current Opinion in Psychology*, *29*, 119—125. https://doi.org/10.1016/j.copsyc.2019.01.003

Giesbrecht, B., Sy, J. L., & Guerin, S. A. (2013). Both memory and attention systems contribute to visual search for targets cued by implicitly learned context. *Vision Research*, *85*, 80–89. https://doi.org/10.1016/j.visres.2012.10.006

Green, B. F., & Anderson, L. K. (1956). Color coding in a visual search task. *Journal of Experimental Psychology*, *51*(1), 19–24. https://doi.org/10.1037/h0047484

Hodsoll, J., & Humphreys, G. W. (2001). Driving attention with the top down: The relative contribution of target templates to the linear separability effect in the size dimension. *Perception \textbackslash& Psychophysics*, *63*(5), 918—926. https://doi.org/10.3758/bf03194447

Hout, M. C., & Goldinger, S. D. (2015). Target templates: The precision of mental representations affects attentional guidance and decision-making in visual search. *Attention, Perception \textbackslash& Psychophysics*, *77*(1), 128—149. https://doi.org/10.3758/s13414-014-0764-6

Hulleman, J. (2010). Inhibitory tagging in visual search: Only in difficult search are items tagged individually. *Vision Research*, *50*(20), 2069–2079. https://doi.org/10.1016/j.visres.2010.07.017

Hulleman, J., & Olivers, C. N. L. (2017). The impending demise of the item in visual search. *Behavioral and Brain Sciences*, *40*, e132. https://doi.org/10.1017/S0140525X15002794

Kerzel, D. (2019). The precision of attentional selection is far worse than the precision of the underlying memory representation. *Cognition*, *186*, 20—31. https://doi.org/10.1016/j.cognition.2019.02.001

Kriegeskorte, N., Mur, M., & Bandettini, P. (2008). Representational Similarity Analysis – Connecting the Branches of Systems Neuroscience. *Frontiers in Systems Neuroscience*, *2*. https://doi.org/10.3389/neuro.06.004.2008

Lee, S.-H., Kravitz, D. J., & Baker, C. I. (2013). Goal-dependent dissociation of visual and prefrontal cortices during working memory. *Nature Neuroscience*, *16*(8), 997—999. https://doi.org/10.1038/nn.3452

Lleras, A., Wang, Z., Ng, G. J. P., Ballew, K., Xu, J., & Buetti, S. (2020). A target contrast signal theory of parallel processing in goal-directed search. *Attention, Perception, \textbackslash& Psychophysics*, *82*(2), 394—425. https://doi.org/10.3758/s13414-019-01928-9

Long, N. M., & Kuhl, B. A. (2018). Bottom-Up and Top-Down Factors Differentially Influence Stimulus Representations Across Large-Scale Attentional Networks. *The Journal of Neuroscience*, *38*(10), 2495—2504. https://doi.org/10.1523/jneurosci.2724-17.2018

Malcolm, G. L., & Henderson, J. M. (2010). Combining top-down processes to guide eye movements during real-world scene search. *Journal of Vision*, *10*(2), 4–4. https://doi.org/10.1167/10.2.4

Martin, A., & Becker, S. I. (2018). How feature relationships influence attention and awareness: Evidence from eye movements and EEG. *Journal of Experimental Psychology: Human Perception and Performance*, *44*(12), 1865—1883. https://doi.org/10.1037/xhp0000574

Navalpakkam, V., & Itti, L. (2007). Search Goal Tunes Visual Features Optimally. *Neuron*, *53*(4), 605—617. https://doi.org/10.1016/j.neuron.2007.01.018

Nili, H., Wingfield, C., Walther, A., Su, L., Marslen-Wilson, W., & Kriegeskorte, N. (2014). A Toolbox for Representational Similarity Analysis. *PLoS Computational Biology*, *10*(4), e1003553. https://doi.org/10.1371/journal.pcbi.1003553

Olivers, C. N. L., Peters, J., Houtkamp, R., & Roelfsema, P. R. (2011). Different states in visual working memory: When it guides attention and when it does not. *Trends in Cognitive Sciences*. https://doi.org/10.1016/j.tics.2011.05.004

Pelli, D. G. (1997). The VideoToolbox software for visual psychophysics: Transforming numbers into movies. *Spatial Vision*, *10*(4), 437—442. https://doi.org/10.1163/156856897x00366

Rajsic, J., & Woodman, G. F. (2020). Do we remember templates better so that we can reject distractors better? *Attention, Perception, & Psychophysics*, *82*(1), 269–279. https://doi.org/10.3758/s13414-019-01721-8

Ratcliff, R., & Childers, R. (2015). Individual Differences and Fitting Methods for the Two-Choice Diffusion Model of Decision Making. *Decision (Washington, D.C.)*, *2015*.

Ratcliff, R., & McKoon, G. (2008). The Diffusion Decision Model: Theory and Data for Two-Choice Decision Tasks. *Neural Computation*, *20*(4), 873—922. https://doi.org/10.1162/neco.2008.12-06-420

Reynolds, J. H., & Heeger, D. J. (2009). The Normalization Model of Attention. *Neuron*, *61*(2), 168—185. https://doi.org/10.1016/j.neuron.2009.01.002

Rosenholtz, R. (2017). Those pernicious items. *Behavioral and Brain Sciences*, *40*, e154. https://doi.org/10.1017/S0140525X16000248

Scolari, M., Byers, A., & Serences, J. T. (2012). Optimal Deployment of Attentional Gain during Fine Discriminations. *The Journal of Neuroscience*, *32*(22), 7723—7733. https://doi.org/10.1523/jneurosci.5558-11.2012

Scolari, M., & Serences, J. T. (2009). Adaptive Allocation of Attentional Gain. *Journal of Neuroscience*, *29*(38), 11933—11942. https://doi.org/10.1523/jneurosci.5642-08.2009

Soto, D., Hodsoll, J., Rotshtein, P., & Humphreys, G. W. (2008). Automatic guidance of attention from working memory. *Trends in Cognitive Sciences*, *12*(9), 342—348. https://doi.org/10.1016/j.tics.2008.05.007

Treisman, A. M., & Gelade, G. (1980). A feature-integration theory of attention. *Cognitive Psychology*, *12*(1), 97—136. https://doi.org/10.1016/0010-0285(80)90005-5

Treue, S., & Trujillo, J. C. M. (1999). Feature-based attention influences motion processing gain in macaque visual cortex. *Nature*, *399*(6736), 575—579. https://doi.org/10.1038/21176

Wiecki, T. V., Sofer, I., & Frank, M. J. (2013). HDDM: Hierarchical Bayesian estimation of the Drift-Diffusion Model in Python. *Frontiers in Neuroinformatics*, *7*. https://doi.org/10.3389/fninf.2013.00014

Wolfe, J. M. (2012). Saved by a log: How do humans perform hybrid visual and memory search? *Psychological Science*, *23*(7), 698—703. https://doi.org/10.1177/0956797612443968

Wolfe, J. M. (2021). Guided Search 6.0: An updated model of visual search. *Psychonomic Bulletin & Review*. https://doi.org/10.3758/s13423-020-01859-9

Woodman, G. F., Carlisle, N. B., & Reinhart, R. M. G. (2013). Where do we store the memory representations that guide attention? *Journal of Vision*, *13*(3). https://doi.org/10.1167/13.3.1

Wu, R., Scerif, G., Aslin, R. N., Smith, T. J., Nako, R., & Eimer, M. (2013). Searching for something familiar or novel: ERP correlates of top-down attentional selection for specific items or categories. *Journal of Cognitive Neuroscience*, *25*(5), 719—729. https://doi.org/10.1162/jocn_a_00352

Yu, X., & Geng, J. J. (2019). The Attentional Template Is Shifted and Asymmetrically Sharpened by Distractor Context. *Journal of Experimental Psychology: Human Perception and Performance*, *45*(3), 336–353. https://doi.org/10.1037/xhp0000609

Chapter 5: Visual Search Guidance uses Coarser Template Information than Target-match Decisions

The following chapter consists of a manuscript under review at *Psychological Bulletin and Review*.

Abstract

When searching for an object, we use a target template in memory that contains task-relevant information to guide visual attention to potential targets and to determine the identity of attended objects. These processes in visual search have typically been assumed to rely on a common source of template information. However, our recent work (Yu, et al., in press) argued that attentional guidance and target-match decisions rely on different information during search, with guidance using a “fuzzier” version of the template compared to target decisions. However, that work was based on the special case of search for a target amongst linearly separable distractors (e.g., search for an orange target amongst yellower distractors). Real-world search targets, however, are infrequently linearly separable from distractors, and it remains unclear whether the differences between the precision of template information used for guidance compared to target decisions also applies under more typical conditions. In four experiments, we tested this question by varying distractor similarity during visual search and measuring the likelihood of attentional guidance to distractors and target misidentifications. We found that early attentional guidance is indeed less precise than that of subsequent match decisions under varying exposure durations and distractor set sizes. These results suggest that attentional guidance operates on a coarser code than decisions, perhaps because guidance is

constrained by lower acuity in peripheral vision or the need to rapidly explore a wide region of space while decisions about selected objects are more precise to optimize decision accuracy.

Introduction

When looking for an object, we engage in a continuous look-and-identify cycle in which we use target information in memory (i.e., the target or attentional template) to guide eye-movements to probable targets and then make decisions about the match (Desimone & Duncan, 1995; Duncan & Humphreys, 1989; Wolfe, 2021). These processes are typically assumed to rely on the same information from a single target template. However, our recent work (Yu, et al., in press) found that the precision of attentional guidance and target-identity decisions differed when searching for a target amongst linearly separable distractors (e.g., an orange target amongst yellower distractors). Real-world search, however, rarely involves linearly separable distractors. Therefore, in the current studies, we test if attentional guidance uses a “fuzzier” version of the target template compared to target decisions during more typical visual search conditions.

Most models of visual search (Bundesen, 1990; Desimone & Duncan, 1995; Wolfe, 2021) include the concept of the attentional template (Duncan & Humphreys, 1989). It refers to an internal representation of target information held in working or long-term memory during visual search (Carlisle et al., 2011; Woodman et al., 2013). Activated shortly before the search task (Grubert & Eimer, 2018), the target template guides selective attention towards objects with template-matching attributes (Eimer, 2014) and is used to decide of the object is a target-match (Cunningham & Wolfe, 2014). Attentional guidance towards template-similar objects is presumed to occur because information in the target template is used to modulate sensory gain (Reynolds & Heeger, 2009). For example, when looking for a red colored object, it is assumed that the sensory gain of neurons that preferentially encode “red” anywhere in the visual field is enhanced (Andersen et al., 2008; Liu et al., 2007; Treue & Trujillo, 1999).

Once attention selects a candidate object, a decision must be made regarding the exact identity of the stimulus as a target-match or non-match (Castelhano et al., 2008; Rajsic & Woodman, 2020). This decision is a time-consuming portion of the look-identify cycle and must be accurate if visual search is to be ultimately successful. Therefore, more precise attentional templates are expected to improve visual search efficiency by enhancing attentional guidance to the correct targets and by accelerating target-match decisions (Hout & Goldinger, 2015; Malcolm & Henderson, 2009, 2010).

Although attentional guidance and match decisions are often hypothesized to rely on the same template information, Wolfe (2021) recently argued that the search template should be separated into two: a “guiding” template in working memory that is used to deploy attention to potential targets; and a “target” template in long-term memory that is used to determine if a candidate object is the target. Consistent with this idea, our recent study (Yu et al., in press) provided evidence that the informational code of the search template differs based on the stage of processing. Specifically, when looking for an orange target that appears predictably amongst linearly separable (e.g., yellow) distractors, early attentional guidance is based on relational information (e.g., prioritizing the “reddest” object regardless of its exact hue) whereas subsequent match decisions are made against an “optimal” off-target feature (e.g., the slightly redder version of the orange target). Our findings suggest that attentional guidance operates on a coarser code to weight sensory information than target-match decisions, which uses more precise information to determine identity (Kerzel, 2019; Rajsic & Woodman, 2020).

The aim of the current experiments is to test if attentional guidance and target-match decisions rely on different degrees of template precision during more common visual search conditions. The experiments involve randomly intermixing frequent *search decision* trials with infrequent *guidance probe* trials (Figure 5.1A). On *search decision* trials, participants perform a visual search task to locate a predefined target color and make a manual response. Error rates on these *decision* trials are used as an index of misidentifications of a distractor as the target in the final binary decision. On *guidance probe* trials, letters rapidly appear inside each search stimulus on the initial search array (Gaspelin et al., 2015; Kim & Cave, 1995). On these trials, participants attempt to recall as many letters as possible (and are not required to respond specifically to the search target). The probability that the probe letter at a given location is reported is used as an index of attentional guidance because participants will be more likely to report the letter at an attended location than to report the letter at an unattended location (Gaspelin & Luck, 2018). If guidance uses coarser template information than decisions, then participants will report letter probes on a wider range of distractors than those that are ultimately misidentified as targets. Alternatively, if a single fixed representation is used at the two stages, we expect the range of distractors that capture attention to be the same as the range of distractors that will be misidentified as the target.

Experiments 1AB

Method

Participants. To determine the sample size for Experiment 1, we first conducted a pilot study with 32 participants (data were not included in Experiment 1) using similar methods and procedures in Experiment 1A. The smallest effect size of the two dependent measures of interest (in this case the probability of reporting the probe letter at critical distractor location, *d* = .393) was entered into G*power calculation (http://www.gpower.hhu.de/). The results estimated that *N* = 70 was necessary to detect significant effects (*p* = .05, two-tailed) with a power .9. Data were collected online using the Testable platform (https://www.testable.org/) until we obtained a sample of 70 participants after exclusion criteria were applied. 45 participants in Experiment 1A and 47 participants in Experiment 1B were excluded from the analysis because of poor performance in search decision trials (accuracy in decision trials with far critical distractors (±50° to ±100°) was below 80%) and insufficient guidance probe trials (the number of effective guidance trials was below 80%; see *statistical analysis* for which guidance trials were excluded from the analysis). A large number of outliers was expected due to the fact that the experiment was conducted online through SONA and course credit was not tied to performance. 140 participants (Experiment 1A: *N* = 70, self-reported 12 males, self-reported 58 females, 2 left-handed, ages from 18 – 26 years; Experiment 1B: *N* = 70, self-reported 14 males, self-reported 56 females, 7 left-handed, ages from 18 – 43 years) from University of California, Davis participated online in Experiment 1 in partial fulfillment of a course requirement. A given participant completed only one experiment (Experiment 1A or 1B). Each participant provided written informed consent in accordance with the local ethics clearance as approved by the National Institutes of Health. Each participant's color vision was assessed by self-report. All participants had normal or corrected-to-normal vision, and all had normal color vision.

Stimuli. All experiments were conducted online through Testable. All stimuli were created in Illustrator, saved as PNG files, and uploaded to Testable.org. All stimuli were presented against a gray background (color hue = '#808080'). The target and distractor colors were selected from a color wheel defined in LAB color space (a, b coordinates = 0, 0; luminance = 70; from Bae et al., 2015). Two target colors (218°, 258°) were counterbalanced across participants. Each participant was assigned a single target color throughout the experiment. We used the colors that were ±20° rotated from the focal blue color (i.e., the best representative of the blue color category) as the target colors (Figure 5.1B). Non-focal colors were used to assess if the expected memory bias for the target color towards the category center would also be present in visual search guidance and decisions (Bae et al., 2015; Nako et al., 2016). Two target colors were used to ensure that our results were not due to spurious effects associated with one color and yet minimize noise in perception due to uncontrolled color variation caused by participants' environments (e.g., monitors, graphic cards, screen specifications, and lighting conditions). Because the target colors did not affect performance (Experiment 1A: *ps* > .13; Experiment 1B: *ps* > .06), the data were collapsed in all subsequent analyses to maximize statistical power. For descriptive simplicity, the target color will always be referred to as +20° rotations from the focal blue color. The experiments included three types of trials: 1) *color wheel memory* trials to measure the template content in long-term memory and independent of simultaneous distractor competition; 2) *search decision* trials to assess how target templates are used during the target decision making stage of visual search; 3) *guidance probe* trials to test how target templates are used during the initial guidance stage of visual search.

The color wheel in the *memory* trials (Figure 5.1A) was divided into 72 bins (5° per bin) and each bin had a number attached. Participants reported the number of the color wedge that best matched the target color in memory. There was a total of six possible rotations of the color wheel. *Search decision* trials were composed of a target and 3 distractor circles (radius: 50 pixels), evenly arrayed around a virtual circle with a radius of 350 pixels (Figure 5.1A). The first distractor (referred to as the "critical distractor") was constructed in steps of 10° from the target color to ±100° rotations from the target color, resulting in a total of 20 distractor colors (Figure 5.1B). Among the 20 colors, the -20° distractor was the focal blue color (Figure 5.1B) and served to interrogate the response bias towards the category center. The second distractor color was always rotated 180° from the target color and was expected to interfere very little with target selection (Figure 5.1B). The color of the last distractor changed on a trial-by-trial basis and was selected from the rest of the color wheel (110° - 250°) in steps of 10° in order to inject visual variability in the search display (Figure 5.1B). To vary the absolute positions of objects, the search array was randomly rotated 40° clockwise or counterclockwise along an imaginary circle on every trial. Each search item had a small notch that appeared at the top or bottom. The notch on the target and the critical distractor appeared equally often on the top and bottom (50% each). The position of the notch on the target and the critical distractor was the same on 50% of trials. The notch positions of the two non-critical distractors varied randomly with the constraint that amongst the four objects, there were always two with notches at the top and two with notches at the bottom on every trial. On *guidance probe* trials (Figure 5.1A), an uppercase letter in the English alphabet was presented in white Arial typeface at the center of each search item. The font size of letters

(15pt) was set to be very small to encourage participants to move their eyes to identify the letter. The letters on a given trial were selected at random, without replacement, from a letter list composed of Q, W, E, U, P, A, J, L, Z, and M. A subsequent response screen displayed six letters in white, including the four presented in the previous probe displays and two fillers randomly chosen from the letter list.

Design. Participants completed 16 practice trials composed of all three types of trials. The main experiment was composed of 12 color wheel memory trials, 160 search decision trials and 80 guidance probe trials. Trials were presented in 80 mini-blocks, each containing 1-3 decision trials and 1 guidance trial. The color wheel memory trials were presented randomly, with the constraint that there could never be two consecutive memory trials.

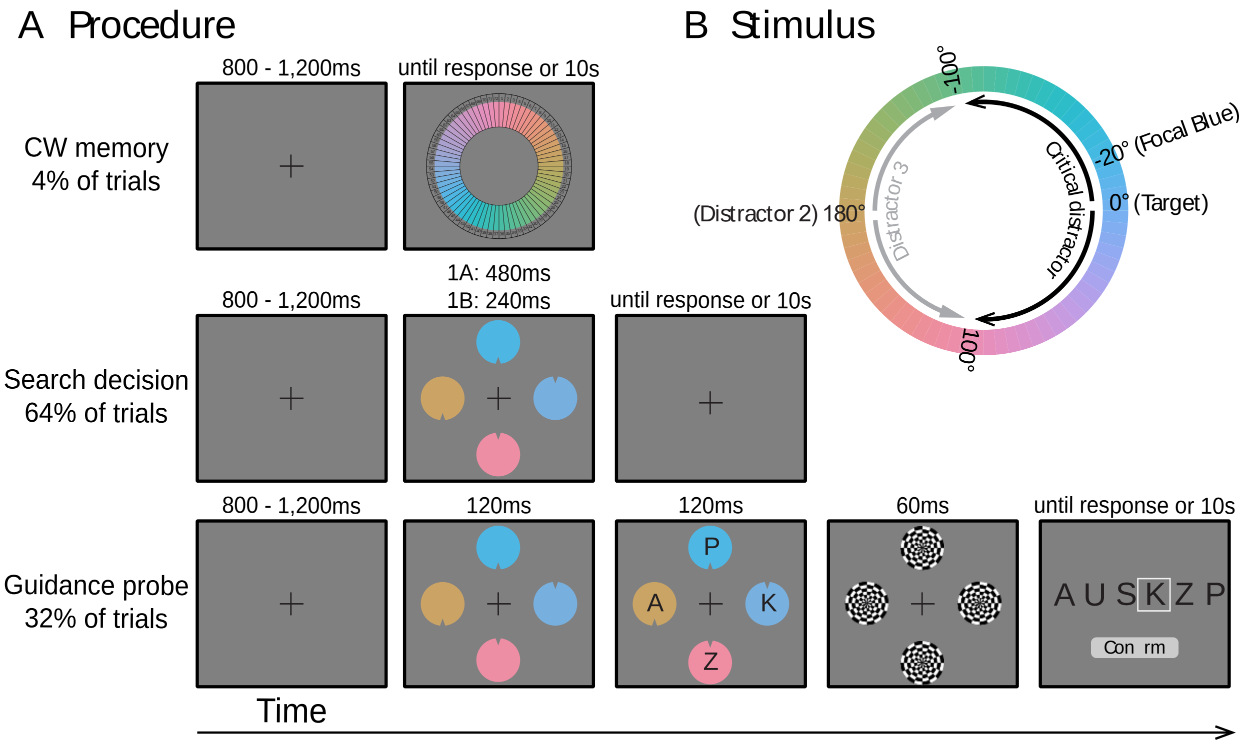

Figure 5.1. A) Example of *color wheel memory, search decision*, and *guidance probe* trials in Experiments 1AB. *Color wheel memory* trials: Participants were instructed to type the number

corresponding to the remembered target color. *Search decision* trials: Participants were instructed to locate the target color circle and report the position of the notch. Visual feedback was given immediately after the response. *Guidance probe* trials: Participants were instructed to report all letters on the response screen that they remembered seeing in the probe display. B) The color wheel used in both experiments. The illustrated target blue color (0°) was 20° rotated from the focal color within the blue color category. The black band indicates the range of colors used for critical distractors (-100° - 100°). The -20° critical distractor was the focal blue color. The second distractor was always 180° rotated from the target. The light gray band indicated the range of colors used for the last distractor (110° - 250°).

Procedure. An example of the target color was presented prior to the beginning of the experiment. On *color wheel memory* trials (4% of trials), participants were required to type the number of the color wedge that best matched the target color in memory in a response box at the bottom of the screen. The color wheel remained on the screen until response. On *search decision* trials (64% of trials), the search array appeared on the screen for 480ms in Experiment 1A. Upon presentation of the display, participants searched for the predefined target-color circle and reported the notch position by pressing the keyboard button “O” for top and button “K” for bottom. Visual feedback was provided immediately following the response. On *guidance probe* trials (32% of trials), the search array was presented for 120ms, followed immediately by a letter superimposed on each search item for 120ms (the letter-probe array). Next, the search array was replaced with circular checkerboard masks (radius: 50 pixels) for 60ms, which served to minimize shifts of attention within iconic memory after the probe array disappeared (Loftus & Shimamura, 1985). Finally, the response display screen appeared until response. Participants used the mouse to choose all probe letters on the response screen that they remembered seeing on the probe display. Participants clicked on zero to four letters: a white box surrounded the letter when it was selected. They pressed “confirm” when selection was complete. If no response was recorded within 10s, all three types of trials automatically terminated. After response, a central fixation cross was presented for 800-1200ms before the next trial started. Participants were instructed to fixate on the center cross until task stimuli were presented.

Because target identification requires the accumulation of perceptual evidence, we presented the *search decision* trials for longer than the *guidance probe* arrays in Experiment 1A. However, this design allows for the possibility that observed differences between the two trial types are due to differences in display duration. To control for this possibility, Experiment 1B was identical to 1A except that the exposure duration of the search displays on *decision* trials was shortened to 240ms. If longer display durations are necessary for decision processes to be more precise than guidance, then there should be no differences between the precision of guidance and decisions in this experiment. However, if decisions are still more precise than guidance with shorter display durations, the results would indicate that the information underlying attentional guidance vs. target decisions is inherently different.

Statistical Analysis. The color wheel in the *memory* task was composed of 72 color wedges sampling color hues in steps of 5°. Therefore, the relative click distance from the veridical target color, which reflects the degree of error in the reported color, was divided into 5° bins (Figure 5.2A). Trials where the response errors were beyond ±60° were removed from data analyses, which accounted for .60% data in Experiment 1A and .48% data in Experiment 1B. The distribution of color wheel clicks was then fitted with a Gaussian function (Figure 5.2A). This resulted in the estimation of parameter μ_{mem} (mean of the color wheel click frequency distribution), which corresponds to the central tendency in the color judgments, and the estimation of parameter σ_{mem} (standard deviation of the click frequency distribution), which corresponds to the precision of color judgments where smaller values indicate higher precision.

Search decision trials with an RT less than 250ms or greater than 2500ms were also excluded from the analyses, which resulted in 1.11% and .70% of the decision trials being dropped in Experiment 1A and 1B, respectively. When analyzing error rates on decision trials, we exclusively analyzed trials where the notch position of the critical distractor and that of the target were opposite, i.e., “notch-opposite” trials (see Supplemental Materials for full description of error rates). The notch positions of the two non-critical distractors on these trials were also opposite. Thus, if one of the two non-critical distractors was selected as the target, the error would have an equal probability of being coded as a "target correct" or a "critical distractor error"; however, such errors were rare (see Figure S5.1 in Supplemental Materials). The majority of errors were due to selection of the critical distractor and therefore errors on these “notch-opposite” trials were used as an estimate of the probability that participants misidentified the critical distractor as the target. We calculated the frequency of misidentifications attributed to selection of each critical distractor for each participant as a metric of decision precision. For example, if the participant made 9 out of 10 errors on trials with the -10° critical distractor, we calculated the frequency of identification errors for the -10° distractor as .9. This calculation was made for every critical distractor separately. We then fitted the error frequencies with a Gaussian function. This resulted in the estimation of parameter μ_{dec} (mean of the decision error frequency distribution), which corresponds to the central tendency of match decisions, and the estimation of parameter σ_{dec} (standard deviation of the error frequency distribution), which corresponds to the precision of decision process.

Guidance probe trials were discarded if more than one probe letter was recalled or when the reported letters were not present in the probe array. This resulted in a loss of 11.46% guidance trials in Experiment 1A and 11.68% guidance trials in Experiment 1B. These trials were excluded because we wished to only measure the first object that participants attended. Report of multiple probe letters precluded the ability to know which object was attended first. The percentage of trials in which only the probe letter at the critical distractor location was reported was used as the index of initial attentional guidance to the critical distractor. Consistent with search decision trials, we fitted a Gaussian function to the reported frequency of letters on critical distractors. This resulted in the estimation of parameter μ_{gui} (mean of the guidance probe recall frequency distribution), which corresponds to the central tendency of attentional guidance, and the estimation of parameter σ_{gui} (standard deviation of the recall frequency distribution), which corresponds to the precision of initial guidance.

All parameters from the Gaussian functions were estimated using a hierarchical Bayesian parameter (HBA) estimation method. To perform HBA, we used the R package, Bayesian Regression Models using ‘Stan’ (brms) (Bürkner, 2017, 2018) and the probabilistic programming language Stan (Carpenter et al., 2017). Normal and Gamma distributions were used to set the hyper priors of the normal mean ($\mu \sim$ Normal (0, 1)) and standard deviation ($\sigma \sim$ Gamma (5, 1)). Given the small number of data points per participant (due to constraints in online experimentation), we only estimated the group parameter values to capture commonalities across individuals. Each chain was run with

5000 samples, with the first 2500 warm-up samples discarded as burn-in. A total of 4 chains were run, leading to 10,000 total posterior samples. Convergence was assessed by computing the Gelman-Rubin $\hat{R}$ statistic for each parameter. The range of $\hat{R}$ values across all group parameter estimates was between 0.99-1.05, suggesting satisfactory convergence. Goodness of fit was visually inspected with the posterior predictive check method (Figures 5.2 and 5.4). For each posterior distribution, we reported the mean posterior estimates and 95% credible intervals. Because all parameters were estimated with a hierarchical Bayesian approach, we conducted hypothesis testing directly on the posteriors rather than relying on frequentist statistics. For example, to assess whether μ_{mem} was significantly more negative than 0°, indicating a memory bias towards the color category center (i.e., the most typical color exemplar of the target category), we report the probability of posterior values being less than zero (Figure 5.2B).

Results

Analysis of the contents of the target template in memory. The distributions of color wheel click on memory trials were estimated by fitting the Gaussian function (Figure 5.2A). We found significantly negatively shifted μ_{mem} values (Figure 5.2B) in both experiments (M_{1A} = -5.45°, CI_{1A} = [-6.05° -4.84°]; M_{1B} = -7.99°, CI_{1B} = [-8.63° -7.36°]), probability > .99, suggesting that colors exhibited memory biases towards the category center (focal blue color: -20°) (Bae et al., 2015; Hardman et al., 2017). Additionally, the estimated σ_{mem} (Figure 5.2C) in both experiments were around 10° (M_{1A} = 10.67°, CI_{1A} = [10.25° 11.10°]; M_{1B} = 10.91°, CI_{1B} = [10.49° 11.44°]), indicating that the memory representation of the target was very precise. If this target template in memory was used to generate target-match decisions and/or guide attention (Yu et al., in press), we expect the precision of those processes to match the precision of the target representation in memory.

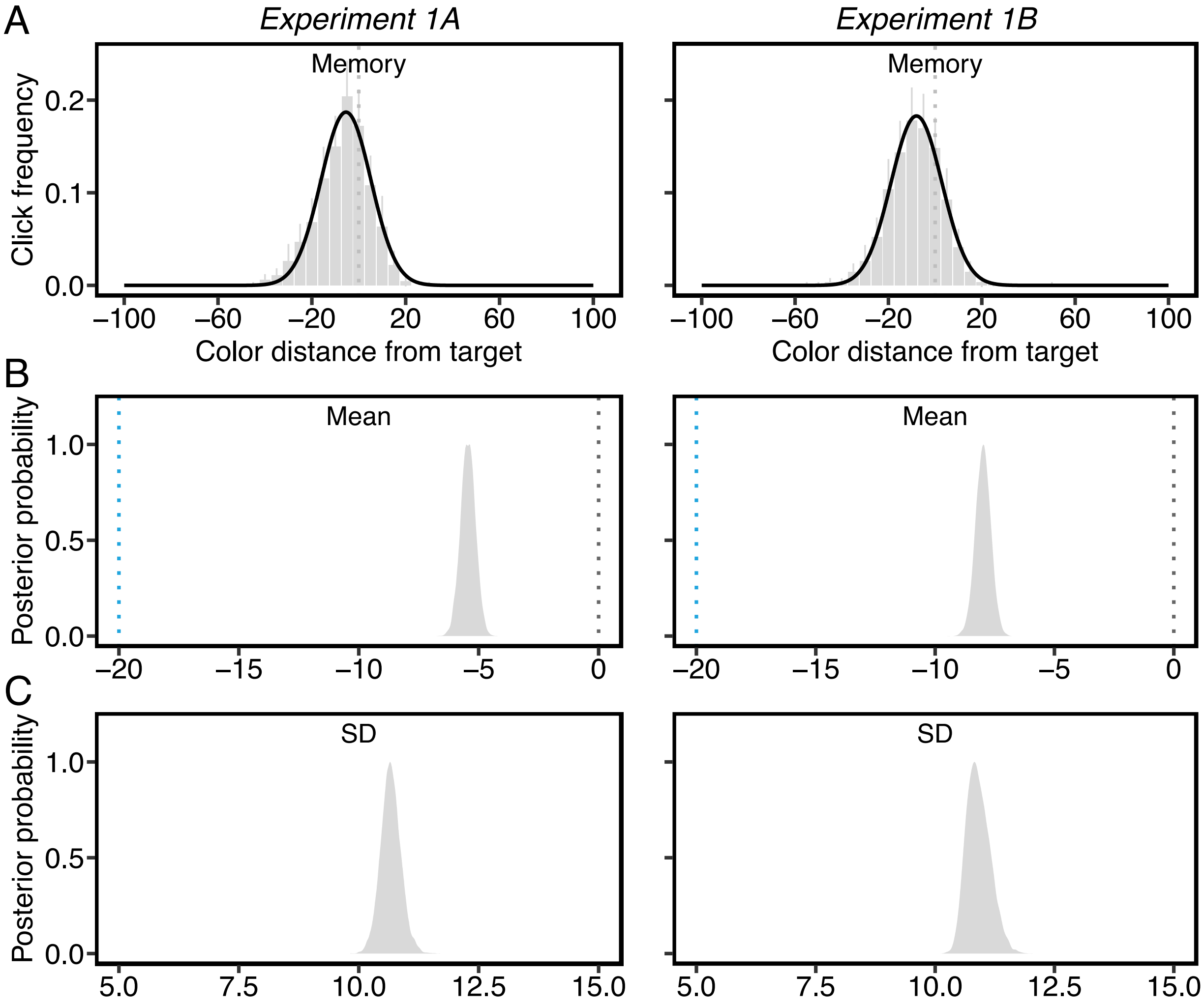

Figure 5.2. A) Group averages of click distance from the target color in the color wheel memory task. Raw data divided into 5° bins. Black solid lines are Gaussian distribution fits. All error bars are the 95% confidence intervals. B) Posterior distribution of μ_{mem} values from Gaussian fits. The gray dotted lines indicate the true target color (0°), and the blue lines indicate the focal blue color (-20°) at the category center. C) Posterior distribution of σ_{mem} values from Gaussian fits.

Analysis of the precision of attentional guidance and match decisions. To test our main hypothesis that guidance would be less precise than decisions, we first directly compared percentages of letters reported on critical distractors on guidance probe trials and error rates on search decision trials using a paired *t* test (Figure 5.3). The two measures provide information about whether critical distractors attracted initial attention and whether they were eventually misidentified as targets. The probe letter recall on critical distractors (M_{1A} = 17.97%, CI_{1A} = [16.56% 19.37%]; M_{1B} = 17.48%, CI_{1B} = [16.20% 18.75%]) was significantly higher than the decision error rate (M_{1A} = 9.90%, CI_{1A} = [8.48% 11.33%]; M_{1B} = 11.60%, CI_{1B} = [10.30% 12.89%]) (Experiment 1A: $t(69) = 8.76$, $p < .0001$, $d = 1.04$, $BF_{10} > 1{,}000$; Experiment 1B: $t(69) = 7.45$, $p < .0001$, $d = .89$, $BF_{10} > 1{,}000$). Moreover, comparisons between probe letter recall and error rates remained significant when each was normalized against response chance level (probe recall: 16.67%; error rates: 50%), Experiment 1A: $t(69) = 44.70$, $p < .0001$, $d = 5.37$, $BF_{10} > 1{,}000$, Experiment 1B: $t(69) = 49.65$, $p < .0001$, $d = 5.93$, $BF_{10} > 1{,}000$ (see also Figure S5.2 in Supplemental Materials for comparisons of probe letter recall on critical distractors against non-critical distractors).

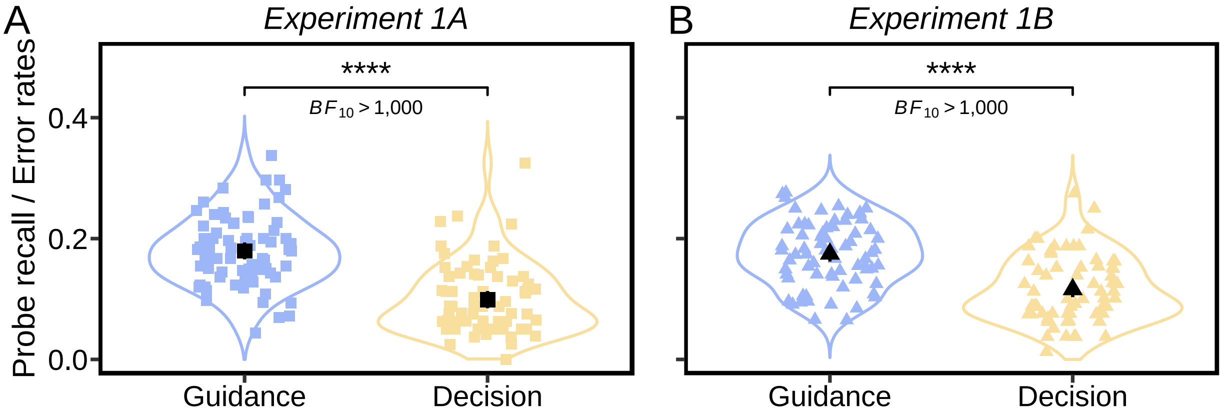

Figure 5.3. The percentages of letters reported on critical distractors on guidance probe trials and the error rates on search decision trials. The two measures provide information about the likelihood of attending to critical distractors and misidentifying them as the target. The colored dots represent individual data points, and the black ones indicate the mean values. All error bars are the 95% confidence intervals.

Next, we examined the frequency of letter recall (Figure 5.4A) and decision errors (Figure 5.4B) as a function of *each* critical distractor condition and fitted the response frequencies with the Gaussian distribution. First, both μ_{gui} (M_{1A} = -10.32°, CI_{1A} = [-13.62°

-7.08°]; M_{1B} = -6.70°, CI$_{1B}$ = [-9.59° -3.83°]) and μ_{dec} (M_{1A} = -4.80°, CI$_{1A}$ = [-5.76° -3.92°]; M_{1B} = -3.53°, CI$_{1B}$ = [-4.82° -2.23°]) were significantly negatively shifted (Figure 5.4C), probability > .99, suggesting that the two subprocesses of visual search were both biased towards the category center. The memory bias for the target color measured from the color wheel memory task was present in both guidance and decisions, consistent with the notion that the target template is encoded in memory and used as the source information for visual search guidance and decisions.

To assess whether a wider range of critical distractors attracted attention than those that were misidentified as the target, we compared the σ values estimated from the fitted Gaussian distributions, which serve as the statistical analogue for the magnitude of precision. As can be seen from the nonoverlapping posteriors (Figure 5.4D), σ_{gui} (M_{1A} = 36.78°, CI$_{1A}$ = [33.17° 40.80°]; M_{1B} = 35.28°, CI$_{1B}$ = [31.83° 39.02°]) was significantly larger than σ_{dec} (M_{1A} = 13.99°, CI$_{1A}$ = [12.91° 15.14°]; M_{1B} = 18.41°, CI$_{1B}$ = [17.00° 19.96°]) in both experiments, probability > .99. The difference in σ values provide strong evidence in support of the hypothesis that the precision of attentional guidance is coarser than the precision of target-match decisions.

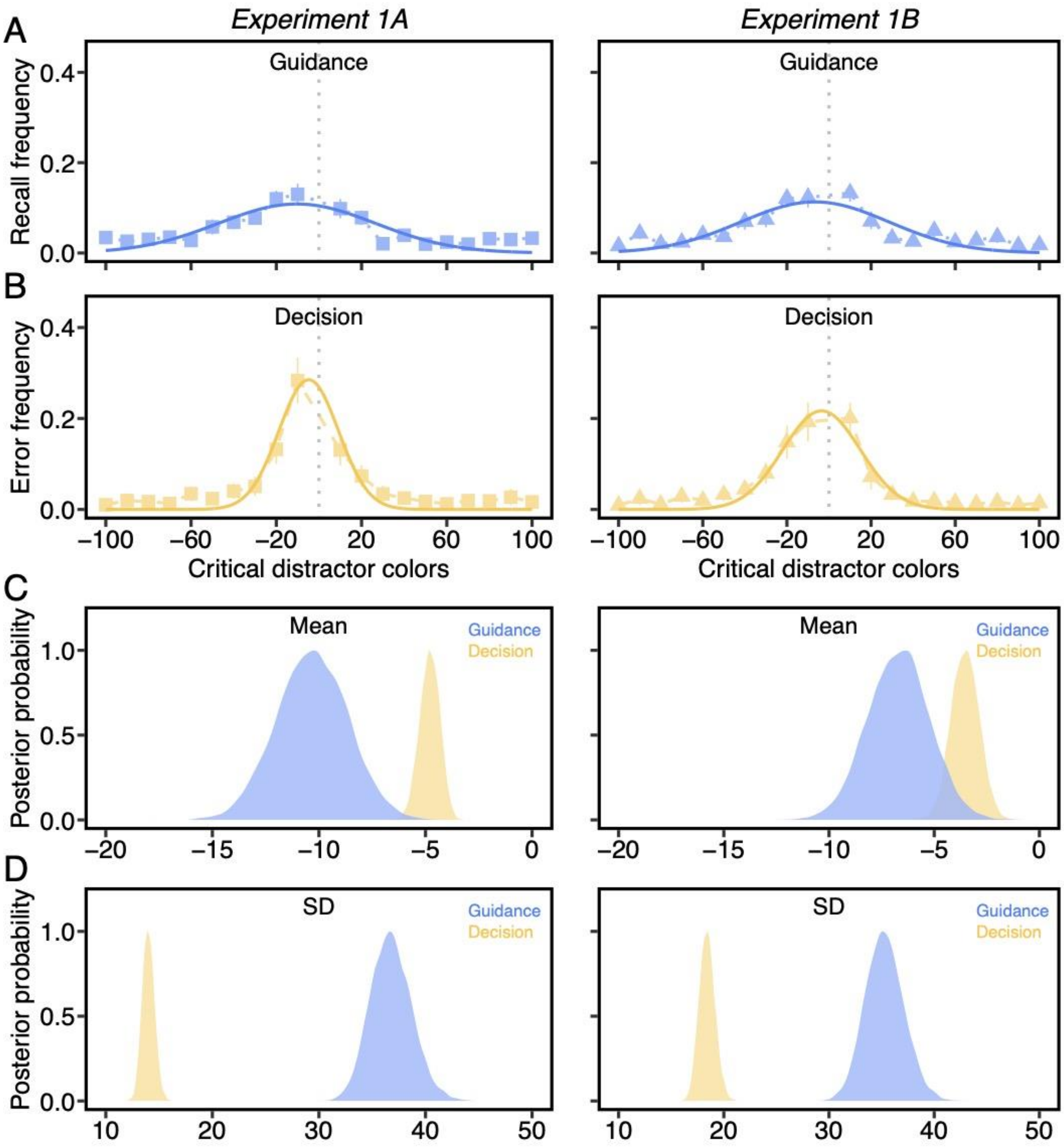

Figure 5.4. A) The frequency with which letters were recalled on each critical distractor. B) The frequency with which each critical distractor was misidentified as the target. Solid curved lines are Gaussian distribution fits. The gray dash line indicates the true target color. All error bars are the 95% confidence intervals. C) Posterior distribution of μ values from Gaussian fits. D) Posterior distribution of σ values from Gaussian fits.

Comparisons of guidance and decisions against memory precision. Next, we compared the precision of the color wheel memory performance, which represents the upper limit in the precision of the template, against guidance and decisions. The precision of guidance (σ_{gui}) was significantly poorer than memory (σ_{mem}) in both experiments (Experiment 1A: M_{diff} = 26.11°; Experiment 1B: M_{diff} = 24.38°), probability > .99. This suggests that the cause of broader attentional guidance to target-similar stimuli is not due to imprecision in the underlying memory representation, but rather due to poor attentional selectivity (Kerzel, 2019). Although there was also a statistical difference between σ_{dec} and σ_{mem}, probability > .99, the average difference was more modest, 3.33° in Experiment 1A and 7.50° in Experiment 1B. The larger difference in Experiment 1B was likely due to limitations in evidence accumulation following the shorter exposure duration of the search array. Together, the results indicate that the target decision process uses more precise template information compared to initial attentional guidance. Interestingly, both were less precise than the actual memory for the target itself. This suggests that the limiting factor in guidance and decision precision during visual search is related to temporal or visual pressures rather than the fidelity of the template memory itself.

Experiment 2AB

The purpose of Experiment 2 was to provide a conceptual replication of Experiment 1 and test if imprecisions in attentional guidance will still occur on visual search trials with small set sizes. In this experiment, we modified the visual search paradigm to include a target and only one distractor. We predicted the precision of attentional guidance would increase but still be worse than the precision of target-match decisions.

Method

Participants. 195 new participants from University of California, Davis participated online in Experiment 2A and 2B in partial fulfillment of a course requirement. 55 subjects were excluded by the same criteria in Experiment 1, which led to a total of 140 undergraduates (self-reported 22 males, self-reported 118 females, 11 left-handed, ages from 18 – 39 years). A given participant completed only one experiment (Experiment 2A or 2B). Each participant provided written informed consent in accordance with the local ethics clearance as approved by the National Institutes of Health. Each participant's color vision was assessed by self-report. All participants had normal or corrected-to-normal vision, and all had normal color vision.

Stimuli, Design, Procedure & Statistical Analysis. All aspects of Experiment 2 were identical to Experiment 1, with the following exceptions. *Search decision* trials (Figure 5.5) consisted of two bilaterally presented target and critical distractor circles (distance between the center points: 350 pixels). Participants were instructed to indicate whether the target color appeared at the left side by pressing button "K" or at the right side by pressing button "L". The stimuli appeared on the screen for 480ms in Experiment 2A and 240ms in Experiment 2B. *Guidance probe* trials (Figure 5.5) started like search decision trials, but the search array appeared for only 120ms. Then, probe letters were superimposed on the search items for 120ms, after which all items disappeared. The letter list was the same as the list used in Experiment 1, except that the letter "L" was replaced with the letter "B" because "L" was now used for search trial responses. The subsequent response screen displayed four letters, including the two in probe displays and two fillers randomly chosen from the letter list. The two target colors were counterbalanced across participants and because there were no spurious differences (*ps* > .18), the data were collapsed in all subsequent analyses. Overall, 3.9% of trials in Experiment 2A and 3.9% of trials in Experiment 2B were removed from data analysis by the same criteria in Experiment 1.

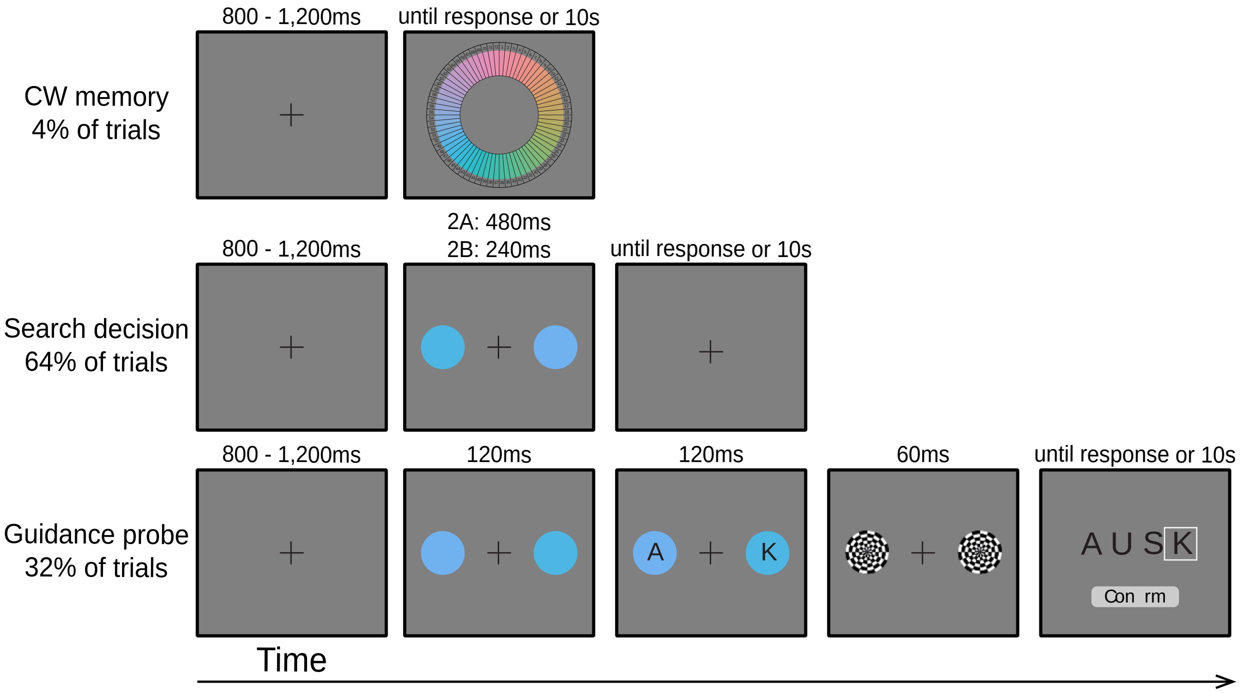

Figure 5.5. Example of *color wheel memory*, *search decision*, and *guidance probe* trials in Experiments 2AB.

Results

Analysis of the contents of the target template in memory. The distributions of relative click distance on color wheel memory trials were fitted with the Gaussian function (Figure 5.6A). The μ_{mem} values (M_{2A} = -5.63°, CI_{2A} = [-6.21° -5.05°]; M_{2B} = -8.13°, CI_{2B} = [-8.71° -7.55°]) were significantly negatively shifted (Figure 5.6B), probability > .99. This result replicated those from Experiment 1, suggesting that the color memory is pulled towards the nearest category center. In addition, we found no difference in memory precision (M_{2A} = 10.60°, CI_{2A} = [10.18° 11.01°]; M_{2B} = 10.49°, CI_{2B} = [10.05° 10.89°]) between

Experiment 1 and 2 (Figure 5.6C), $\text{probability}_{1A>2A} = .58$, $\text{probability}_{1B>2B} = .91$, indicating that the stable search target is stored in long-term memory with high precision (Woodman et al., 2013) irrespective of whether it is used for four-item or two-item search.

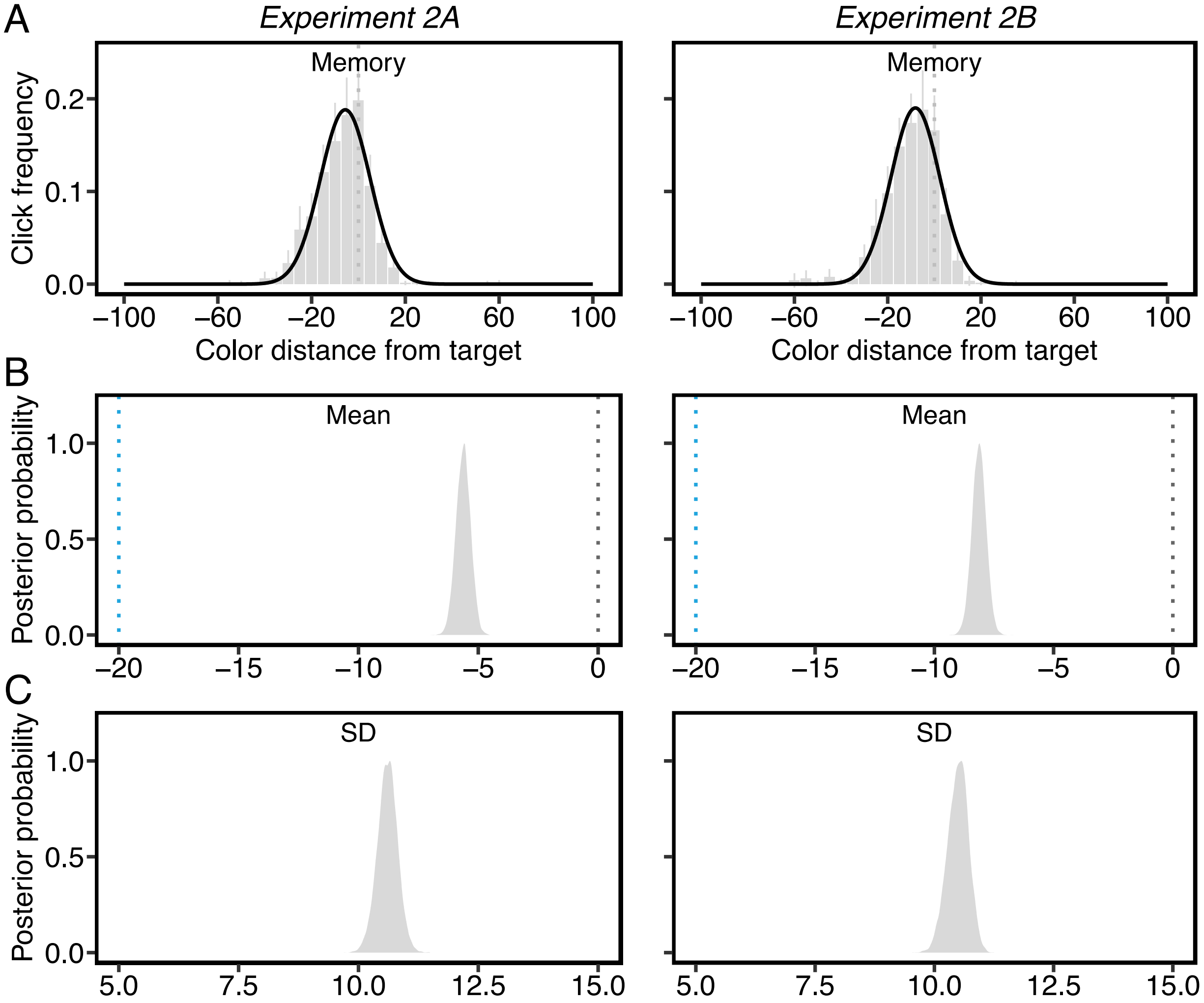

Figure 5.6. A) Group averages of click distance from the target color in the color wheel memory task. Raw data divided into 5° bins. Black solid lines are Gaussian distribution fits. All error bars are the 95% confidence intervals. B) Posterior distribution of μ_{mem} values from Gaussian fits. The gray dotted lines indicate the true target color (0°), and the blue lines indicate the focal blue color (-20°) at the category center. C) Posterior distribution of σ_{mem} values from Gaussian fits.

Analysis of the precision of attentional guidance and match decisions. A paired *t* test (Figure 5.7) confirmed a significantly higher percentage of letters reported on critical distractors (M_{2A} = 15.82%, CI_{2A} = [13.25% 18.38%]; M_{2B} = 13.17%, CI_{2B} = [11.16%

15.18%]) than the error rate of selecting critical distractors as the target (M_{2A} = 6.32%, CI_{2A} = [5.46% 7.17%]; M_{2B} = 6.24%, CI_{2B} = [5.59% 6.89%]) (Experiment 2A, $t(69) = 7.56$, $p < .0001$, $d = 0.90$, $BF_{10} > 1,000$; Experiment 2B, $t(69) = 7.22$, $p < .0001$, $d = .86$, $BF_{10} > 1,000$). Comparisons remained significant when probe letter recall and error rates were normalized against response chance level (probe recall: 25%; error rates: 50%), Experiment 2A: $t(69) = 34.07$, $p < .0001$, $d = 4.07$, $BF_{10} > 1,000$; Experiment 2B: $t(69) = 41.99$, $p < .0001$, $d = 5.02$, $BF_{10} > 1,000$. In replication of Experiment 1, participants were more likely to direct their attention to critical distractors, but easily reject them as nontargets.

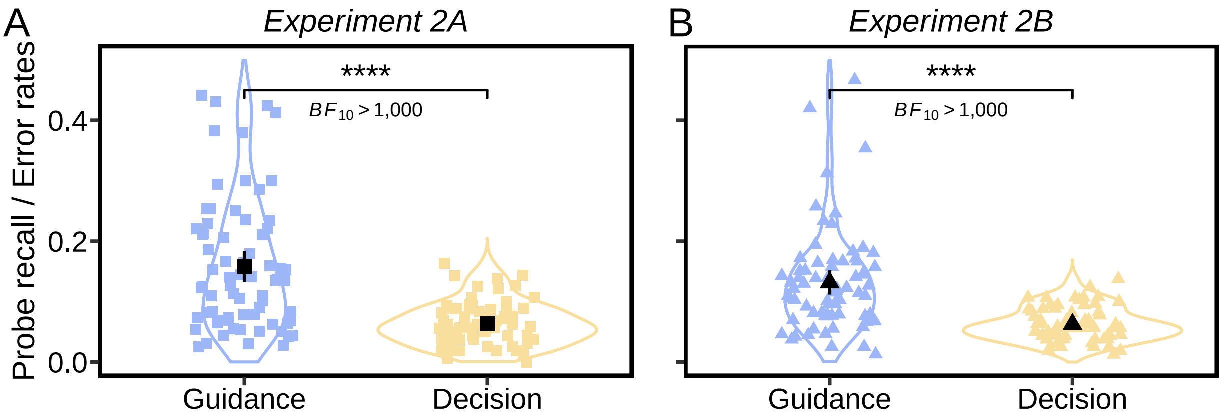

Figure 5.7. The percentages of letters reported on critical distractors on guidance probe trials and the error rates of selecting critical distractors as the target on search decision trials. The colored dots represent individual data points, and the black ones indicate the mean values. All error bars are the 95% confidence intervals.

We next computed the frequency of letter recall (Figure 5.8A) and decision errors (Figure 5.8B) as a function of *each* critical distractor condition and fitted the Gaussian function to frequency distributions in the same way as Experiment 1. First, both μ_{gui} (M_{2A} = -4.23°, CI_{2A} = [-5.62° -2.91°]; M_{2B} = -4.86°, CI_{2B} = [-6.15° -3.63°]) and μ_{dec} (M_{2A} = -4.39°, CI_{2A} = [-5.21° -3.61°]; M_{2B} = -4.31°, CI_{2B} = [-5.07° -3.57°]) were significantly negatively shifted (Figure 5.8C), probability > .99, demonstrating a bias in guidance and decisions towards the category center. The shift in memory towards the category center was recapitulated in guidance and decisions, supporting the notion that a single memory template underlies both processes.

The comparisons of σ values, which were used to index the precision of guidance and decisions, showed that σ_{gui} (M_{2A} = 20.23°, CI_{2A} = [18.27° 22.41°]; M_{2B} = 19.14°, CI_{2B} = [17.67° 20.74°]) was significantly larger than σ_{dec} (M_{2A} = 12.70°, CI_{2A} = [12.01° 13.44°]; M_{2B} = 12.54°, CI_{2B} = [11.88° 13.21°]) in both experiments (Figure 5.8D), probability > .99. This pattern converges with Experiment 1, suggesting that attentional guidance is a less precise process during visual search than match decisions. Furthermore, the σ_{gui} values (Experiment 1A - 2A: M_{diff} = 16.54°; Experiment 1B - 2B: M_{diff} = 16.14°) were much smaller, probability > .99, compared to Experiment 1, showing that the precision of attentional guidance improved substantially with smaller set sizes. In contrast, the set size effect on σ_{dec} (Experiment 1A - 2A: M_{diff} = 1.29°; Experiment 1B - 2B: M_{diff} = 5.87°) was significant but relatively weak, $probability_{1A>2A}$ = .97, $probability_{1B>2B}$ > .99.

Comparisons of guidance and decisions against memory precision. The σ_{gui} values were significantly greater than the σ_{mem} values (Experiment 2A: M_{diff} = 9.63°; Experiment 2B: M_{diff} = 8.65°), probability > .99, again suggesting that imprecise attentional guidance is not because of poor memory representations. In contrast, the average difference between σ_{dec} and σ_{mem} was only 2.10° in Experiment 2A and 2.04° in Experiment 2B, but statistically significant, probability > .99, highlighting the fact that the precision of decision process was closer to the precision of the target color held in long-term memory.

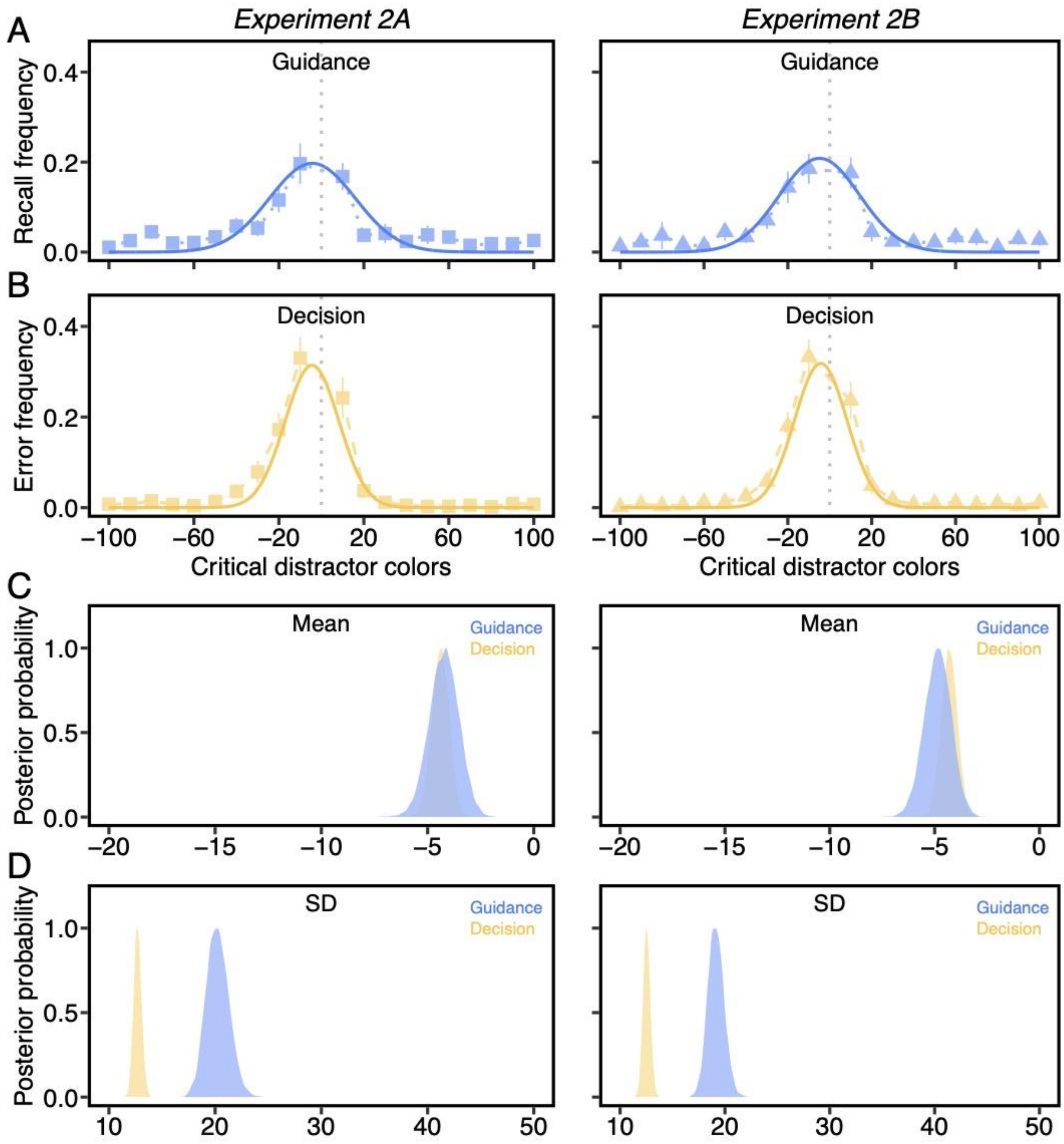

Figure 5.8. A) The frequency with which letters were recalled on each critical distractor. B) The frequency with which each critical distractor was misidentified as the target. Solid curved lines are Gaussian distribution fits. The gray dash line indicates the true target color. All error bars are the 95% confidence intervals. C) Posterior distribution of μ values from Gaussian fits. D) Posterior distribution of σ values from Gaussian fits.

Discussion

The purpose of the current experiments is to test if attentional guidance is coarser than target-match decisions during visual search. To this end, we measured the likelihood of attentional guidance and misidentification decisions across of a range of distractors from 10° up to 100° of separation from the target in color space. The results showed that a broader range of distractors capture initial attention than those that were ultimately misidentified as targets. Our findings provide strong evidence that template information operates at different scales of precision to guide attention and make identity decisions (Wolfe, 2021).

The target template has long been hypothesized to allocate attention to candidate objects by converting display-wide enhancement of template-matching features into spatially specific enhancement (Berggren et al., 2017; Eimer, 2014). However, recent research has found that target-similar cues that do not completely match the template contents also strongly capture attention (Kerzel, 2019), suggesting that attentional selection is imprecise compared to the memory template. In the current study, we found convergent evidence that the "tuning" of guidance was 8 ~ 26° broader than the target template in memory. In contrast, decisions about the identity of the target after a candidate object was selected were only 2° ~ 3° less precise than the template. The exception was in Experiment 1B when the search display was short and there were four items, suggesting that the precision of decision processes depends on sufficient time to accumulate perceptual evidence (Yu et al., in press).

Together, these experiments suggest that attentional guidance and target-match decisions differ in precision during visual search. What could cause this difference between guidance and decisions? The low precision of attentional guidance is perhaps due to the need to rapidly prioritize attention to stimuli in peripheral vision where color and spatial acuity are poor (Hulleman, 2009; Rosenholtz, 2017). This would explain why the precision of the initial guidance improved substantially when the set size was smaller and there was less visual crowding (Experiment 2). In contrast, when making identity decisions, there is greater pressure for accuracy and more detailed information is available because the attended stimulus is in foveal vision (Castelhano et al., 2008; Rajsic & Woodman, 2020).

So far, our assumption has been that attentional guidance and decisions rely on the same target template but are constrained by differences in visual acuity (i.e., in peripheral vs. central vision) and perhaps response criterion. However, it is also possible that there are two sources of information with independent target representations. For example, Wolfe and colleagues have argued that when looking for a large number of potential targets, search is guided by a "guiding template" in working memory that contains simple guiding features like color and orientation, and target identification, or object recognition, is determined by a precise "target template" in long-term memory (Cunningham & Wolfe, 2014; Wolfe, 2021). Depending on the processing stage at hand, the appropriate representation would be selected to optimally meet the task requirements. Because we only used a single color as the target throughout the experiment, our data do not speak to whether guidance is based on a working memory template that is separate from the long-term memory representation of the target, or whether guidance only reflects a coarser manifestation of the same target template in memory. Future work is necessary to flesh out how working and long-term memory representations of the target differ and are used to guide attention and make target decisions.

In conclusion, we used an attention-probe paradigm to compare the precision of attentional guidance and the precision of target-match decisions during visual search. Under different exposure durations and distractor set sizes, we consistently observed that guidance was coarser than match decisions. Our results offer a novel view of the search template that considers the unique demands of attentional guidance vs. decisions during visual search.

Supplemental Material

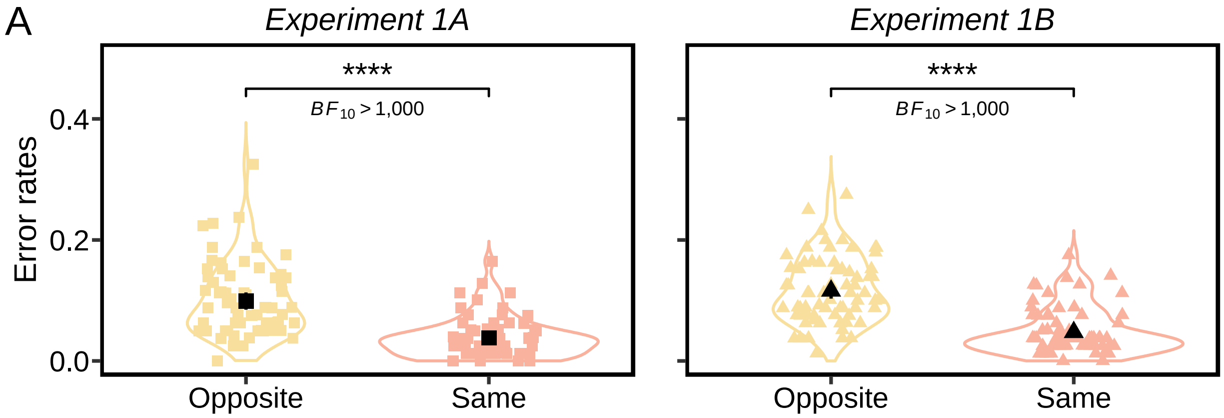

Figure S5.1. Error rates on *search decision* trials where the notch position of the critical distractor and that of the target were opposite or the same in Experiments 1AB. Because the target and critical distractor had the same response on the "same" trials, the error rates reflect the likelihood of misidentifying one of the two non-critical distractors as the target. The error rates on these trials were low (M_{1A} = 3.79%, CI_{1A} = [2.99% 4.58%]; M_{1B} = 4.75%, CI_{1B} = [3.82% 5.68%]), suggesting that participants had a very low probability of selecting the non-critical distractors as the target. This supports the notion that error on "opposite" trials (on which the two non-critical distractors also had opposite notch positions) reflect the rate of erroneously selecting the critical distractor as the target.

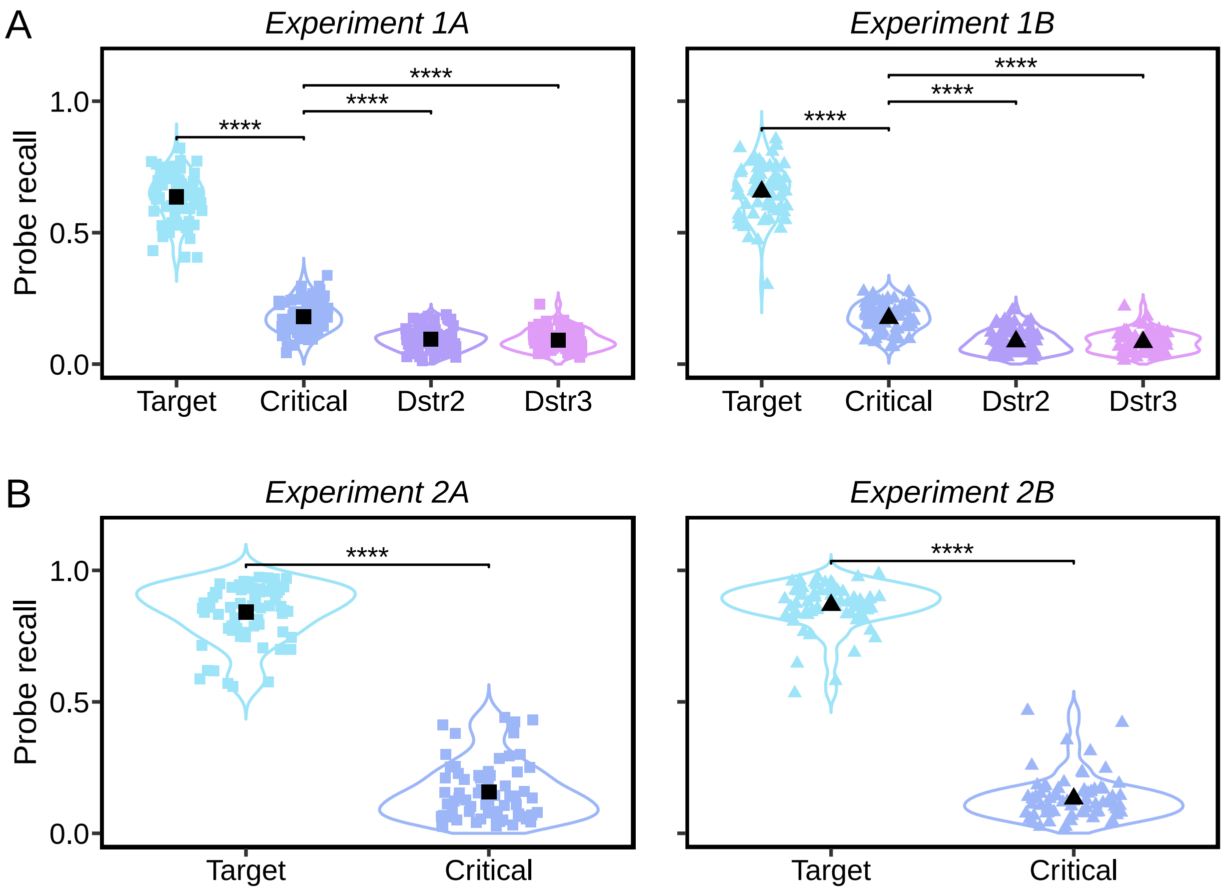

Figure S5.2. A) The percentages of probe letter reported on the target, critical distractors, and non-critical distractors on *guidance probe* trials in Experiments 1AB. The probe letter recall on the target was significantly higher than the probe letter recall on all three distractors, *ts* > 36.13, *ps* < .0001, *ds* > 4.31, BF_{10} > 1,000. The probe letter recall on the critical distractor was significantly higher than the probe letter recall on two non-critical distractors, *ts* > 10.62, *ps* < .0001, *ds* > 1.26, BF_{10} > 1,000. B) The percentages of probe letter reported on the target and critical distractors on *guidance probe* trials in Experiments 2AB. The probe letter recall on the target was significantly higher than the probe letter recall on the critical distractor, *ts* > 26.57, *ps* < .0001, *ds* > 3.17, BF_{10} > 1,000. Trials included in these analyses were ones in which only one letter was reported, which represented 80% or more of the guidance probe trials.

References

Andersen, S. K., Hillyard, S. A., & Müller, M. M. (2008). Attention Facilitates Multiple Stimulus Features in Parallel in Human Visual Cortex. *Current Biology*, *18*(13), 1006–1009. https://doi.org/10.1016/j.cub.2008.06.030

Bae, G.-Y., Olkkonen, M., Allred, S. R., & Flombaum, J. I. (2015). Why some colors appear more memorable than others: A model combining categories and particulars in color working memory. *Journal of Experimental Psychology. General*, *144*(4), 744—763. https://doi.org/10.1037/xge0000076

Berggren, N., Jenkins, M., McCants, C. W., & Eimer, M. (2017). The spatially global control of attentional target selection in visual search. *Visual Cognition*, *25*(1–3), 196–214. https://doi.org/10.1080/13506285.2017.1287806

Bundesen, C. (1990). A theory of visual attention. *Psychological Review*, *97*(4), 523—547. https://doi.org/10.1037/0033-295x.97.4.523

Bürkner, P.-C. (2017). **brms**: An *R* Package for Bayesian Multilevel Models Using *Stan*. *Journal of Statistical Software*, *80*(1). https://doi.org/10.18637/jss.v080.i01

Bürkner, P.-C. (2018). Advanced Bayesian Multilevel Modeling with the R Package brms. *The R Journal*, *10*(1), 395. https://doi.org/10.32614/RJ-2018-017

Carlisle, N. B., Arita, J. T., Pardo, D., & Woodman, G. F. (2011). Attentional Templates in Visual Working Memory. *Journal of Neuroscience*, *31*(25), 9315–9322. https://doi.org/10.1523/JNEUROSCI.1097-11.2011

Carpenter, B., Gelman, A., Hoffman, M. D., Lee, D., Goodrich, B., Betancourt, M., Brubaker, M., Guo, J., Li, P., & Riddell, A. (2017). *Stan*: A Probabilistic Programming Language. *Journal of Statistical Software*, *76*(1). https://doi.org/10.18637/jss.v076.i01

Castelhano, M. S., Pollatsek, A., & Cave, K. R. (2008). Typicality aids search for an unspecified target, but only in identification and not in attentional guidance. *Psychonomic Bulletin & Review*, *15*(4), 795–801. https://doi.org/10.3758/PBR.15.4.795

Cunningham, C. A., & Wolfe, J. M. (2014). The role of object categories in hybrid visual and memory search. *Journal of Experimental Psychology. General*, *143*(4), 1585—1599. https://doi.org/10.1037/a0036313

Desimone, R., & Duncan, J. (1995). Neural Mechanisms of Selective Visual Attention. *Annual Review of Neuroscience*, *18*(1), 193—222. https://doi.org/10.1146/annurev.ne.18.030195.001205

Duncan, J., & Humphreys, G. W. (1989). *Visual Search and Stimulus Similarity*. 26.

Eimer, M. (2014). The neural basis of attentional control in visual search. *Trends in Cognitive Sciences*, *18*(10), 526—535. https://doi.org/10.1016/j.tics.2014.05.005

Gaspelin, N., Leonard, C. J., & Luck, S. J. (2015). Direct Evidence for Active Suppression of Salient-but-Irrelevant Sensory Inputs. *Psychological Science*, *26*(11), 1740–1750. https://doi.org/10.1177/0956797615597913

Gaspelin, N., & Luck, S. J. (2018). Distinguishing among potential mechanisms of singleton suppression. *Journal of Experimental Psychology: Human Perception and Performance*, *44*(4), 626–644. https://doi.org/10.1037/xhp0000484

Grubert, A., & Eimer, M. (2018). The Time Course of Target Template Activation Processes during Preparation for Visual Search. *The Journal of Neuroscience*, *38*(44), 9527–9538. https://doi.org/10.1523/JNEUROSCI.0409-18.2018

Hardman, K. O., Vergauwe, E., & Ricker, T. J. (2017). Categorical working memory representations are used in delayed estimation of continuous colors. *Journal of Experimental Psychology: Human Perception and Performance*, *43*(1), 30–54. https://doi.org/10.1037/xhp0000290

Hout, M. C., & Goldinger, S. D. (2015). Target templates: The precision of mental representations affects attentional guidance and decision-making in visual search. *Attention, Perception \textbackslash& Psychophysics*, *77*(1), 128—149. https://doi.org/10.3758/s13414-014-0764-6

Hulleman, J. (2009). No need for inhibitory tagging of locations in visual search. *Psychonomic Bulletin & Review*, *16*(1), 116–120. https://doi.org/10.3758/PBR.16.1.116

Kerzel, D. (2019). The precision of attentional selection is far worse than the precision of the underlying memory representation. *Cognition*, *186*, 20—31. https://doi.org/10.1016/j.cognition.2019.02.001

Kim, M.-S., & Cave, K. R. (1995). Spatial Attention in Visual Search for Features and Feature Conjunctions. *Psychological Science*, *6*(6), 376–380.

Liu, T., Larsson, J., & Carrasco, M. (2007). Feature-Based Attention Modulates Orientation-Selective Responses in Human Visual Cortex. *Neuron*, *55*(2), 313—323. https://doi.org/10.1016/j.neuron.2007.06.030

Loftus, G. R., & Shimamura, A. P. (1985). How Much Is an Icon Worth? *Journal of Experimental Psychology: Human Perception and Performance*, *11*(1), 1–13.

Malcolm, G. L., & Henderson, J. M. (2009). The effects of target template specificity on visual search in real-world scenes: Evidence from eye movements. *Journal of Vision*, *9*(11), 8–8. https://doi.org/10.1167/9.11.8

Malcolm, G. L., & Henderson, J. M. (2010). Combining top-down processes to guide eye movements during real-world scene search. *Journal of Vision*, *10*(2), 4–4. https://doi.org/10.1167/10.2.4

Nako, R., Grubert, A., & Eimer, M. (2016). Category-based guidance of spatial attention during visual search for feature conjunctions. *Journal of Experimental Psychology: Human Perception and Performance*, *42*(10), 1571—1586. https://doi.org/10.1037/xhp0000244

Rajsic, J., & Woodman, G. F. (2020). Do we remember templates better so that we can reject distractors better? *Attention, Perception, & Psychophysics*, *82*(1), 269–279. https://doi.org/10.3758/s13414-019-01721-8

Reynolds, J. H., & Heeger, D. J. (2009). The Normalization Model of Attention. *Neuron*, *61*(2), 168—185. https://doi.org/10.1016/j.neuron.2009.01.002

Rosenholtz, R. (2017). Those pernicious items. *Behavioral and Brain Sciences*, *40*, e154. https://doi.org/10.1017/S0140525X16000248

Treue, S., & Trujillo, J. C. M. (1999). Feature-based attention influences motion processing gain in macaque visual cortex. *Nature*, *399*(6736), 575—579. https://doi.org/10.1038/21176

Wolfe, J. M. (2021). Guided Search 6.0: An updated model of visual search. *Psychonomic Bulletin & Review*. https://doi.org/10.3758/s13423-020-01859-9

Woodman, G. F., Carlisle, N. B., & Reinhart, R. M. G. (2013). Where do we store the memory representations that guide attention? *Journal of Vision*, *13*(3). https://doi.org/10.1167/13.3.1

Yu, X., Hanks, T. D., & Geng, J. J. (in press). Attentional guidance and match decisions rely on different template information during visual search.

Chapter 6: General Discussion

The idea of template is a core construct within all models of attention. Most hypothesize that template information is used to bias sensory processing towards target features and serve as a decisional boundary for target selection (Bundesen, 1990; Desimone & Duncan, 1995; Duncan & Humphreys, 1989; Liu et al., 2007; Martinez-Trujillo & Treue, 2004; Reynolds & Heeger, 2009). The target template is typically characterized as a single, static, and veridical representation of what we are looking for. Across the experiments presented here we found that the template contents are modulated by the distractor context and that the precision of template information differs based on the stage of processing. Together, these results illuminate that the template should be understood as a custom set of information that will change based on environments and task demands.

Template modulation mechanism

Previous findings demonstrated that when the distractor set is linearly separable from the target, the target representation in memory shifts away from distractor features (Becker, 2010; Kerzel, 2020; Navalpakkam & Itti, 2007) and develop a sharper boundary with distractors (Geng et al., 2017). These changes in the target template are presumed to increase the target-to-distractor psychological distinctiveness and lead to better attentional selection. In Chapter 2, we extended those findings by demonstrating the exact properties of the visual context that contribute to template shifting and sharpening. Specifically, the template representation shifts whenever the distractor set is linearly separable from the target, but that asymmetrical sharpening only occurs when linearly separable distractors are highly target-similar. These results suggest that asymmetrical sharpening is a more effortful strategy and is only used when necessary to counteract pressure from highly competitive distractors, potentially to avoid cognitive effort (Tünnermann et al., 2021). In contrast, a systematic shift occur even when distractor colors are easily distinguishable from the target, and the magnitude of this shift is insensitive to increased distractor competition. Thus, template shifting appears to occur in response to the entire distractor features space, but not to specific feature values. It remains an interesting question what specific conditions affect the magnitude of shift in target representation.

Although the contents of the template are expected to affect both sensory processing as well as decisional processes, the match-to-sample probe task only obtained a measurement of target decisions independent from distractor processing and competition during active visual search. Therefore, the pattern we have seen should reflect a memory representation that impacts visual search processes by facilitating target-match decisions instead of biasing sensory selection during attentional guidance. Taken together, shifting and sharpening are sensitive to different qualities of distractor pressure (linear separability and similarity, respectively), but both increase the representational distinctiveness of targets from expected distractors to better identify targets.

One open question remains in Chapter 2 regarding the brain mechanisms that support these changes in target representation. Using the same task, in Chapter 3, we sought to find out how brain encodes the template information to optimize target-match decisions. We targeted networks for which have long been known of template maintenance, namely the frontoparietal control network and the visual cortical network

(Bichot et al., 2015, 2019; D'Esposito & Postle, 2015; Harrison & Tong, 2009; Schaefer et al., 2018). We successfully decoded the off-veridical template that maximized the target-to-distractor discrimination in prefrontal cortex in the probe task when no actual distractors presented. The results suggest that prefrontal cortex engages in target decisions using templates that are held in long-term memory and shaped by the recent search context. The results corroborate previous research that target representations in frontoparietal regions are often biased to optimize different task demands (Ester et al., 2016; Lee et al., 2013; Long & Kuhl, 2018). In contrast to the pattern in prefrontal cortex, stimulus responses in early visual cortex reflected veridical target inputs, suggesting that match decisions are based on a transformation of veridical target information in sensory cortex into a biased template space in service of facilitating decision processes. As previously mentioned, the template information are also used to set sensory gains, besides determine target identify. A remaining question is if the same template information stored in prefrontal cortex is used to guide sensory selection. If so, how the template information is transformed to visual cortex to select any relational matching stimuli (Chapter 4 results)? If not, which brain regions flexibly control the template contents for better target selection? Future work will be necessary to address those questions.

Coarse guidance and precise decisions

In Chapter 2 and 3, we demonstrated the flexibility of the template contents as a function of distractor context. In Chapter 4 and 5, we further explored how template information changed as a function of the stage of processing during visual search. Although previous studies have used eye metrics to measure the effect of templates during guidance and decisions (Hout & Goldinger, 2015; Malcolm & Henderson, 2010, 2010), few have considered whether the information is the same or different. In Chapter 4, we used the same visual search paradigm in which all distractors were linearly separable but highly similar to the target and were known to shift the target representation away from the distractor features. In separate critical search trials, we systematically varied the color of the critical distractor and assessed how frequently it captured initial attention and how long and how likely it was rejected as a non-target. In line with Becker and colleagues' relational account (Becker, 2010; Martin & Becker, 2018), we found that all stimuli that were relational matches captured attention and first saccades more strongly than stimuli that were relational mismatches. Therefore, attention appears to be initially guided by the relative feature of the target, not specific feature values. However, the fixation dwell times and the DDM drift rates, as measurements of target-match decisions, were based on an optimally tuned target template with a central value shifted away from distractors. These results suggest that the decision process operates on an optimally shifted and precisely tuned template. In addition, we observed a close relationship between the target memory representation and the decision process during visual search, suggesting that the long-term memory representation of the target is more closely aligned with decision processes in visual search than guidance.

Real-world search, however, rarely involves linearly separable distractors. In Chapter 5, we tested if guidance uses a coarser version of the template compared to decisions during more typical search conditions. We used an attention-probe paradigm (Gaspelin et al., 2015) and measured the likelihood of attentional guidance and misidentification decisions across of a range of distractors from 10° up to 100° of separation from the target in color space. The results showed that a broader range of distractors captured initial attention than those that were ultimately misidentified as targets, suggesting that the precision of attentional guidance is worse than the precision of target-match decisions. Interestingly, both processes were less precise than the actual memory for the target itself. This suggests that the limiting factor in guidance and decision precision during visual search is related to temporal pressure or visual acuity rather than the fidelity of the memory itself. Taken together, our findings in the two chapters provide strong evidence that template information operates at different scales of precision to guide attention and make identity decisions.

An open question remains about what could cause this difference between guidance and decisions. One possible reason is due to the poor color and spatial acuity when there is a need to rapidly prioritize attention to stimuli in peripheral vision (Hulleman, 2009, 2010; Rosenholtz, 2017). In contrast, when making identity decisions, there is greater pressure for accuracy and more detailed information is available because the attended stimulus is in foveal vision (Rajsic & Woodman, 2020). Another possibility is that participants set different criterions: a liberal criterion to broadly capture all potential targets and a more conservative criterion for more precise decisions. So far, the assumption has been that guidance and decisions rely on the same target template but are constrained by differences in visual acuity and response criterion. However, it is also possible that there are two sources of information with independent target representations. For example, Wolfe and colleagues have argued that when looking for a large number of potential targets, search is guided by a “guiding template” in working memory that contains simple guiding features like color and orientation, and target identification, or object recognition, is determined by a precise “target template” in long-term memory (Cunningham & Wolfe, 2014; Wolfe, 2021). Future work is necessary to address how memory representations of the target differ and are used to guide attention and make target decisions.

Conclusion

Attentional templates have held an important place in our understanding of search behavior. The traditional definition of templates often assumed that the template contains a veridical copy of the target. The experiments presented here demonstrate the flexibility of template contents as a function of distractor context and stage of processing during visual search. Our results strongly argued against a perfectly veridical target. Instead, the template contents are customized according to search environments and task demands. In summary, the study of flexible target templates provide information about how the internal representation of the target is modulated to best discriminate the target from distractors at present moment.

References

Anderson, B. A. (2014). On the precision of goal-directed attentional selection. *Journal of Experimental Psychology: Human Perception and Performance*, *40*(5), 1755—1762. https://doi.org/10.1037/a0037685

Becker, S. I. (2010). The Role of Target–Distractor Relationships in Guiding Attention and the Eyes in Visual Search. *Journal of Experimental Psychology: General*, *139*(2), 247–265. https://doi.org/10.1037/a0018808

Becker, S. I., Harris, A. M., Venini, D., & Retell, J. D. (2014). Visual search for color and shape: When is the gaze guided by feature relationships, when by feature values? *Journal of Experimental Psychology: Human Perception and Performance*, *40*(1), 264—291. https://doi.org/10.1037/a0033489

Bichot, N. P., Heard, M. T., DeGennaro, E. M., & Desimone, R. (2015). A Source for Feature-Based Attention in the Prefrontal Cortex. *Neuron*, *88*(4), 832—844. https://doi.org/10.1016/j.neuron.2015.10.001

Bichot, N. P., Xu, R., Ghadooshahy, A., Williams, M. L., & Desimone, R. (2019). The role of prefrontal cortex in the control of feature attention in area V4. *Nature Communications*, *10*(1). https://doi.org/10.1038/s41467-019-13761-7

Bravo, M. J., & Farid, H. (2012). Task demands determine the specificity of the search template. *Attention, Perception, \textbackslash& Psychophysics*, *74*(1), 124—131. https://doi.org/10.3758/s13414-011-0224-5

Bravo, M. J., & Farid, H. (2016). Observers change their target template based on expected context. *Attention, Perception, \textbackslash& Psychophysics*, *78*(3), 829—837. https://doi.org/10.3758/s13414-015-1051-x

Bundesen, C. (1990). A theory of visual attention. *Psychological Review*, *97*(4), 523—547. https://doi.org/10.1037/0033-295x.97.4.523

Castelhano, M. S., Pollatsek, A., & Cave, K. R. (2008). Typicality aids search for an unspecified target, but only in identification and not in attentional guidance. *Psychonomic Bulletin & Review*, *15*(4), 795–801. https://doi.org/10.3758/PBR.15.4.795

Cunningham, C. A., & Wolfe, J. M. (2014). The role of object categories in hybrid visual and memory search. *Journal of Experimental Psychology. General*, *143*(4), 1585—1599. https://doi.org/10.1037/a0036313

Desimone, R., & Duncan, J. (1995). Neural Mechanisms of Selective Visual Attention. *Annual Review of Neuroscience*, *18*(1), 193—222. https://doi.org/10.1146/annurev.ne.18.030195.001205

D’Esposito, M., & Postle, B. R. (2015). The Cognitive Neuroscience of Working Memory. *Annual Review of Psychology*, *66*(1), 115—142. https://doi.org/10.1146/annurev-psych-010814-015031

Duncan, J., & Humphreys, G. W. (1989). *Visual Search and Stimulus Similarity*. 26.

Eriksen, C. W. (1953). Object location in a complex perceptual field. *Journal of Experimental Psychology*, *45*(2), 126–132. https://doi.org/10.1037/h0058018

Ester, E. F., Sutterer, D. W., Serences, J. T., & Awh, E. (2016). Feature-Selective Attentional Modulations in Human Frontoparietal Cortex. *Journal of Neuroscience*, *36*(31), 8188—8199. https://doi.org/10.1523/jneurosci.3935-15.2016

Gaspelin, N., Leonard, C. J., & Luck, S. J. (2015). Direct Evidence for Active Suppression of Salient-but-Irrelevant Sensory Inputs. *Psychological Science*, *26*(11), 1740–1750. https://doi.org/10.1177/0956797615597913

Geng, J. J., DiQuattro, N. E., & Helm, J. (2017). Distractor Probability Changes the Shape of the Attentional Template. *Journal of Experimental Psychology: Human Perception and Performance*, *43*(12), 1993–2007. https://doi.org/10.1037/xhp0000430

Geng, J. J., & Witkowski, P. (2019). Template-to-distractor distinctiveness regulates visual search efficiency. *Current Opinion in Psychology*, *29*, 119—125. https://doi.org/10.1016/j.copsyc.2019.01.003

Green, B. F., & Anderson, L. K. (1956). Color coding in a visual search task. *Journal of Experimental Psychology*, *51*(1), 19–24. https://doi.org/10.1037/h0047484

Harrison, S. A., & Tong, F. (2009). Decoding reveals the contents of visual working memory in early visual areas. *Nature*, *458*(7238), 632—635. https://doi.org/10.1038/nature07832

Hodsoll, J., & Humphreys, G. W. (2001). Driving attention with the top down: The relative contribution of target templates to the linear separability effect in the size dimension. *Perception \textbackslash& Psychophysics*, *63*(5), 918—926. https://doi.org/10.3758/bf03194447

Hout, M. C., & Goldinger, S. D. (2015). Target templates: The precision of mental representations affects attentional guidance and decision-making in visual search. *Attention, Perception \textbackslash& Psychophysics*, *77*(1), 128—149. https://doi.org/10.3758/s13414-014-0764-6

Hulleman, J. (2009). No need for inhibitory tagging of locations in visual search. *Psychonomic Bulletin & Review*, *16*(1), 116–120. https://doi.org/10.3758/PBR.16.1.116

Hulleman, J. (2010). Inhibitory tagging in visual search: Only in difficult search are items tagged individually. *Vision Research*, *50*(20), 2069–2079. https://doi.org/10.1016/j.visres.2010.07.017

Kerzel, D. (2019). The precision of attentional selection is far worse than the precision of the underlying memory representation. *Cognition*, *186*, 20—31. https://doi.org/10.1016/j.cognition.2019.02.001

Kerzel, D. (2020). Direct evidence for the optimal tuning of attention. *Journal of Experimental Psychology: Human Perception and Performance*, *46*(7), 716–728. https://doi.org/10.1037/xhp0000744

Lee, S.-H., Kravitz, D. J., & Baker, C. I. (2013). Goal-dependent dissociation of visual and prefrontal cortices during working memory. *Nature Neuroscience*, *16*(8), 997—999. https://doi.org/10.1038/nn.3452

Liu, T., Larsson, J., & Carrasco, M. (2007). Feature-Based Attention Modulates Orientation-Selective Responses in Human Visual Cortex. *Neuron*, *55*(2), 313—323. https://doi.org/10.1016/j.neuron.2007.06.030

Long, N. M., & Kuhl, B. A. (2018). Bottom-Up and Top-Down Factors Differentially Influence Stimulus Representations Across Large-Scale Attentional Networks. *The Journal of Neuroscience*, *38*(10), 2495—2504. https://doi.org/10.1523/jneurosci.2724-17.2018

Malcolm, G. L., & Henderson, J. M. (2009). The effects of target template specificity on visual search in real-world scenes: Evidence from eye movements. *Journal of Vision*, *9*(11), 8–8. https://doi.org/10.1167/9.11.8

Malcolm, G. L., & Henderson, J. M. (2010). Combining top-down processes to guide eye movements during real-world scene search. *Journal of Vision*, *10*(2), 4–4. https://doi.org/10.1167/10.2.4

Martin, A., & Becker, S. I. (2018). How feature relationships influence attention and awareness: Evidence from eye movements and EEG. *Journal of Experimental Psychology: Human Perception and Performance*, *44*(12), 1865—1883. https://doi.org/10.1037/xhp0000574

Martinez-Trujillo, J. C., & Treue, S. (2004). Feature-Based Attention Increases the Selectivity of Population Responses in Primate Visual Cortex. *Current Biology*, *14*(9), 744—751. https://doi.org/10.1016/j.cub.2004.04.028

Nako, R., Wu, R., & Eimer, M. (2014). Rapid guidance of visual search by object categories. *Journal of Experimental Psychology: Human Perception and Performance*, *40*(1), 50—60. https://doi.org/10.1037/a0033228

Navalpakkam, V., & Itti, L. (2007). Search Goal Tunes Visual Features Optimally. *Neuron*, *53*(4), 605—617. https://doi.org/10.1016/j.neuron.2007.01.018

Olivers, C. N. L., Peters, J., Houtkamp, R., & Roelfsema, P. R. (2011). Different states in visual working memory: When it guides attention and when it does not. *Trends in Cognitive Sciences*. https://doi.org/10.1016/j.tics.2011.05.004

Rajsic, J., & Woodman, G. F. (2020). Do we remember templates better so that we can reject distractors better? *Attention, Perception, & Psychophysics*, *82*(1), 269–279. https://doi.org/10.3758/s13414-019-01721-8

Ratcliff, R., & McKoon, G. (2008). The Diffusion Decision Model: Theory and Data for Two-Choice Decision Tasks. *Neural Computation*, *20*(4), 873—922. https://doi.org/10.1162/neco.2008.12-06-420

Ratcliff, R., Smith, P. L., Brown, S. D., & McKoon, G. (2016). Diffusion Decision Model: Current Issues and History. *Trends in Cognitive Sciences*, *20*(4), 260–281. https://doi.org/10.1016/j.tics.2016.01.007

Reynolds, J. H., & Heeger, D. J. (2009). The Normalization Model of Attention. *Neuron*, *61*(2), 168—185. https://doi.org/10.1016/j.neuron.2009.01.002

Rosenholtz, R. (2017). Those pernicious items. *Behavioral and Brain Sciences*, *40*, e154. https://doi.org/10.1017/S0140525X16000248

Schaefer, A., Kong, R., Gordon, E. M., Laumann, T. O., Zuo, X.-N., Holmes, A. J., Eickhoff, S. B., & Yeo, B. T. T. (2018). Local-Global Parcellation of the Human Cerebral Cortex from Intrinsic Functional Connectivity MRI. *Cerebral Cortex*, *28*(9), 3095—3114. https://doi.org/10.1093/cercor/bhx179

Schmidt, J., & Zelinsky, G. J. (2009). Short article: Search guidance is proportional to the categorical specificity of a target cue. *Quarterly Journal of Experimental Psychology*, *62*(10), 1904–1914. https://doi.org/10.1080/17470210902853530

Scolari, M., Byers, A., & Serences, J. T. (2012). Optimal Deployment of Attentional Gain during Fine Discriminations. *The Journal of Neuroscience*, *32*(22), 7723—7733. https://doi.org/10.1523/jneurosci.5558-11.2012

Scolari, M., & Serences, J. T. (2009). Adaptive Allocation of Attentional Gain. *Journal of Neuroscience*, *29*(38), 11933—11942. https://doi.org/10.1523/jneurosci.5642-08.2009

Serences, J., Saproo, S., Scolari, M., Ho, T., & Muftuler, L. (2009). Estimating the influence of attention on population codes in human visual cortex using voxel-based tuning functions. *NeuroImage*, *44*(1), 223—231. https://doi.org/10.1016/j.neuroimage.2008.07.043

Treisman, A. M., & Gelade, G. (1980). A feature-integration theory of attention. *Cognitive Psychology*, *12*(1), 97—136. https://doi.org/10.1016/0010-0285(80)90005-5

Treue, S., & Trujillo, J. C. M. (1999). Feature-based attention influences motion processing gain in macaque visual cortex. *Nature*, *399*(6736), 575—579. https://doi.org/10.1038/21176

Tünnermann, J., Chelazzi, L., & Schubö, A. (2021). How feature context alters attentional template switching. *Journal of Experimental Psychology: Human Perception and Performance*. https://doi.org/10.1037/xhp0000951

Wolfe, J. M. (2012). Saved by a log: How do humans perform hybrid visual and memory search? *Psychological Science*, *23*(7), 698—703. https://doi.org/10.1177/0956797612443968

Wolfe, J. M. (2021). Guided Search 6.0: An updated model of visual search. *Psychonomic Bulletin & Review*. https://doi.org/10.3758/s13423-020-01859-9

Won, B.-Y., Haberman, J., Bliss-Moreau, E., & Geng, J. J. (2020). Flexible target templates improve visual search accuracy for faces depicting emotion. *Attention, Perception, & Psychophysics*, *82*(6), 2909–2923. https://doi.org/10.3758/s13414-019-01965-4